Murine Models of Cerebral Ischemia: Development of a Mouse Model of Global Cerebral Ischemia; Response of GluR2 Knockout Mice in a Model of Permanent Focal Cerebral Ischemia

by

Sunu Samuel Thomas

A thesis submitted in conformity with the requirements for the degree of Master's of Science

Institute of Medical Science
University of Toronto

Abstract I

Development of a Four-Vessel Occlusion Model of Murine Global Cerebral Ischemia: Influence of Strain, Ischemic Duration and Reperfusion Time

Cerebral ischemia resulting from cardiac arrest leads to delayed selective neuronal death. A similar pathological outcome is observed in a variety of experimental animal models of global ischemia. However, a reproducible murine model of ischemia resulting in delayed selective neuronal death has yet to be established. Such a model could be applied to transgenic and knockout mice to further elucidate the roles of specific genes and their products in the underlying pathophysiology resulting from cerebral ischemia. **Purpose:** To develop a model of global cerebral ischemia in the mouse. **Hypothesis:** Mice subjected to global ischemia produced by a four-vessel occlusion (*4-VO*) model will yield the delayed selective death of >90% of pyramidal neurons in the CA1 region of the hippocampus. **Methods:** Under halothane anesthesia, the vertebral arteries of male CD1 mice (28-35g), were permanently occluded by electrocoagulation through the alar foramina. Twenty-four hours later, the subjects were re-anesthetized and their carotid arteries were transiently occluded for 15 min (n=5) and 20 min (n=5) to produce the four-vessel occlusion model of global ischemia. To test for strain-related susceptibility to ischemic damage, C57Bl/6 mice were subjected to 15- (n=5) and 20-min (n=5) of four-vessel occlusion. The effect of extended reperfusion times was tested in C57Bl/6 sacrificed 7 (n=5) and 14 days (n=3) after 20 min of ischemia. All mice were monitored by an EEG. Sham-operated animals (n=3) had their vertebral arteries coagulated while their carotid arteries were only exposed. Seven days post-ischemia or sham-procedure, the brains were perfusion-fixed and the number of ischemic CA1 pyramidal neurons were counted following histological staining by cresyl violet. **Results:** Histological analysis of the CA1 region of the hippocampus in CD1 mice subjected to up to 20 min ischemia did not show a statistically significant difference in the number of ischemic neurons between challenged and sham-operated mice (~3% cell death). Similarly, 15 and 20 min ischemia in C57Bl/6 mice, and prolonging the reperfusion period in this strain from 7 to 14 days also did not enhance hippocampal neuronal injury. Intra-ischemic isoelectric silence was recorded for all subjects. **Conclusions:** Although the model possesses a scientifically acceptable rate of mortality (40 to 50%) and all mice record flat EEG traces, the data suggest that the four-vessel occlusion model to be inadequate in yielding CA1 neuronal death.

Abstract II

Mice Lacking GluR2 are NOT More Susceptible to Focal Cerebral Ischemia

The massive influx of Ca^{2+} ions through neuronal glutamate receptors has been implicated in the pathophysiology of focal cerebral ischemia. AMPA receptor ion channels are composed of heteromeric combinations of four subunits (GluR1, 2, 3 & 4). The inclusion of GluR2 in its composition renders AMPA receptors Ca^{2+}-impermeable. The GluR2 Hypothesis states that cerebral ischemia induces the selective loss of this subunit, and consequently, increases Ca^{2+}-permeability through GluR2-less AMPA receptors. **Purpose:** We have therefore tested the response of mice lacking this subunit in a model of permanent focal cerebral ischemia. **Hypothesis:** GluR2(-/-) mutant mice will be more susceptible to ischemic injury resulting from the permanent occlusion of their middle cerebral artery. **Methods:** Under halothane anesthesia, the middle cerebral artery (MCA) of wild-type $Glur2^{(+/+)}$ and mutant $Glur2^{(-/-)}$ mice was occluded intraluminally using a 6-0 monofilament suture. Changes in ipsilateral cerebral blood flow (CBF) were monitored by laser Doppler flowmetry. Neurologic outcome was evaluated immediately prior to sacrifice using a neurobehavioural deficit score system (0: no deficits; 1: inability to flex right forepaw; 2: circling behaviour; 3: loss of righting reflex; 4: no spontaneous movement.) Animals were sacrificed 24 hours after the onset of ischemia by perfusion-fixation with 10% formalin-saline solution. Brains were subsequently cut into four 2 mm thick slices and processed for histological analysis. Infarction areas were quantified for each tissue slice using an image analysis system (MCID) and then integrated to calculate the overall infarction volume for each brain. **Results:** The results show that the extent of ischemic tissue damage between wild-type (n=7) and mutant mice (n=8) was not statistically different ($Glur2^{(+/+)}$: 67.82 +/- 7.22 mm^3 vs $Glur2^{(-/-)}$: 69.32+/- 5.53 mm^3.) Similarly, differences in neurobehavioural deficit scores were also not significant ($Glur2^{(+/+)}$: 2.86 +/- 4.04 and $Glur2^{(-/-)}$: 3.00 +/- 4.23.) **Conclusions:** These data suggest that the genetic deletion of the AMPA receptor GluR2 subunit does not enhance susceptibility to focal ischemic damage resulting from 24 hours of permanent MCA occlusion.

Dedication

This thesis is dedicated to my loving parents,
Samuel & Susamma Thomas,
who through the passion and diligence
by which they lead their lives,
truly symbolize the very meaning of the word
perseverance.

Acknowledgements

I wish to express my utmost appreciation to those who through their mentorship, patience, support and camaraderie helped mould my Master's experience. The brevity in the writing of these acknowledgements in no way reflects my sincere gratitude to them or the enormity of their contribution to my growth as a student and person.

Chris Wallace	for his supervision in allowing me the freedom to set my own course, yet with enough guidance to keep me on track.
James Eubanks	for never failing to believe in me.
John Roder David Hampson Andres Lozano W.M Burnham	for investing in my development as a graduate student through journal clubs, committee meetings and for their willingness to answer my simplest of questions.
Lucy Teves Richard Logan	for whips & chains, infectious smiles and serving as Chris Wallace's most potent weapons in the art of graduate student focus.

This list would be incomplete without the mention of those post-doctoral fellows and graduate students whose friendships highlight so many of the fond memories I have of my Master's studies.

Koji Iihara, Joseph Francis, Warren Ho, Benjamin Jung, Hany Elgandy, Guanming Zhang, Timothy Mertens and Rajesh Khanna

Table of Contents

I. List of Abbreviations

AMPA	alpha-amino-3-hydroxy-5-methyl-4-isoxazolepropionate
ANOVA	Analysis of Variance
ATP	Adenosine-tri-phosphate
MCA	Middle Cerebral Artery
MCAO	Middle Cerebral Artery Occlusion
NMDA	N-Methyl-*D*-aspartate
SD	Standard Deviation
SEM	Standard Error of the Mean
TTC	2,3,5-triphenyltetrazolium chloride
VAO	Vertebral Artery Occlusion
VSCC	Voltage Sensitive Calcium Channel
4VO	Four-Vessel Occlusion

II. Table of Figures

III. Introduction

III.i. Overview of Stroke

III.i.a. Stroke: A Definition

A stroke is a circulatory disturbance resulting in neurological impairments that are sustained for at least a 24 hour time period[1]. Strokes are classified into two categories according to the vascular cause of aberrant cerebral blood flow. Occlusive strokes result from the blockage of an artery by a clot of possible thrombo- or cardioembolic origin. The rupturing of blood vessels, as in the case of a haemorrhage, potentially leads to a second class of stroke of which intracerebral and subarachnoid types exist depending on the site of extravasational bleeding[2].

III.i.b. Stroke Epidemiology

Stroke continues to be the third most common cause of death in the industrialized nations, behind only cardiovascular disease and cancer[3]. It accounts for approximately 10% of all mortalities in developed nations and has a worldwide incidence rate estimated to be between an alarming 150 and 200 cases per 100 000 people[2]. About 85% of all strokes are thromboembolic in nature. Cerebral hemorrhages account for approximately 10 to 15% of all incidences of stroke[4].

Stroke survival is highly influenced by its etiology. The 30 day mortality rate for victims of occlusive, intracerebral and subarachnoid haemmorrhagic strokes is 15%, 45%, and 48-82%, respectively[5].

Stroke is the leading cause of disability in adults. In fact, stroke survivors account for approximately 3 million individuals in the United States alone[6]. Unfortunately, those who do survive suffer a range of compounded permanent disabilities depending upon the extent and type of ischemic damage, including paralysis, speech impediments, dementia, memory loss, and depression[5].

The economic impact of stroke has been estimated to total $30 billion dollars annually in the United States. This figure accounts for both the direct costs derived from hospital, physician, rehabilitation and equipment expenses, as well as the indirect costs from lost wages and individual productivity[5].

III.i.c. Stroke Prevention

The identification and management of stroke risk factors remain an important means by which the incidence of stroke may be reduced. Improvements in the management of hypertension, and increased public awareness of the ills of tobacco use and cardiac disease has been credited with the steady decline in both stroke incidence and mortality.

Nevertheless, stroke susceptibility increases with age, and the risks associated with gender, race and genetic predisposition are not modifiable[3,6].

III.i.d. Stroke Treatment

Effective pharmacotherapy to reduce cerebral damage resulting from a stroke is currently inadequate. Thrombolytic agents have been shown to ameliorate neurological impairments by restoring cerebral blood flow through occluded arteries[7]. However, the neuroprotective efficacy of such drugs is dependent upon their timely administration immediately following the onset of the stroke event. Hence, the limited usefulness of the available pharmacology necessitates improvements in the diagnosis of stroke, and further elucidation of its pathophysiology for the development of novel therapeutic strategies.

III.ii. The Cerebrovascular System

III.ii.a. Cerebral Metabolism - General

The adult human brain accounts for only 2% of total body weight, yet it consumes 20% of cardiac output and 15% of the total inspired oxygen. This disproportionate consumption of energy resources reflects the brain's dependence on the oxygen and glucose borne of its blood supply. ATP derived from the oxidative metabolism of glucose is responsible for supporting all cerebral function. Paradoxically, the brain

possesses only minimal energy reserves in the event of a circulatory disturbance[8]. Neurological impairments and syncope may be observed within seconds following a disruption in cerebral blood flow.

III.ii.b. Cerebrovascular Anatomy

Arterial blood is delivered to the brain through the internal carotid and vertebral arteries. The basilar artery, arising from the conjunction of the vertebral arteries, anastamoses with branches of the internal carotid arteries to form the Circle of Willis at the base of the brain. This arterial ring is composed of the right and left anterior, middle and posterior cerebral arteries[9,10]. The circle is made intact by a pair of anterior and posterior communicating arteries that connect the two anterior cerebral arteries, and the internal carotid and posterior cerebral arteries, respectively.

The Circle of Willis, by virtue of its anastamoses, ensures a constant supply of blood to the brain in the event of a vascular obstruction originating in the carotid or vertebral arteries. Therefore, following an arterial occlusion, blood flow may be restored to compromised tissue by the shunting of blood from the anterior or posterior circulation, or from the contralateral hemisphere[11].

III.ii.c. Cerebrovascular Hemodynamics

Variations in cortical blood flow have been shown to correspond to region-specific cerebral activity. The coupling of cerebral blood flow, neuronal activity and cerebral metabolism is believed to be mediated by vasoactive substances including CO_2, H^+, O_2, adenosine, K^+, Ca^{2+} and nitric oxide gas[12,13].

Cerebral blood flow may be further regulated by the parasympathetic and sympathetic innervation of the cerebrovasculature. Whereas parasympathetic innervation is a potent neural vasodilator, the vasoactive properties of the sympathetic nervous system is dependent upon the adrenergic receptor subtype. Alpha-adrenoceptor activation promotes vasoconstriction, while nor-adrenaline binding to beta-adrenoreceptors stimulates arterial vasodilation[14-16].

Despite localized fluctuations, total cerebral blood flow, under normal physiological conditions, is always held constant[17,18]. Cerebral autoregulation is the intrinsic capacity of the cerebral circulation to maintain constant blood flow in the brain over a range of systemic arterial blood pressures between 60 and 150 mmHg[9]. Thus, the delivery of oxygen and glucose is preserved even in conditions of either low blood pressure or chronic hypertension.

III.ii.d. Cerebral Blood Flow Thresholds

Measurements of cerebral blood flow have established the basal rate of cerebral perfusion to be 40 to 60 ml / min / 100 g of brain tissue. Neurological deficits emerge following the reduction of blood flow levels below 20 ml / min / 100 g of brain tissue, indicative of neuronal dysfunction and synaptic failure. However, a further reduction of cerebral blood flow below 8 and 10 ml / min / 100 g of tissue fails to sustain cellular viability, leading to areas of dead cerebral tissue[17,19,20].

III.ii.e. Cerebral Metabolic Adaptation

If cerebral blood flow is reduced beyond the lower limits of autoregulatory compensation, i.e. 60 mmHg, the brain is capable of increasing oxygen uptake from a limited arterial supply[17]. This enhanced efficiency of energy utilization is critical for maintaining the cerebral metabolic rate of oxygen consumption ($CMRO_2$) required to preserve neuronal function and viability. However, like autoregulation, this adaptive capacity is limited to a finite range of arterial pressures between 25 and 60 mmHg. A reduction of cerebral blood flow below 25 mmHg renders the tissue ischemic and susceptible to death[8,14,20].

III.iii. Cerebral Ischemia - Definitions

Ischemia refers to a reduction in cerebral blood flow to levels incompatible with tissue viability[21]. Two types of cerebral ischemia exist according to the regional distribution of the affected arterial territories:

III.iii.a. Focal Cerebral Ischemia

Focal ischemia refers to a localized reduction in cerebral blood flow, typically resulting from the occlusion of an artery by a thrombotic or cardio-embolic clot[22].

III.iii.b. Global Cerebral Ischemia

Global ischemia arises from conditions of cardiac arrest (pump failure), massive brain swelling (increased intracranial pressure), or severe systemic hypotension, in which blood flow to the entire brain is compromised[22].

The functional deficits attributed to stroke neuropathology are indicative of the cerebral territories that have been hemodynamically compromised. It is for this reason that brain damage sustained from an occlusive stroke is disparate from that of a cardiac arrest[9].

III.iv. Experimental Cerebral Ischemia: Animal Models

The validity of any animal model of cerebral ischemia is ultimately determined by its ability to reproducibly yield a lesion similar to that observed in the human stroke condition. It is essential that the magnitude of damage and its distribution within the cerebral tissue be controlled to facilitate statistical comparisons. The lesion produced must also be amenable and sensitive to change such that the experimental perturbation of the model may elucidate the pathogenic mechanisms of cerebral ischemia[23]. Hence, the delayed development of symmetrical and selective neuronal death in the CA1 subfield of the hippocampus is a prerequisite for models of global cerebral ischemia[24]. Similarly, the most studied models of focal ischemia are those that consistently produce relatively consistent infarction volumes[25-27].

III.iv.a. Choice of Animal

Which animal species and strain should be used in a model of cerebral ischemia? The neuroanatomy, physiology and cerebrovasculature of a chosen animal should be similar to those found in humans so as to yield a clinically analogous ischemic lesion[23]. In animals for which these criteria are met and subsequently tested, one must assume that the damage sustained from experimental cerebral ischemia is governed by a pathophysiology that is conserved in humans. This necessary assumption has led to criticisms, as therapeutic strategies found to be neuroprotective in animal models have as yet to be proven successful clinically.

The induction of cerebral ischemia first requires surgical access to the arteries that feed the brain. Early models were developed in larger animals, and in particular primates for which the surgical preparation was similar to neurosurgical procedures conducted in humans. However, the need to control outcome variability for the statistical validation of a given model has influenced the development of different models of stroke in a variety of animal species and even their strains[25]. For this reason, models have been developed in dogs, rabbits, pigs and cats[28]. Models using rats and gerbils, in particular, have been extensively used due to their amenability to a variety of outcome measures that characterize the morphological, biochemical and electrophysiological changes that occur as a pathological consequence of cerebral ischemia[23]. Controlling those physiological parameters that may influence lesion variability, including temperature, systemic blood pressure, arterial blood gases, and levels of glucose and acidity, are more manageable in rodents. Moreover, the relatively lower costs associated with rats and gerbils enables larger sample sizes that improve the power of statistical comparisons in the studies that employ them[23].

III.iv.b. Controlling Outcome Variability: Physiological Parameters

Aberrant changes in body temperature, systemic blood pressure, arterial carbon dioxide, pH, glucose and hematocrit may potentially confound the interpretation of the ischemic outcome. Therefore, it is imperative that these parameters are controlled to pre-ischemic values throughout a study.

Temperature

Hypothermia is so potently neuroprotective that it has been successfully implemented clinically during specific neurosurgical procedures. Hypothermia greatly reduces the extent of brain damage sustained in models of both focal and global cerebral ischemia. In contrast, hyperthermia is known to exacerbate ischemic injury[29-32].

Arterial Blood Pressure

Systemic blood pressure is determined by the cardiac output, the total peripheral vascular resistance, blood volume and arterial compliance. Control of these determinants is necessary to maintain mean arterial blood pressure. Hypotension reduces cerebral blood flow; a property that has been implemented in the development of models of global cerebral ischemia[33].

$PaCO_2$ and pH

Increasing levels of P_aCO_2 and blood acidity produce vasodilation, resulting in an increase in total cerebral blood flow . In contrast, hyperventilation induces arterial conditions of alkalinity and low P_aCO_2 that promote vasoconstriction and reduction in cerebral blood flow[13,14].

Glucose

Hyperglycemia is known to exacerbate ischemic injury by contributing to the production of tissue acidosis. Cerebral blood flow tends to become sluggish with increasing levels of blood sugar. In general , hypoglycemia reduces tissue damage induced by cerebral ischemia[34,35].

Arterial Blood Hematocrit

The hematocrit ratio is defined as the proportion of red blood cells (erythrocytes) in a given volume of blood. If this ratio is zero, the viscosity of blood is that of the plasma alone. Therefore, in conditions of polycythemia, resulting from an abnormally excessive blood erythrocyte concentration, blood flow is diminished. In contrast, blood flow is enhanced by anaemia due to a decrease blood viscosity.

III.v. Focal Cerebral Ischemia

III.v.a. Focal Cerebral Ischemia: Neuropathology

The middle cerebral artery (MCA) is predisposed to potential occlusion by arterial debris, e.g. thrombotic clot, due to the step-down reduction in its lumenal calibre distal to its bifurcation from the internal carotid artery in the Circle of Willis. The lesion that subsequently evolves is characterized by a region of tissue damage, termed infarction, that resides within the vascular territory of the MCA. The liquefactive dissolution of the infarcted tissue, and the presence of edema in the affected hemisphere clearly demarcate the lesion from viable tissue. With time, the dead tissue is replaced by either a cavity or a cyst that remains with the individual for life. On a microscopic level, the infarct zone is defined by a region of pannecrosis in which all cells, i.e. neurons, glia and endothelial cells, have succumbed to death. The tissue matrix, called the neuropil, spreads and expands as a consequence of edamatous swelling[36,37].

The degree of motor and sensory dysfunction, e.g. paralysis, following an occlusive stroke is a direct consequence of the size and distribution of the infarcted tissue within the affected cerebral hemisphere.

III.v.b. Experimental Focal Cerebral Ischemia: Basic Concepts

III.v.b.i. Anatomy of the Middle Cerebral Artery

The internal carotid artery bifurcates into the middle and anterior cerebral arteries. The vascular territory of the middle cerebral artery encompasses the external surface of the hemisphere, including the lateral parts of the frontal, parietal, occipital and temporal lobes[10]. Perforating arteries that branch off the middle cerebral artery supply deeper cerebral tissues. Specifically, numerous lentriculostriate arteries arise from the proximal segment of the middle cerebral artery to supply parts of the internal capsule, the caudate putamen and the globus pallidus[38].

III.v.b.ii. Middle Cerebral Artery Occlusion

The occlusion of the middle cerebral artery (MCAO) produces an ischemic lesion resembling that observed in victims of embolic or thrombotic stroke. In models of focal ischemia, the quantification of the infarction volume remains the ultimate endpoint upon which statistical comparisons are made. Thus, it is imperative that the size and distribution of the ischemic lesion be controlled[25].

The volume and location of the infarction has been shown to be dependent upon the precise site of the occlusion along the middle cerebral artery[39]. Occlusions distal to the origin of the lentriculostriate arteries result in predominantly cortical lesions[26,40,41]. Infarctions that penetrate deeper tissue arise from more proximal occlusions to the origin

of the middle cerebral artery itself. However, the final lesion seldom encompasses the whole of the susceptible MCA territory. Aside from that core region solely dependent upon the middle cerebral artery, peripheral tissues may be rescued by collateral circulation from the anterior and posterior cerebral arteries[42,43]. In fact, though the location of the resulting lesion is centrally defined by the middle cerebral artery, minor shifts in its position is dependent upon the relative flows from the two collateral arteries, moving it in the direction of lesser compensation.

III.v.c. Animal Models of Focal Cerebral Ischemia

The relative conservation of the middle cerebral artery in a variety of animal species has facilitated the development of models of focal ischemia in primates, dogs and cats. In particular, many models have been designed in the rat and their descriptions are forthcoming.

In the development of focal models of cerebral ischemia, two approaches have been established for the occlusion of the middle cerebral artery: extravascular and intravascular.

Extravascular Occlusion of the Middle Cerebral Artery (MCA)

With this approach, the surgeon is afforded the opportunity to visually confirm both the cessation and reperfusion of blood flow through the middle cerebral artery. In these models of focal ischemia, the removal of a portion of the skull by a craniectomy is necessary to expose the middle cerebral artery[26,27,44]. Manipulation of the artery requires an additional incision into the protective dural sheath of the brain, thereby, breaching the integrity of the cerebral environment. Therefore, to minimize exposure damage to the cerebral cortex, the parenchymal tissue is continuously irrigated with warm saline or artificial cerebrospinal fluid (CSF).

Models of both permanent and temporary focal ischemia are possible with this surgical approach. However, the reversibility of the ischemia is dependent upon the method of occlusion. The use of micro-aneurysm clips, ligatures and vasoconstrictors, i.e. endothelin, are amenable to investigations of transient focal ischemia[23,45,46]. In contrast, electrocoagulation is used as a means of permanently occluding the middle cerebral artery. Usually, the MCA is transected following cautery to avoid reflow as a result of the recannulation of the artery.

Rat: Distal MCA Occlusion

In early models, focal ischemia was induced by the distal occlusion of the middle cerebral artery. Cerebral tissue damage was minimal and also restricted to the cortex[40]. In fact, the incidence of infarction was poor as a result of compensatory collateral

circulation from the lenticulostriate arteries, and the end-arterioles of the anterior and posterior cerebral arteries.

Rat: Tandem Occlusion of Distal MCA & CCA

Brint et al. introduced a novel model of focal ischemia in which the distal middle cerebral artery is occluded in conjunction with its ipsilateral common carotid artery[26]. The occlusion of the latter was deemed necessary to increase the severity of the ischemia, and to restrict the contribution of collateral blood flow through the lenticulostriate arteries to infarct variability. The tandem occlusion technique gives rise to consistent infarctions isolated to the cortical tissue.

Rat: Proximal MCA Occlusion

In this model of focal ischemia, the stem of the proximal middle cerebral artery is occluded through a subtemporal craniectomy[27,43]. As the occlusion is made lateral to the lenticulostriate arteries, cerebral infarction is produced consistently in the cortex and in deeper tissue residing in the lateral part of the caudate putamen.

Intravascular Occlusion of the Middle Cerebral Artery

Rat: MCA Occlusion by an Intraluminal Suture

A great disadvantage to the aforementioned models is the potential injury to cerebral tissue from thermal and mechanical trauma during surgery. Despite the reproducibility of such models, the influences of procedurally-related factors on the ischemic outcome cannot be neglected.

The intravascular occlusion of the middle cerebral artery provides a technique that is minimally invasive, and preserves intracranial pressure, blood brain barrier permeability and intracerebral temperature. Exposure injury is avoided as the brain is never exposed. In addition, the reversibility of the occlusion by suture withdrawal facilitates the study of reperfusion in the pathophysiology of focal cerebral ischemia[47-50].

In this model, a suture is inserted into the external carotid artery and advanced a known distance through the internal carotid artery to occlude the middle cerebral artery at its origin[47]. As the site of the occlusion is proximal to the lentriculostriate arteries, the influence of collateral circulation on the variability of the ischemic lesion is minimized. The cerebral damage sustained in the intraluminal model encompasses the bulk of the vascular territory of the MCA to include the neocortex, caudate putamen and hippocampus[51].

The major drawback to this model is the surgeon's inability to visually confirm the successful occlusion of the middle cerebral artery. The reliability of the model has been enhanced by the intra-operative monitoring of cerebral blood flow using laser Doppler flowmetry as a means of verifying the occlusion[52]. In addition, the occluding tip of the filament must be modified, either by heat-blunting or silicone-coating, to avoid perforating the artery[53,54]. The calibre of the suture must be carefully matched to the mass of the animal to effectively block the lumen of the middle cerebral artery[47]. Residual blood flow derived from the posterior communicating artery has been known to circumvent a thin suture and reperfuse the MCA.

III.v.d. Outcome Measures: Evaluation of Focal Ischemic Damage

III.v.d.i. Diagnosis of the Lesion

Gross Tissue Stains

Identification of the lesion in cerebral tissue is achieved histochemically by indicator dyes. The staining properties of each dye, and the mode and timing of their usage determine their efficacy in delineating the infarction from viable tissue. For instance, 2,3,5-triphenyltetrazolium chloride (TTC) stains living tissue brick red based on the presence of a mitochondrial dehydrogenase enzyme[55,56]. Ischemic tissue is clearly detected as it fails to stain. Neutral red is a intracellular pH indicator whose tissue staining intensity increases with the degree of cerebral blood flow decrease[57].

The need for fresh tissue for effective staining avoids the processing and fixing of tissue required for histological analysis. Brain tissue is either immersed in the stain, or the dye is infused into the cerebrovasculature by an intra-arterial injection. However, the perfusion method has been shown to be better correlated to standardized histological stains in estimating the size of the infarction than by that determined from tissue immersion[56].

However, the efficacy of gross tissue stains is dependent upon the timing of their administration. In contrast to histology which is able to identify ischemic damage at a cellular level, detection by gross tissue stains requires the development of a critical volume of infarction[55]. Thus, reliable diagnosis of tissue damage by these dyes requires a minimum of four hours. Earlier detection of ischemic damage is facilitated by histology.

Histological Analysis

The ultimate pathological assessment of ischemic damage requires the analysis of tissue at a cellular level by histology. Fixation, and subsequent processing by alcohol and xylene are essential steps required for the preparation of tissue for histological analysis. Under light microscopy, cellular structures are distinguished by the differential staining patterns of histological dyes, including hematoxylin-eosin (H&E) and cresyl violet (Nissl stain). Selectivity and intensity of staining is dependent upon the binding characteristics of each dye. Cresyl violet is an acidophilic stain with an affinity for charged proteins. Hematoxylin & eosin provide contrast by staining for both acidophilic

(hematoxylin) and basophilic moieties (eosin)[58]. Thus, morphological changes characteristic of ischemic cell change may be distinguished from normal cells in viable tissue. In addition, the efficacy of staining and damage detection is not dependent on the time of animal sacrifice following the onset of the ischemia.

III.v.d.ii. Quantification of Ischemic Damage

The size of the ischemic lesion is reported as either a total infarction volume or as a series of infarction areas calculated at specific coordinates along the brain's long axis[53,59]. Typically, the infarction volume is calculated by a mathematical integration of the ischemic brain's infarct areas, the latter of which is determined by imaging devices. In some studies, comparisons are made between the size of the ischemic and contralateral hemispheres as a means of correcting for the contribution of edema and tissue swelling to the apparent infarct volume[37].

III.v.e. Outcome Measures: Assessment of Functional Deficits

III.v.e.i. Neurobehavioural Deficit Score System

The degree of motor impairments following the occlusion of the middle cerebral artery is correlated to the severity of ischemic damage. The development of these deficits is also an indirect indicator of the temporal evolution of the infarction. Scoring systems have been established to statistically validate the evaluation of neurobehavioural impairments[39,49,60]. These scales are based on a rank-order of scores in which higher scores are indicative of a more severe deficit. For instance, specific behavioural tendencies may be assigned the following test scores: 0 - absence of any observable motor impairment; 1 - inability to extend right forepaw; 2 - circling behaviour; 3 - loss of righting reflex; 4 - no spontaneous movement; 5 - death.

III.v.f. Outcome Measures: Measurement of Cerebral Blood Flow

III.v.f.i. Relative Measurement of Cerebral Blood Flow

Laser Doppler Flowmetry

Laser Doppler flowmetry provides a non-invasive method of monitoring relative changes in cortical blood flow continuously, without the need to sacrifice the animal. The precise location and depth of blood flow measurement is limited to the recording properties of the laser probe. Studies have shown that laser Doppler recordings correlate well with absolute measures of blood flow changes determined by autoradiography[52].

Indicator Dyes

Vascular injections of carbon black solution, India ink and Evan's blue dye provide a qualitative assessment of the measure of tissue perfusion during periods of ischemia[42]. Thus, tissues directly affected by the ischemia remain unstained, whereas zones of low, e.g. penumbra, to normal blood flow are delineated by differential staining patterns.

III.v.f.ii. Absolute Measurements of Cerebral Blood Flow

Autoradiography by ^{14}C-iodoantipyrine

Autoradiography provides a quantitative, multi-regional measure of cerebral blood flow based on the accumulation of radioactive tracers, e.g. ^{14}C-iodoantipyrine, within the brain. The technique is not conducive to either continuous or long-term monitoring of blood flow changes, as the animal must be sacrificed following the intravenous injection of the radioactive tracer[43,61].

Hydrogen Clearance

Cerebral blood flow is quantified at a specific polarographic coordinate within the brain by an electrode that measures changes in the tissue concentration of hydrogen[61]. The technique enables repeated monitoring of blood flow without the need to sacrifice the animal. The intracerebral insertion of an electrode, and the unreliability of

measurements in severely ischemic tissue are potential drawbacks to the Hydrogen Clearance method[62].

Microspheres

As with autoradiography, the regional accumulation of microspheres in proportion to blood flow provides a quantitative assessment of the cerebral circulation in models of ischemia. Long-term or continuous measurements of cerebral blood are not possible with this technique[61].

III.v.g. Spatial and Temporal Profiles of Focal Ischemic Damage

The occlusion of the middle cerebral artery produces a region of infarction confined to the frontoparietal aspect of the affected hemisphere[63,64]. As previously described, the depth of the ischemic damage is dependent upon the segment of the MCA that is occluded; the more proximal the site of occlusion, the greater the size of the lesion.

At a cellular level, energy failure following the arterial occlusion leads to almost immediate irreversible cell death in that region of tissue in which the ischemia is most dense. However, total damage sustained by the onset of focal ischemia is progressive. In most animal species tested, infarcts appear within 1 to 2 hours of sustained ischemia, and are near maximal within 3 to 6 hours[28,65]. By these time points, the lesion is clearly demarcated from viable tissue. During the evolution of the infarction, tissue damage is

further exacerbated by edema formation and inflammatory responses induced by the ischemia[37].

Primary damage to cerebral tissue resulting from temporary or permanent focal ischemia is believed to be complete by 24 hours[47]. For this reason, the infarction outcome in models of focal ischemia is typically evaluated 24 hours following the MCA occlusion as a statistically valid temporal endpoint. However, secondary damage attributed to neuronal degeneration of the axonal projections to and from the substantia nigra and thalamus has been shown to occur 72 to 96 hours following the occlusion of the MCA[36]. Subsequent to its peak at 24 hours, both the infarction and ipsilateral hemisphere are gradually reduced in size as a consequence of reduced edema formation, the resorption of excess tissue fluid and the elimination of dead cells by macrophages[60,66].

III.v.g.i. Hemodynamic Consequences

Reduction of blood flow within the vascular territory of the occluded middle cerebral artery is not uniformly distributed. Rather, a gradient exists in which cerebral blood flow improves the further the tissue is removed from the site of the arterial occlusion. Two regions of tissue are defined according to their ischemic severity: the ischemic core, and the penumbra.

Ischemic Core

The ischemic core denotes that region of tissue closest to the site of the MCA occlusion in which the reduction of blood flow is most severe[63,64,67]. The degree of residual perfusion is incompatible with sustaining cellular viability. Within this region, ATP is depleted and no longer synthesized, contributing to the loss of ion homeostasis and membrane integrity. Thus, in the evolution of the stroke lesion, core tissue is the first to succumb. Histologically, cerebral tissue within the ischemic focus is pannecrotic such that cells of all types are dead.

Ischemic Penumbra

The penumbra is the region of cerebral tissue found between the ischemic core and that outside the vascular territory of the middle cerebral artery[68,69]. Within this "shadow" of the ischemic focus, the reduction in blood flow, though significant, is still less severe as compared to core tissue[17,42]. Thus, the viability of penumbral tissue is temporarily sustained by collateral circulation from the end-arterioles of the anterior and posterior cerebral arteries that maintain blood flow above the ischemic threshold[19]. In contrast to the ischemic core, the active maintenance of ion homeostasis and membrane integrity in penumbral tissue are fuelled by near physiological levels of ATP[64].

However, the penumbral zone is characterized by synaptic failure and severe lactic acidosis. Therefore, despite viability, cells in the periphery of the ischemic focus are functionally compromised[69]. The loss of their functionality appears to be reversible

with rapid and adequate reperfusion. Otherwise, sustained focal ischemia promotes the evolution of the infarction[68]. Thus, it is possible, that within a given window of opportunity, penumbral tissue may be rescued from recruitment into the ischemic core.

III.vi. Global Cerebral Ischemia

III.vi.a. Global Cerebral Ischemia: Neuropathology

Survival from a cardiac arrest decreases with longer durations of circulatory stasis. Those who have been successfully resuscitated, however, suffer deficits ranging from amnesia to coma[70-72]. However, unlike the lesions confined to the vascular territory of the MCA with an occlusive stroke, neuropathological analyses of brains subjected to a cardiac arrest revealed distinct regions of bihemispherical tissue damage not prescribed to a specific artery. In particular, selectively vulnerable populations of neurons were identified in the CA1 subfield of the hippocampus and layers III, V and VI of the neocortex[73-77]. Interestingly, the pathology of global ischemia was determined to occur in a delayed fashion, presenting itself only days after the initial ischemic episode[78,79].

Studies have shown that the memory deficits sustained in survivors of cardiopulmonary arrest to be attributed to CA1 hippocampal lesions[80-82]. However, the assessment of the morbidity following a cardiac arrest is further complicated by systemic derangements owing to a "global" ischemia limited not just to the brain, but to the body as a whole[70,72].

III.vi.b. Global Cerebral Ischemia: Animal Models

An effective model of global cerebral ischemia must reproduce the clinical outcome of CA1 hippocampal neuronal death in a selective and delayed manner. The degree of ischemia must be sufficiently severe to induce a near maximal neuronal dropout (>90%) from the CA1 subfield for statistical comparisons to be valid. To this end, a variety of animal models of global ischemia have been developed differing in the consistency of the ischemic outcome, the uniformity of the blood flow reduction, the ease of the surgical preparation, and the amenability to the long-term recovery of challenged animals[23].

III.vi.b.i. Complete versus Incomplete Global Cerebral Ischemia

In model development, the term global ischemia refers loosely to a reduction in cerebral blood flow to at least both hemispheres of the brain. Models are classified into two categories according to the totality of the overall blood flow reduction.

Complete global cerebral ischemia, as produced by a cardiac arrest, is characterized by a state of circulatory stasis within the brain. In contrast, models of incomplete global ischemia are defined by a severe reduction of blood flow primarily to the forebrain (cerebrum) with adequate perfusion to the midbrain and cerebellum[23].

III.vi.b.ii. Animal Types

Strategies to develop these models have entailed the occlusion of a combination of arteries and / or the manipulation of hemodynamic determinants of cerebral blood flow, i.e. systemic blood pressure and intracranial pressure[23]. The approach taken is largely dependent upon the size and manageability of the animal species, and the degree of the arterial development of their Circle of Willis.

Complete global ischemia is produced either by a cardiac arrest or by blocking aortic blood flow. This has been facilitated in larger animals, including primates, dogs, rabbits and pigs that provide surgical access to the heart and thereby, permitting the intrathoracic clamping of the brachiocephalic and left subclavian arteries. Other methods used to produce global ischemia in large animals include the elevation of intracranial pressure, and the inflation of a neck tourniquet with induced hypotension in order to reducing total cerebral blood flow[23].

In contrast, rodent models of global cerebral ischemia have primarily been developed by reducing blood flow in major arteries that directly supply the brain. Thus, in gerbils that possess a poorly developed Circle of Willis, the occlusion of the carotid arteries is sufficient to produce severe forebrain ischemia[77]. However, a similar strategy is inadequate in rats due to collateral blood flow arising from the vertebro-basilar system. Therefore, to produce a rat model of global ischemia, the occlusion of the carotid arteries must be accompanied by the induction of systemic hypotension, or the additional occlusion of the vertebral or basilar arteries[33,83,84].

III.vi.c. Rodent Models of Incomplete Global Ischemia

Gerbil: Bilateral Common Carotid Artery Occlusion (BCCAO)

The lack of posterior communicating arteries renders the gerbil susceptible to forebrain ischemia following the occlusion of both common carotid arteries[77,85,86]. The absence of these arteries in an incomplete Circle of Willis denies compensatory collateral circulation from the vertebro-basilar system. The simplicity of the surgical technique, and the induction of delayed CA1 neuronal death following less than five minutes of ischemia are advantages to the model. However, excessive interanimal variability in the degree of hippocampal damage, and the onset of epileptic seizures in challenged animals have limited the extensive use of gerbils as the animal model of choice for global ischemia[23].

Rat: Two-Vessel Occlusion & Systemic Hypotension

In contrast to the gerbil, the rat possesses a complete of Circle of Willis. Consequently, the occlusion of only the common carotid arteries is insufficient in reducing cerebral blood flow below ischemic thresholds. For this reason, Smith *et al.*, introduced a novel model of global cerebral ischemia in which the occlusion of the two arteries is combined with an induction of systemic hypotension[33]. The reduction in mean arterial blood pressure is initially achieved by exsanguination and further enhanced by hypotensive drugs, e.g. Arfonad (a ganglioside blocker).

The ischemia produced in this model is uniformly distributed to all cerebral regions. An ischemic duration of 15 minutes is sufficient to produce symmetrical damage to the CA1 hippocampal region in a delayed fashion. Furthermore, graded levels of ischemic injury may be sustained by manipulating the degree of systemic hypotension in the model.

Rat: Four-Vessel Occlusion

In another popular model, global ischemia is produced by occluding the four major arteries that supply the brain with blood[83,84]. In a two stage surgical procedure, the vertebral arteries are permanently occluded by electrocautery through the alar foramina of the first cervical vertebrae. Twenty-four hours later, both common carotid arteries are transiently occluded by microaneurysm clips in either anesthetized or unanesthetized animals. The absence of anesthesia during the ischemia eliminates the confounding influences that it may have on the ischemic outcome. An ischemic duration of 15 minutes is sufficiently severe to reproducibly yield >90% CA1 hippocampal neuronal death 7 days following the ischemia.

The model was initially criticized for its inconsistency in the ischemic outcome of challenged animals. This was attributed to collateral blood flow from the vertebro-basilar system originating from the anterior spinal artery[62,87]. Consequently, a gradient of ischemia is produced yielding greater CA1 injury in the dorsal hippocampus[88]. Ischemic criteria were established such that only those animals displaying a lack of responsiveness,

pupil dilation and the recording of a flat EEG trace during the four-vessel occlusion were to be included in any study[89]. The model is associated with a high mortality rate (~50%) owing to the invasiveness of the surgical procedure and potential damage sustained to the cardio and respiratory centres in the midbrain from the electrocoagulation of the vertebral arteries.

Rat: Modified Four-Vessel Occlusion

To improve the consistency of the ischemic damage induced in early versions of the four-vessel occlusion model, Sugio et al. recognized the need to restrict suspected collateral blood flow through vessels running through the cervical and paravertebral muscles[90]. The tightening of these muscles by a suture during the four-vessel occlusion was shown to significantly improve the success rate of the model and the consistency of CA1 hippocampal damage. However, care must be taken to avoid autonomic nerve damage and respiratory arrest attributed to overtightening of the muscle stitch[91,92].

III.vi.d. Rodent Models of Complete Global Ischemia

Rat: Three-Vessel Occlusion

In this approach, the basilar artery is occluded in combination with the common carotid arteries to produce a model of complete global cerebral ischemia[79]. The occlusion of the basilar artery eliminates the collateral blood flow from the anterior spinal and

vertebral arteries believed to be responsible for variable degrees of ischemia in other rat models. Although levels of cerebral blood flow produced by the three-vessel occlusion are near zero, characterization of the neuropathological outcome of the model is lacking. In addition, an intradural approach is required for the occlusion of the basilar artery, increasing the technical difficulty of the surgery and the risk of brainstem injury.

Rat: Seven-Vessel Occlusion

Complete global cerebral ischemia is produced by the occlusion of the basilar artery in combination with the right and left pterygopalatine, external carotid and common carotid arteries[93]. Like its three-vessel occlusion counterpart , this model was intended to improve the consistency of the ischemic outcome produced by the occlusion of the vertebral and carotid arteries in the four-vessel model. Hence, the invasiveness of the surgical protocol is apparently justified by the need to better control collateral circulation from the anterior spinal artery derived from blood flow through vessels distal to the points of vertebral and carotid artery occlusion. Cerebral blood flow in the model is almost completely eliminated. However, full characterization of the consistency and extent of ischemic damage is lacking. The model has not achieved widespread use in studies of global cerebral ischemia.

Rat: Cardiac Arrest

In this model, animals are administered a dose of a nondepolarizing neuromuscular junction blocker, e.g. vecuronium, to induce respiratory muscle paralysis[94]. Cardiac arrest results from the ensuing apnea. The animal is resuscitated after breathing has ceased for 8 min.

Despite their clinical relevance, the use of cardiac arrest models in rats, dogs and primates has been limited in the field of global ischemia. Animals tested in the model require extensive post-operative care to treat pulmonary edema, the obstruction of airways by mucus and a host of systemic derangements attributed to anoxia and circulatory stasis[23]. The consistency of ischemic damage is poor and non-selective. Furthermore, studies of long-term survival following the arrest are not possible due to high animal mortality.

III.vi.e. Outcome Measures: Evaluation of Ischemic Damage

III.vi.e.i. Diagnosis of Ischemic Lesion

Cellular damage in regions of selective neuronal vulnerability are not detectable by the gross tissue stains often employed in the pathological assessment of focal ischemia. The primary method of lesion detection in models of global cerebral ischemia is by histological staining, e.g. cresyl violet (Nissl stain).

III.vi.e.ii. Quantification of Ischemic Damage

Selective regions of the brain are susceptible to damage following global cerebral ischemia[73-77]. Specifically, the degree of neuronal death in the CA1 subfield of the hippocampus is used as a measure of the severity of ischemic damage. Hippocampal damage may be calculated as a percentage of the number of pyknotic neurons in the CA1 region divided by the total neuronal count in that subfield[95]. As a means of standardization, the latter value is usually derived from the total number of neurons from the CA1 hippocampus of a sham-operated animal. Alternatively, hippocampal damage may be quantified as a density of the number of dead neurons within a defined distance of the CA1. Ranked scores have also been used as a qualitative measure of hippocampal damage following global cerebral ischemia[96].

III.vi.f. Outcome Measures: Assessment of Functional Deficits

A common development in patients who have survived a cardiac arrest is memory loss. This deficit has been associated with a lesion in the CA1 region of the hippocampus[81]. In models of experimental ischemia, the behavioural response of rodents tested in a variety of mazes is an indicator of the degree of CA1 hippocampal neuronal death. Specifically, rodents are subjected to either the Morris water maze, radial or T-maze as a means of evaluating deficits in their learning, memory and spatial navigational skills.

III.vi.g. Outcome Measures: Electrical & Cerebral Blood Flow Deficits

Electroencephalography (EEG)

Electroencephalography (EEG) has been used extensively in diagnosing global cerebral ischemia in both experimental models of stroke and intra-operatively during surgical procedures that potentially perturb cerebral blood flow[89]. EEG tracings do not directly measure cerebral blood flow. Rather, the electroencephalogram records global cortical electrical activity. Conditions of severe metabolic dysfunction, as induced by cerebral ischemia, abolishes this activity, and is recorded on an EEG tracing as a flat line.

Previously described methods of cerebral blood flow measurement have also been extensively used in models of global cerebral ischemia.

III.vi.h. Spatial and Temporal Profiles of Global Ischemic Damage

Neuronal death sustained following global cerebral ischemia evolves in a delayed manner in selectively vulnerable regions of the brain. The profile of ischemic damage is relatively conserved in a variety of models and animal species tested.

The response of brain tissue to global cerebral ischemia is heterogeneous. Ischemic damage within the hippocampus is restricted to the subiculum, hilus and the pyramidal neurons of the CA1. In contrast, the CA3 and dendate gyrus are markedly resistant to even severe global ischemia. Selective death is also observed in the small and medium-sized neurons of the striatum and layers III, V and VI of the neocortex[73-77].

Within the CA1 region of the hippocampus, neuronal death is only observed to occur 48 to 72 hours following the ischemic event[78]. In fact, neurons that are destined to die are functionally normal 24 hours after transient forebrain ischemia. Hence, the delay between the onset of ischemia and the ensuing cell death serves as an intriguing therapeutic window for the development of neuroprotective strategies.

III.vii. Transgenic & Knockout Mice in Experimental Cerebral Ischemia

Much of our current understanding of stroke pathophysiology has been derived from the pharmacological manipulation of rat models of ischemia. However, it has become increasingly clear that the complex mechanisms of cerebral ischemia exist at both cellular and molecular levels. Unfortunately, advances in the field have been limited by the lack of subcellular pharmacology. Even though agonists and antagonists to these molecular targets may exist, questions regarding their selectivity and pharmacokinetics, specifically, their ability to cross the blood brain barrier in effective yet nonlethal doses, has hindered their use.

To this end, genetically engineered mice, either lacking or overexpressing specific genes, have provided the opportunity to investigate the role of particular proteins in the mechanisms of cerebral ischemia. Mutant mice act as genetic tools that may be tested in models of focal and global ischemia to answer specific questions regarding the genetic and molecular determinants of cerebral ischemia. The power of this technology is clearly evident in the ever growing number of studies that are published employing them (Tables 1 & 2.)

Two general classes of mutant mice exist as distinguished by the nature of the genetic manipulation that has produced them. Transgenic mice are constructed by the genomic insertion of a novel gene or the overexpression of one that is endogenous to the host animal. In contrast, knockout mice, also called null mutants, are produced following

the deletion or inactivation of a specific gene. A wild-type mouse refers to a normal animal whose genome has not been altered.

III.vii.a. Murine Models of Cerebral Ischemia

The study of genetically engineered mice in the pathophysiology of stroke has necessitated the development of murine models of cerebral ischemia. The design of these models have been adapted from existing models used to test other rodents. Thus, cerebral blood flow monitoring, the assessment of functional deficits and the diagnosis and quantification of the ischemic lesion are similar to that used in rat and gerbil models of cerebral ischemia.

Mouse Focal Cerebral Ischemia

In early investigations, the mouse middle cerebral artery was occluded by electrocoagulation[138]. However, most studies currently being published test transgenic and knockout mice using the intraluminal occlusion model of focal ischemia. As previously stated, the model is amenable to the study of both the permanent and temporary occlusion of the middle cerebral artery, and has been well-characterized in the literature[47,48,50,139].

Mouse Global Cerebral Ischemia

A reproducible model of murine global ischemia has yet to be established. Attempted models of global ischemia produced in the mouse either by a three-vessel occlusion of both the basilar and carotid arteries, or by the bilateral occlusion of the carotid arteries alone have been unreliable in the consistency and selectivity of sustained hippocampal damage[24,96,140,141].

III.viii. Cerebral Ischemia: Pathophysiology

Although models of focal and global ischemia produce lesions by reducing cerebral blood flow, differences exist in the spatial and temporal profiles of their resulting damage. This is attributed to the distribution and severity of the ischemia; the latter of which is determined by the duration and degree of blood flow reduction. Thus, the delayed death of selectively vulnerable neuronal populations produced by a global ischemia of short duration, contrasts the pannecrosis observed in the vascular territory of a permanently occluded middle cerebral artery.

At present, the pathogenic mechanisms underlying focal and global ischemia remain unclear. Although the disparity of their pathological profiles suggest distinct cytotoxic pathways, specific mediators of cell death following both types of ischemia have been identified, including ischemia-induced energy failure and the concomitant perturbation of glutamate and calcium ion homeostasis.

III.viii.a. Consequences of Energy Failure

The onset of cerebral ischemia produces a state of energy failure in which the delivery of oxygen and glucose to the affected tissues is severely compromised. This leads to an impairment of ATP synthesis and the rapid depletion of minimal energy reserves[97,98]. As all cellular processes are intimately linked to ATP, the vitality of the cell is jeopardized after the onset of cerebral ischemia. Without intervention, the cell

succumbs as a consequence of internal derangements that have been initiated by the lack of ATP.

ATP depletion impairs the operation of the Na^+/K^+ ATPase which is responsible for maintaining sodium and potassium ion concentration gradients across the neuronal membrane. The ensuing rise in intracellular Na^+ and extracellular K^+ ion concentrations produces a state of maintained membrane depolarization[97]. This results in the perturbation of voltage-dependent cellular mechanisms, and the subsequent loss of cellular ion homeostasis triggered in part to the unregulated release of neurotransmitters into the synapse.

III.viii.b. Disruption of Ca^{2+} Homeostasis

Calcium is a ubiquitous divalent cation that acts a second messenger responsible for the activation of a myriad of cellular processes including membrane excitability, synaptic transmission, gene expression and cell growth and differentiation[99,100]. This activity is dependent upon the maintenance of an intracellular concentration of free Ca^{2+} that is four times less than that found in the extracellular space. Cytosolic Ca^{2+} levels are maintained by a dynamic balance of those mechanisms that control for calcium influx, extrusion, and sequestration[99]. Calcium may enter the cell through ion channels, exchangers and pumps. Subsequently, free Ca^{2+} ions may then be bound to specific cytosolic binding proteins or stored in the endoplasmic reticulum or mitochondria. The

intracellular concentration may be further regulated by the removal of Ca^{2+} ions from the cell through additional pumps and exchangers[100-102].

Cerebral ischemia disrupts normal calcium ion homeostasis by impairing the regulation of Ca^{2+} influx and efflux pathways[34]. This results in an elevation of its intracellular concentration. Consequently, the calcium overload triggers a variety of catabolic processes initiated by proteases, phospholipases, endonucleases, free radicals and the disruption of mitochondrial function that ultimately destroy the cell[98,103].

III.viii.c. Routes of Ca^{2+} Influx Activated by Cerebral Ischemia

A description of those sources of cytosolic Ca^{2+} influx that are perturbed during cerebral ischemia is as follows:

Na^+ / Ca^{2+} Exchanger

The movement of Ca^{2+} across the neuronal membrane by the Na^+ / Ca^{2+} exchanger is driven by sodium electrochemical gradient. Under normal physiological conditions, the exchanger operates to extrude one Ca^{2+} for every three Na^+ ions transported into the cell. However, during cerebral ischemia in which the Na^+ gradient falls, the exchanger reverses the direction of ion movement by importing rather than exporting Ca^{2+}[99].

Voltage Sensitive Calcium Channels (VSCC)

The sustained neuronal depolarization during cerebral ischemia facilitates the movement of Ca^{2+} from the extracellular space into the cell through voltage-dependent calcium channels. L, T, N and P subtypes of VSCCs exist differing in the kinetics of their activation states[99]. Of these, the L-subtype (long-lasting) has been most extensively studied using specific antagonists from the dihydropyridine family of drugs, including nimodipine[104].

Glutamate Receptors

In addition to the activation of voltage-sensitive calcium channels, the ischemia induced membrane depolarization triggers the unregulated release of neurotransmitters into the synapse. Although both excitatory and inhibitory neurotransmitters are released during the ischemic episode, glutamate has been the most extensively studied in its role in cerebral ischemia.

Glutamate is the major excitatory neurotransmitter of the mammalian central nervous system, and has been implicated in memory, cognition, and motor and sensory perception[105]. Glutamate binds to specific post-synaptic receptors, of which both ionotropic and metabotropic classes exist[106]. Ionotropic glutamate receptors are directly coupled to ion channels, and are subdivided into two types according to their binding affinities to selective exogenous ligands: N-methyl-D-aspartate (NMDA) and alpha-amino-3-hydroxy-5-methyl-4-isoxazolepropionate/kainate (AMPA/kainate). In contrast,

metabotropic receptors mediate their activity via G-protein linked second messenger systems[106].

During cerebral ischemia, excessive neurotransmitter release by neuronal depolarization and the failure of clearance mechanisms result in the sustained accumulation of glutamate in the synapse. This leads to the overstimulation of post-synaptic glutamate receptors and mediates cell death by a phenomenon described as excitoxicity[107,108]. Consequently, increased Ca^{2+} permeability through stimulated glutamate receptors has been implicated in the neurotoxicity of glutamate exposure[103]. The mechanisms by which these receptors contribute to the calcium overload is as follows:

Metabotropic Glutamate Receptors

Three classes of metabotropic glutamate receptors exist encompassing eight different subtypes. Though not directly linked to ion channels, mGluR1 and 5 of Class I metabotropic glutamate receptors trigger a second messenger cascade involving the phospholipase C-mediated hydrolysis of polyphosphoinositides that ultimately liberates Ca^{2+} ions from the internal stores of the endoplasmic reticulum. Moreover, this class facilitates the activation of Ca^{2+}-permeable NMDA receptors[106].

NMDA Receptors

NMDA receptors are coupled to ion channels that are permeable to Na^+, K^+ and Ca^{2+} ions. However, ion permeability is dependent upon receptor activation by specific ligand binding and the removal of the depolarizing blockade of the channel by Mg^{2+}[106]. Calcium influx through NMDA receptors has been shown to mediate glutamate neurotoxicity[109]. An overwhelming body of evidence has demonstrated the neuroprotective efficacy of NMDA receptor antagonists in models of focal ischemia[109-112]. In fact, infarct volumes have been reduced up to 88% over untreated controls following the administration of the noncompetitive NMDA antagonist, MK-801[111,113]. Similarly, CA1 hippocampal loss was ameliorated in early studies testing MK-801 in models of global ischemia[114,115]. However, subsequent studies confirmed that the neuroprotective effects of NMDA antagonists in global ischemia to be attributed to the induction of cerebral hypothermia[116,117]. Interestingly, NMDA-mediated neuroprotection was not observed when brain temperature was regulated.

AMPA Receptors

AMPA receptors are ionotropic glutamate receptors that are readily permeable to Na^+ and K^+ ions facilitating their role as the principle mediators of fast excitatory synaptic transmission in the central nervous system[106]. AMPA receptor antagonists, including NBQX and CNQX, have been extensively studied in their capacity to protect CA1 hippocampal neurons in models of global cerebral ischemia[118,119]. However, in a seemingly reversal of roles with NMDA antagonists, the reduction of infarction volumes

by the blockade of AMPA receptors in focal ischemia has been controversial, and at best, their neuroprotective efficacy to be modest, i.e. <30 %[101,120-125].

It is believed that activated AMPA receptors mediate ischemic damage by the bi-directional movement of Na^+ and K^+ ions through its ionophores that subsequently depolarize the neuronal membrane[106]. As a consequence, Ca^{2+} enters the cell indirectly by the reversal of the Na^+ / Ca^{2+} exchanger, and through the activation of voltage-dependent Ca^{2+} channels and NMDA receptor ion channels whose depolarizing blockade has been removed by the AMPA-mediated membrane depolarization. In fact, Ca^{2+} permeability through AMPA receptors was considered to be negligible. However, recent evidence has shown that Ca^{2+} influx through AMPA receptors to be dependent upon the channel's subunit composition[127,128].

III.viii.d. The GluR2(B) Hypothesis

AMPA receptor ion channels are composed of heteromeric combinations of four subunits termed GluR1, 2, 3 and 4[106]. Inclusion of the GluR2 subunit restricts Ca^{2+} permeability through AMPA receptors due to the presence of a positively-charged arginine residue in the subunit's second transmembrane domain[128,129]. In fact, subpopulations of neurons including cerebellar glial cells[155], hippocampal basket cells, and neocortical nonpyramdial cells[156] possess GluR2-less Ca^{2+} permeable AMPA receptors[130,131].

In a model of transient global ischemia, it was recently observed that the delayed death of CA1 hippocampal neurons was preceded by the selective downregulation of GluR2 mRNA[132-135]. The proposed GluR2 Hypothesis states that this change in gene expression, as triggered by ischemia, will lead to the formation of AMPA receptors lacking the GluR2 subunit. Consequently, in the presence of endogenous glutamate, Ca^{2+} influx through these GluR2-less receptors contributes to or causes ischemic cell death[136,137].

Thesis Objective 1:

To further study the role of the GluR2 subunit in delayed neuronal death, I have proposed to test the relative susceptibility of the GluR2 null mutant mouse to global cerebral ischemia. However, the lack of a reproducible model of murine global ischemia necessitates its development. Therefore, I propose to develop a four-vessel occlusion model of global cerebral ischemia in the mouse. Therefore, by occluding both the vertebral and carotid arteries, I will attempt to produce selective neuronal damage in the CA1 subfield of the mouse hippocampus in a delayed manner.

Thesis Objective 2:

As models of murine focal ischemia have been well-established in the literature, I have proposed to study the response of the GluR2 null mutant mouse in a model of permanent focal ischemia. Hence, I will determine the relative susceptibility of these mutant mice to the filamentous occlusion of the middle cerebral artery, as compared to wild-type controls.

IV. Thesis Objectives and Hypotheses

V. Development of a Mouse Model of Global Cerebral Ischemia

General Objective: To develop a reproducible model of murine global cerebral ischemia.

Specific Objective: To reproduce the four-vessel occlusion rat model of global cerebral ischemia in the mouse.

Hypothesis I: Occlusion of both vertebral and carotid arteries will yield a high percentage (>90%, as with the rat) of delayed neuronal death in the CA1 region of the murine hippocampus.

VI. Response of GluR2 Knockout Mice to Permanent Focal Cerebral Ischemia

General Objective: To elucidate the role of GluR2 subunit in the pathophysiology of focal cerebral ischemia.

Specific Objective: To determine the response of mice lacking the GluR2 gene in a model of permanent focal cerebral ischemia.

Hypothesis I: GluR2 knockout mice will be more susceptible to ischemic injury following 24 hours of permanent filamentous occlusion of the middle cerebral artery, as compared to wild-type control mice.

V. The Development of a Four-Vessel Occlusion Model of Murine Global Cerebral Ischemia

Influence of Strain, Ischemic Duration & Reperfusion Time

V.i. Overview

The complete interruption of cerebral perfusion, as in the case of a cardiac arrest, is termed global cerebral ischemia. Survivors suffer from a range of neurological impairments; the severity of which is dependent upon the length of patient survival, and the duration of circulatory stasis[70-72]. Autopsies performed on the brains of such individuals showed selective tissue damage, suggesting a heterogeneous response of the brain to a global ischemic insult[80]. In particular, the clinical presentation of amnesia in resuscitated patients was associated with lesions specific to the CA1 subfield of the hippocampus[81,82].

Studies using rat and gerbil models of global cerebral ischemia have further characterized the neuropathological profile of hippocampal neuronal death. The CA1 and hilus subfields of the hippocampus were identified as regions of selective neuronal vulnerability, and distinguished from the CA3 and dentate gyrus that were particularly resistant to severe ischemia[73-77]. It was also observed that the death of hippocampal neurons occurred in a delayed manner [52]. In fact, vulnerable CA1 pyramidal neurons remain functionally normal 24 hours after transient forebrain ischemia, degenerating only 2 to 4 days later[79]. Hence, the delay between the onset of ischemia and the ensuing cell

death serves as an intriguing therapeutic window for the development of neuroprotective strategies.

The exact mechanisms by which these cells die are not fully understood. However, recent evidence, including the fragmentation of hippocampal DNA, and neuroprotection by protein synthesis inhibitors in models of global ischemia, has suggested that CA1 hippocampal neurons may die by apoptosis[142-146]. Hence, the recent proliferation of mutant mice, many of which have already been studied in murine models of focal ischemia, provides the opportunity to investigate the role of specific genes in the mechanisms of delayed neuronal death.

However, a reproducible model of murine global ischemia that successfully yields selective, symmetrical and graded CA1 hippocampal injury has yet to be established. Traditionally, the choice of model was dictated by the cerebrovasculature of the rodent. For instance, the Mongolian gerbil, which lacks a complete Circle of Willis, develops severe forebrain ischemia upon bilateral carotid artery occlusion[23]. In contrast, strong collateral circulation renders the rat ischemically resistant to the occlusion of only the carotid arteries. Hence, in order to produce selective neuronal death, a more severe reduction in blood flow can only be achieved by either occluding both vertebral and carotid arteries, known as the "four-vessel occlusion" model, or by bilateral carotid artery occlusion in combination with systemic hypotension[33,83,84]. Murine models of global ischemia produced either by a three-vessel occlusion of both basilar and carotid arteries,

or by the bilateral occlusion of the carotid arteries alone have been unreliable in the consistency and selectivity of hippocampal damage[24,96,140,141].

Thus, we hypothesized that a murine four-vessel occlusion model, in which both carotid and vertebral arteries are occluded, would produce a severe enough ischemia to yield reproducible delayed CA1 neuronal death. Here, we report on the development of the model, and the influences of mouse strain, ischemic duration, and reperfusion time on CA1 hippocampal damage.

V.ii. Objectives

General Objective: To develop a reproducible model of murine global cerebral ischemia.

Specific Objective: To develop a four-vessel occlusion model of global cerebral ischemia in the mouse.

V.iii. Hypotheses

General Hypothesis: Occlusion of both vertebral and carotid arteries will yield a high percentage (>90%, as with the rat) of delayed neuronal death in the CA1 region of the murine hippocampus.

Specific Hypotheses:

i) The degree of CA1 hippocampal damage in the mouse will depend on the duration of the four-vessel occlusion.

ii) The degree of CA1 hippocampal damage will depend on the relative location of the CA1 pyramidal neurons within the hippocampus (i.e. dorsal vs. ventral profiles).

iii) The degree of CA1 hippocampal damage will be enhanced by the tightening of a paravertebral muscle stitch during the four-vessel occlusion.

iv) The degree of CA1 hippocampal damage will depend on the mouse strain and its inherent relative susceptibility to ischemic damage (i.e. CD1, C57BL/6 & SV-129J strains).

v) The degree of CA1 hippocampal damage in the mouse will depend on the duration of the reperfusion period.

V.iv. Materials and Methods

All experiments were performed in strict compliance with guidelines established by the Animal Care Committee of The Toronto Hospital.

V.iv.a. Animal Preparation

Adult male CD1 mice, weighing 25-38g, were anesthetized with 1.5 - 2.0% halothane in 70% N_2O and 30% O_2. Body temperature was monitored by a rectal temperature probe and maintained at 37 °C +/- 0.5 °C using a heating lamp throughout the procedure.

V.iv.b. Four-Vessel Occlusion Model of Murine Global Ischemia

<u>Surgical Procedure for Four-Vessel Occlusion</u>

The surgical procedure for the four-vessel occlusion model in the mouse followed methodology prescribed by Pulsinelli *et al*[84]. A dorsal midline incision of the skin was made posteriorly to the occipital bone and directly overlying the first two cervical vertebrae. The paraspinal muscles were separated from the midline exposing the right and left alar foramina of the first cervical vertebrae. An electrocautery tip was carefully

advanced into each alar foramen, through which the vertebral arteries pass before uniting to form the basilar artery. The vertebral arteries were completely transected by electrocauterization. Surgical bone wax was applied to the space between the two newly formed arterial ends to preserve the permanent occlusion. Deeper penetration of the electrocautery tip into the alar foramina was not attempted, as in the rat version of the model, so as to avoid excessive bleeding and higher rates of mortality. Mice were then allowed to recover from anesthesia following wound closure.

Twenty-four hours later, CD1 mice were re-anesthetized using the same anesthetic regimen, at which time a ventral midline incision was made exposing the common carotid arteries. Following their isolation, anesthesia was shut off, the common carotid arteries were bilaterally occluded by microaneurysm clips, producing the four vessel occlusion model of global ischemia. Anestheisa was shut off immediately prior to the carotid clipping to ensure that only those animals experiencing a loss of consciousness during the occlusion period were included in the study. The clips were removed at the end of the prescribed ischemic duration: 5 min (n= 5); 10 min (n= 5); 15 min (n=3) and restoration of carotid blood flow was verified visually.

Cortical electrical activity was recorded by an EEG, via four needle electrodes inserted under the scalp, for all mice following the clipping of the carotid arteries. Only those animals recording intra-ischemic isoelectric quiescence were included in the study. Animals were also monitored for pupil dilation and the loss of the corneal reflex during the ischemic period.

In all studies, mice subjected to occlusion of only their vertebral arteries served as controls.

Controlling Collateral Circulation

During the development of the well-established rat four-vessel occlusion model of global cerebral ischemia, it was recognized that the reliability of significant CA1 hippocampal damage was dependent on the severity of the ischemic insult. Pulsinelli et al. modified the model by requiring the insertion and tightening of a paravertebral muscle stitch during the ischemic period as a means of controlling collateral circulation derived from arteries in the cervical and paravertebral muscles[91]. Although never described in the context of cerebral ischemia, it may be surmised that the blood supply to these arteries potentially originates from tributaries of the ascending cervical artery, anterior spinal artery and other anastomoses between the carotid / vertebral / subclavian arterial systems that bypass the points of occlusion in the model.

Therefore, the effect of a paravertebral muscle stitch to exacerbate CA1 neuronal damage induced by the four-vessel occlusion was tested in a separate group of male CD1 mice. Following the occlusion of the vertebral arteries, a 3-0 silk suture was inserted through the paravertebral muscles, at the level of the first cervical vertebrae, to form a loop such that it exited the skin on both sides of the ventral incision[90,91]. To control for the contribution of collateral circulation through the neck muscles, the suture was then maintained maximally taut during 5 min (n=8); 10 min (n=3); and 15 min (n=5) of the four-vessel occlusion.

Strain-Related Susceptibility to Four Vessel Occlusion

To explore potential strain-related susceptibility to this model, male C57Bl/6 mice were subjected to 15 min (n=5); 20 min (n=5); and 25 min (n=5) of the four-vessel occlusion with the paravertebral muscle stitch. Male SV-129J mice were subjected to an identical protocol for an ischemic duration of 15 min (n=10).

Effect of Longer Reperfusion Period in C57BL/6 Mice

To determine the effect of a longer reperfusion period on the degree of CA1 hippocampal damage, male C57Bl/6 mice were sacrificed 7 (n=5) and 14 (n=3) days after 20 min of the four-vessel occlusion plus the muscle stitch.

V.iv.c. Histological Analysis of CA1 Hippocampal Neuronal Death

Seven days post-ischemia, challenged animals were re-anesthetized with 2% halothane in 70% N_2O and 30% O_2, and then sacrificed by the transcardiac perfusion of heparinized physiological saline and 4% phosphate-buffered formaldehyde. The brains were harvested from the skull, and subsequently immersed in fresh 4% phosphate-buffered formaldehyde for an additional 24 - 48 hours.

Fixed mouse brains were processed in alcohol and xylene, and subsequently embedded in paraffin. Using a microtome, 6 μm thick coronal slices of brain tissue were cut, and then stained by cresyl violet for histological analysis. This stain recognizes

basophilic cytoplasmic material, including ribosomal RNA, and is a commonly used staining method for this type of neuronal analysis.

CA1 hippocampal damage was assessed by direct visualization using light microscopy (X 400 magnification). In contrast to viable CA1 neurons, dead pyramidal neurons were identified by the appearance of darkly staining neurons with pyknotic nuclei and homogenized cytoplasm, typical of irreversible ischemic cell change. Specifically, CA1 hippocampal damage was evaluated in both the dorsal (Bregma -1.70 & -2.06) and ventral (Bregma -2.70 & -3.16) hippocampus to establish a spatial profile of hippocampal damage for each animal, (Figure 5). The number of dead pyramidal neurons in the whole of the CA1 region of the hippocampus from one 6 μm thick tissue section per hippocampal level for each animal was counted and expressed as a percentage of the total number of CA1 hippocampal neurons [(# of dead neurons / (# of dead neurons + # of viable neurons)) x 100]. The mean percentage neuronal death at each of the four hippocampal levels for all animals within an ischemia group was calculated and compared to the corresponding group means of control animals.

V.iv.d. Statistics

A two-way analysis of variance (ANOVA) was used to calculate significant differences between challenged mice and vertebral artery occlusion controls. Percentage CA1 hippocampal neuronal death, as presented graphically, was converted by an arcsine transformation for statistical analysis by the ANOVA[95, 181]. Factors employed in

statistical calculations for a given study were: Ischemia (VAO-Control, 5 min, 10 min, 15 min) ; Strain (CD1, C57Bl/6) ; Reperfusion Period (7 Days, 14 Days) ; Septotemporal Level (Bregma Coordinates: -1.70, -2.06, -2.70, -3.16). Note: The septotemporal level was one factor in each of the study comparisons, i.e. effects of strain, reperfusion period and ischemia duration with and without a paravertebral muscle stitch, to explore a potential statistically significant difference in the dorsal-ventral profile of CA1 hippocampal neuronal death.

Comparisons between the number of dead CA1 neurons at a given hippocampal level for a given study were performed by the following statistical tests: Ischemia duration (with & without a paravertebral muscle stitch) - one way ANOVA ; Strain - t-test ; Reperfusion - one way ANOVA. Identical analyses were performed for total CA1 hippocampal neurons at each of the prescribed septotemporal levels. Statistical analysis tables are reported in Appendix C.

Data were expressed as mean +/- SD. Results were considered statistically significant for $p < 0.05$.

V.v. Results

Intraischemic EEG Recording

Flat EEG tracings were recorded for all CD1 and C57Bl/6 mice tested in the model, (Figure 7a). SV-129J mice were excluded from the study as isoelectric silence was recorded in only 3 of 10 SV-129J mice during the four-vessel occlusion.

Effect of Strain, Ischemic Duration & Reperfusion Period on CA1 Hippocampal Damage

In this study, there were no differences observed in the degree of CA1 neuronal death in CD1 mice subjected to the four-vessel occlusion, regardless of ischemic durations of 5- (n=5); 10- (n=5); and 15-min (n=3), when compared to control animals. The extent of CA1 hippocampal damage, as determined histologically, was approximately 3% for all test groups (Table Ii). Consequently, a dorsal-ventral gradient of neuronal death within the hippocampus could not be established. The tightening of the paravertebral muscle stitch during the four-vessel occlusion did not enhance CA1 hippocampal damage following 5- (n=8); 10- (n=3) and 15-min (n=5) of ischemia, when compared to controls, (Figure 2). CD1 and C57Bl/6 mice did not differ in their susceptibility to ischemia following either 15-min or 20-min of four-vessel occlusion, (Figure 3; Table Iii). Increasing the reperfusion period from 7 (n=5) to 14 days (n=3) did not significantly increase the percentage of neuronal loss within the CA1 hippocampus of C57Bl/6 mice subjected to 20-min ischemia, (Figure 4; Table I.iii).

All C57Bl/6 mice, (n=5), challenged for 25-min in the four-vessel model subsequently died within 72 hrs of reperfusion. Hippocampal injury in SV-129J mice

could not be evaluated as all animals meeting ischemic criteria, i.e. a flat EEG recording, died either intra-ischemically (n=2) or early within the reperfusion period (n=1).

Histological photographs of the CA1 hippocampus in CD1 and C57Bl/6 mice for their respective ischemic durations and reperfusion periods are presented in Figure 6.

V.vii. Conclusions

The findings of the present study demonstrate that the occlusion of both carotid and vertebral arteries to be inadequate in reliably producing selective delayed neuronal death in the CA1 region of the mouse hippocampus.

VI. Response of GluR2 Knockout Mice in a Model of Permanent Focal Cerebral Ischemia

VI.i. Overview

Focal cerebral ischemia refers to a reduction of blood flow to a localized region of the brain resulting from the occlusion of a cerebral artery[166]. In animal models of focal ischemia, the occlusion of the middle cerebral artery produces a lesion similar to that observed in clinical cases of thrombotic or embolic stroke[25]. Following the occlusion, the ensuing drop in blood flow is most severe in that tissue completely dependent upon the occluded artery. In contrast, surrounding this core is a region of tissue, termed the penumbra, in which the severity of the ischemia is lessened due to collateral circulation[68,69]. As a result, penumbral tissue is temporarily rescued from the rapid infarction experienced in the ischemic focus[67]. Preventing the delayed recruitment of penumbral tissue into the evolving lesion is critical in reducing focal ischemic injury. However, the mechanisms by which viable, yet functionally compromised, penumbral neurons die are still unclear.

It has been well-established that focal cerebral ischemia results in the excessive release of the excitatory neurotransmitter glutamate. The ensuing overactivation of glutamatergic receptor-linked ion channels leads to a rise in the intracellular concentration of Ca^{2+} ions[97,107,167]. The resulting Ca^{2+} overload triggers a catabolic sequence of biochemical reactions initiated by endonucleases, phospholipases, proteases, and free radicals that eventually lead to the demise of the cell[98,103].

Ionotropic glutamate receptors are categorized into N-methyl-D-aspartate (NMDA), and alpha-amino-3-hydroxy-5-methyl-4-isoxazoleproprionate (AMPA)/kainate receptor classes. Both types are coupled to ion channels that upon receptor activation are Na^+ and K^+ ion permeable[106]. However, they are distinct in that NMDA receptors are readily permeable to Ca^{2+} ions, and this provides a plausible mechanism underlying the neuroprotective benefits of its receptor antagonism in models of focal ischemia[102]. However, despite the reduction in ischemic damage by such AMPA receptor antagonists as NBQX, YM872 and YM890, the exact mechanisms by which these quinoxalinediones confer neuroprotection in models of focal ischemia remain unclear[101,120-125].

AMPA receptors are the principle mediators of fast excitatory synaptic transmission in the central nervous system[106]. Therefore, by reducing membrane excitability induced by ischemia, it has been hypothesized that AMPA receptor antagonists reduce the Ca^{2+} influx through NMDA receptors and voltage-sensitive calcium channels[34,123]. The activity of these ion channels is regulated by membrane depolarization. Interestingly, calcium influx through AMPA receptors was initially considered negligible. However, subpopulations of neurons and glia, including cerebellar glial cells[168], hippocampal basket cells, and neocortical nonpyramdial cells[129], have calcium permeable AMPA receptors. It is now known that the regulation of Ca^{2+}-permeability through these channels is dictated by the receptor's subunit composition[127,130].

AMPA receptors are composed of heteromeric combinations of four subunits denoted GluR1, 2, 3 and 4[106]. Inclusion of the GluR2 subunit renders these channels Ca^{2+}-impermeable as a result of electrostatic repulsion by a positively-charged amino acid, arginine (R), in its second transmembrane domain[106,128,129]. In contrast, subunits GluR1, 3 and 4 possess a negatively-charged amino acid, glutamine (Q) in this same position. GluR2 is highly expressed in AMPA receptors located in the principal neurons of both cerebral hemispheres[106,169].

Therefore, it is possible that Ca^{2+} permeability through AMPA receptors lacking the GluR2 subunit may be linked to neurotoxic damage resulting from cerebral ischemia. In fact, studies have shown that the death of CA1 pyramidal neurons in the rat and gerbil hippocampus to be preceded by the selective down-regulation of GluR2 mRNA following transient forebrain ischemia[132-135]. Enhanced Ca^{2+} permeability in these neurons was observed at time points subsequent to the reduced GluR2 expression. The GluR2 Hypothesis states that the down-regulation of GluR2 mRNA may lead to the formation of AMPA receptors lacking this subunit. Consequently, the augmented Ca^{2+} influx through these channels would then increase cellular susceptibility to ischemic death via Ca^{2+}-dependent mechanisms[136,137].

Mutant mice lacking the gene encoding the GluR2 subunit were recently constructed. These GluR2 knockout mice (GluR2(-/-)) possess a relatively normal nervous system, yet exhibit a 9-fold increase in relative hippocampal Ca^{2+}-permeability

following kainate application[131]. This further emphasizes the regulatory role of the GluR2 subunit in gating Ca^{2+} entry through AMPA receptors.

Neuroprotection by Ca^{2+} chelators, calcium channel blockers and glutamate receptor antagonists have underscored the importance of preserving Ca^{2+} homeostasis following the induction of focal cerebral ischemia. Evidence now suggests that Ca^{2+} permeability through AMPA receptors lacking GluR2 may also contribute to an intracellular calcium overload[136,137]. At the present time, a GluR2 subunit specific antagonist does not exist. Therefore, to investigate the potential role of GluR2 in focal cerebral ischemia, we tested the response of GluR2 knockout mice to 24 hours of permanent middle cerebral artery occlusion (MCAO).

VI.ii. Objective

General Objective: To elucidate the role of GluR2 subunit in the pathophysiology of focal cerebral ischemia.

Specific Objective: To determine the response of mice lacking the GluR2 gene in a permanent model of focal cerebral ischemia.

VI.iii. Hypotheses

General Hypothesis: GluR2 knockout mice will be more susceptible to ischemic injury following 24 hours of permanent filamentous occlusion of the middle cerebral artery, as compared to wild-type control mice.

Specific Hypotheses:

i) GluR2 knockout mice will sustain larger infarction volumes 24 hours post-middle cerebral artery occlusion, than wild-type control mice.

ii) GluR2 knockout mice will display more exacerbated neurobehavioural deficits assessed 24 hours post-middle cerebral artery occlusion, than wild-type control mice.

VI.iv. Methods and Materials

VI.iv.a. GluR2 Knockout Mice

All experiments were performed in strict compliance with guidelines established by the Animal Care Committee of the Mount Sinai Hospital. Mice were housed under diurnal lighting conditions and allowed free access to food and water ad libitum.

Vi.iv.b. Polymerase Chain Reaction (PCR) Assay for GluR2 Genotyping

GluR2 null mutant mice (GluR2 (-/-)), a generous donation from Dr. J.C. Roder, were constructed on a CD1 x SV129J background according to the methodology described in detail by Jia *et al*[131]. The identification of knockout mice was accomplished by a polymerase chain reaction (PCR) assay for GluR2 genotyping. In brief, pure genomic DNA was extracted from the tails of heterozygote breeding pair progeny, and then subjected to two PCR reactions. In Reaction #1, the primers CAGCAGATTTAGCCCCTACG and CCTCACAAACACACCATTTCC were added to the DNA for the detection of the wild-type GluR2 allele (623 bp band). In Reaction #2, the primers, CCTCACAAACACACCATTTCC and GGATGATCTGGACGAAGAGC, were added to the DNA to detect the PKG*neo* cassette (1022 bp band) that replaced the transmembrane region TM1 and the pore loop of exon 11 deleted in the targetted construction of the GluR2 mutant mice. DNA from wild-type mice were positive for only Reaction #1, mutants only for Reaction #2 and heterozygotes for both. Following

their identification, male mice were grouped in cages according to their respective genotypes.

VI.iv.c. Model of Permanent Focal Cerebral Ischemia

Adult wild-type (CD1xSV129J) and GluR2 knockout mice, weighing 25-38g, were anesthetized with 1.5 - 2.0% halothane in 70% N_2O and 30% O_2. Body temperature was monitored by a rectal temperature probe and maintained at 37 +/- 0.5°C using a heating lamp throughout the studies.

Occlusion of the middle cerebral artery (MCAO) was achieved using the intraluminal filament technique with minor modifications[48,53,170]. Following a ventral midline incision, the common, internal and external carotid arteries were exposed by blunt dissection. The common and external carotid arteries were loosely ligated by 6-0 silk braided suture and then retracted to retard blood flow. A silicone-coated 6-0 monofilament suture (Prolene) was then inserted through the arteriotomized external carotid artery and then advanced through the internal carotid artery a distance of 10 +/- 0.5 mm to occlude the MCA. The filament was then permanently ligated to the external carotid artery by 6-0 braided silk suture. To avoid potential backbleeding, the external carotid artery was then cauterized and subsequently cut, (Figure 8).

VI.iv.d. Measurement of Regional Cerebral Blood Flow

The filamentous occlusion of the middle cerebral artery was confirmed by laser Doppler flowmetry (Perimed, Stockholm. Local cerebral blood flow recorded pre- and 5- & 15-min post MCAO from a point representative of the ischemic core at 2 mm posterior to bregma and 6 mm lateral to midline on the temporal-parietal bone of the ipsilateral hemisphere. Occlusions were considered successful if regional blood flow values fell to less than 20% of baseline recordings.

VI.iv.e. Quantification of Infarction Volume

Twenty-four hours post-MCAO, mice were re-anesthetized with 2% halothane in 70% N_2O and 30% O_2 and exsanguinated by trans-cardiac perfusion with heparinized saline. Fixation was achieved by the infusion of 10% formalin in saline at a perfusion pressure of 90 mmHg. The brains were removed and subsequently immersed in formalin solution for an additional 24 - 48 hours. Each brain was sliced into 2mm thick coronal slices using the mouse Brain Matrix. Each section was then processed, cut at a thickness of 6 *u*m, and then stained with hematoxylin & eosin stain for histological analysis. Histologically, by twenty-four hours of permanent focal ischemia, the region of infarction, characterized by pannecrosis and neuropil swelling, is clearly delineated from non-ischemic tissue, (Figure 9b). The infarction area of each brain slice was quantified using an image analysis system (MCID) and then integrated to determine the overall infarction volume for each mouse brain. The quantification of the ischemic lesion was

accomplished using the Frustrum Summation method which is described in detail in Appendix D.

VI.iv.f. Assessment of Neurological Deficits

Wild-type and GluR2 knockout mice were evaluated for their motor impairments 24 hours after MCAO using a four-point neurological deficit scoring system[39,171]. Specific behavioural tendencies were assigned the following test scores: 0 - absence of any observable motor impairment; 1 - inability to extend right forepaw; 2 - circling behaviour; 3 - loss of righting reflex; 4 - no spontaneous movement.

VI.iv.g. Statistics

Statistical comparisons in infarction volumes and blood flow measurements between wild-type and GluR2 mutant mice were made using a Student's t test. Neurobehavioural deficit scores were compared with an ANOVA followed by a Mann-Whitney U-test. Data were expressed as mean +/- SD. Results were considered statistically significant for $p < 0.05$.

VI.v. Results

Wild-type and GluR2 knockout mice did not differ in their susceptibility to permanent MCAO, (Figure 10). Infarction volumes for wild-type (n=7) and knockout mice (n=8) were calculated to be 67.82 +/- 19.10 mm^3 and 69.32 +/- 15.64 mm^3, respectively, (Table Iiii.). Histological analysis by hematoxylin and eosin (H & E) staining revealed pannecrosis within the infarction area characterized by pyknotic (red) nuclei, expansion of the neuropil and a generalized pallor of the ischemic tissue, (Figure 9b).

Laser Doppler recordings of residual cerebral blood flow, i.e. the percentage of rCBF following the MCAO compared to a 100% baseline pre-MCAO in wild-type mice (5-min post: 6.59 +/- 1.81%; 15-min post-MCAO: 5.80 +/- 1.77%) was also not statistically different from mutant animals (5-min post: 5.04 +/- 1.29%; 15-min post-MCAO: 4.64 +/- 0.91%), (Table Iii).

Accordingly, neurobehavioural deficit scores did not differ between groups, as all animals were assigned moderate (circling behaviour) to severe (lack of spontaneous movement) scores (wild-type: 2.86 +/- 4.04; mutant: 3.00 +/- 4.23), (Table Iiiii).

VI.vii. Conclusions

The results of this study demonstrate that mice with a null mutation in the GluR2 gene locus are not more susceptible to ischemic injury when tested in a model of permanent focal cerebral ischemia.

VII. Discussions & Future Directions

VII.i. The Development of a Four-Vessel Occlusion Model of Murine Global Cerebral Ischemia

In this study, CD1 and C57Bl/6 mice did not differ in the degree of CA1 hippocampal damage following the occlusion of both vertebral and common carotid arteries, regardless of the ischemic duration or reperfusion time, when compared to controls. SV-129J mice could not be evaluated histologically. These results suggest that the four-vessel occlusion model, though well-established in the rat, to be inadequate in reliably producing murine global cerebral ischemia.

The four-vessel occlusion model when performed in the rat produces a condition of incomplete hemispherical ischemia, sufficiently severe to induce the delayed death of more than 90% of CA1 pyramidal neurons[62,78,84,91,95,147]. Similar degrees of cell death are observed in the hippocampus of rats subjected to a two-vessel occlusion combined with hypotension, and in the gerbil model of transient forebrain ischemia due to bilateral carotid artery occlusion[33,74-77,85]. Why, then, did the technique of occluding both common carotid and vertebral arteries in the mouse not yield the hypothesized measure of CA1 hippocampal damage? Ironically, the answer to this question may require the understanding of those mechanisms underlying selective and delayed neuronal death, for which the model was originally intended to elucidate.

Of importance to this investigation, is the determination of the precise reduction of cerebral blood flow in the mouse forebrain produced by the four-vessel occlusion. In this study, pupil dilation, the losses of both the corneal reflex and apparent consciousness, and electrogencephalographic (EEG) quiescence were used as indicators of cerebral ischemia, according to previously defined ischemic criteria[84]. The EEG is a recording of cerebral electrical activity, and thus, very sensitive to changes in cerebral blood flow[89]. The abolishment of this activity by conditions of severe metabolic dysfunction, as potentially induced by ischemia, are recorded by the EEG as a flat line. Only those animals for which such tracings were made during the four vessel occlusion were included in this study. Interestingly, isoelectric silence was recorded for all CD1 and C57Bl/6 mice tested in this model, despite the lack of significant CA1 hippocampal damage. In this regard, a potential threshold phenomenon may have been exposed that is unique to the mouse. One might surmise that the degree of blood flow reduction between the thresholds for synaptic failure and ischemia to be wider in the mouse than those in the rat and gerbil. Thus, the failure of the EEG to predict the hypothesized ischemic outcome necessitates the implementation of more precise methods of blood flow quantification for model validation.

Historically, three different methods have been routinely employed to measure cerebral blood flow changes in models of ischemia: autoradiography using radioactive traces, hydrogen clearance and laser Doppler flowmetry [52,61,148]. Pulsinelli *et al.* measured a reduction of blood flow of approximately 3% or less of control values in the forebrain of rats subjected to the four-vessel occlusion using ^{14}C-iodoantipyrine[92,149]. When

measured by hydrogen clearance, the residual forebrain blood flow was about 6% of control values[62,147]. Similarly, residual flow in the rat cortex was measured by laser Doppler flowmetry to be on average 12% of baseline recordings in the four-vessel model[150].

Cerebral blood flow in mouse models of bilateral occlusion of the carotid arteries have revealed decreases in blood flow to be about 20% of control values when measured by laser Doppler flowmetry and autoradiography[96]. In a three-vessel occlusion model of murine global ischemia (i.e. basilar + both common carotid arteries), blood flow decreased to less than 10% of baseline[24]. Interestingly, this is the only published mouse model that has achieved a decrease in cerebral blood flow that approaches that of the Pulsinelli model. Therefore, it would be interesting to measure blood flow changes in the four-vessel occlusion model of this study. Although the method of hydrogen clearance allows for the polarographic measurement of blood flow, the requirement of electrode insertion into cerebral tissue, and its relative inaccuracy in severely ischemic tissue render it potentially less favourable in addressing this question[61,87,92]. Rather, future studies employing laser Doppler flowmetry and autoradiography should permit the accurate determination of cerebral blood flow changes in our model of murine global ischemia.

Quantification of this parameter might facilitate in the explanation of the results observed in this investigation. In a preliminary study, EEG tracings made during bilateral carotid artery occlusion in CD1 and C57Bl/6 mice were recorded as flat. Thus,

in the four vessel occlusion model, two possible scenarios exist. In both, blood flow reduction during the occlusion period is sufficiently severe to paralyze synaptic function resulting in electroencephalographic quiescence. However, they may differ in that in one, although the synaptic threshold is surpassed, the decrease in blood flow during the four vessel occlusion does not reach levels of ischemia. In the second, the reduction exceeds the threshold for ischemia, and the cerebral tissue, though ischemic, is either protected or physiologically resistant to damage.

The following is an attempt to explain the failure of the four vessel occlusion model of murine global cerebral ischemia to produce significant neuronal death in the CA1 region of the mouse hippocampus.

Scenario 1: Cerebral Blood Flow Above Ischemia Threshold

Incomplete occlusion of either the carotid or vertebral arteries could account for the potential lack of ischemic severity. However, successful occlusions were visually confirmed for both sets of arteries in all animals tested in the model. It is more likely that blood flow through the anterior spinal artery and vessels through the paravertebral and cervical muscles contributed to the posterior circulation of the Circle of Willis[91].

Measurement of blood flow during the rat four-vessel occlusion have clearly demonstrated milder degrees of ischemia in the caudal structures of the rat forebrain,[33,87,95] potentially accounting for the documented dorsal-ventral gradient of

ischemic damage in CA1 pyramidal neurons[88]. In this study, the degree of CA1 hippocampal damage was quantified at the prescribed four septo-temporal levels (Bregma: -1.70; -2.06; -2.70; -3.16), in an attempt to characterize a corresponding spatial profile in the mouse. Differences in neuronal death along such a gradient was nonexistent in the mouse model. Moreover, Pulsinelli *et al.* introduced the muscle ligation, a technique employed in this study, to control for the collateral circulation arising from the paravertebral and cervical muscles[90,91]. However, the hypothesized increase in ischemic severity by the muscle stitch did not significantly enhance CA1 hippocampal damage. To assess residual cerebral blood in the modified four-vessel model, latex was perfused transcardiacally in a series of post-mortem CD1 mice (n=3). Despite the combination of both the muscle stitch and the complete transection of the vertebral and carotid arteries, latex originating from the anterior spinal artery was observed filling the Circle of Willis through the vertebro-basilar system, (Figure 7b).

A potential drawback to this study is the lack of data concerning the arterial levels of CO_2 and pH during the four-vessel occlusion. Arterial blood samples were not taken from challenged mice owing to their small blood volumes, and to avoid the technical difficulties associated with the cannulation of the femoral artery. However, both parameters are intimately coupled in their regulation of cerebral blood flow[13,14]. Increasing levels of P_aCO_2 and blood acidity produce vasodilation, resulting in an increase in total cerebral blood flow . In contrast, vasoconstriction is induced by arterial conditions of alkalinity and low P_aCO_2. In fact, lowered levels of P_aCO_2 are indicative of hyperventilation, which is known to aid in the restoration of autoregulation through the

reduction of cerebral blood volume by vasoconstriction and increased intracranial pressure[82,151]. Published values for P_aCO_2 for CD1, C57Bl/6 and SV 129J mice were reported to be about 39, 47, and 42 mmHg, respectively during bilateral carotid artery occlusion[96,141]. Thus, the detection of disparate levels of both P_aCO_2 during the four-vessel occlusion could prompt the necessary correction required to ensure consistent ischemic severity.

If the degree of ischemia sustained during the four vessel occlusion does not approach accepted values of blood reduction in similar rat models, alternative procedures to induce murine global ischemia may have to be pursued. Historically, additional rat models emerged as measures were taken to enhance the severity and the uniformity of forebrain ischemia. For instance, in an attempt to better control collateral blood flow derived from the anterior spinal artery flowing through vessels distal to the points of vertebral and carotid artery occlusion, Kameyama *et al.* developed a three-vessel occlusion model (basilar + 2 common carotid arteries) of global ischemia[79]. Shirane *et al.* developed a seven-vessel occlusion model (basilar + 2 pterygopalatine +2 external carotid + 2 common carotid arteries) to further increase the reduction of cerebral blood flow[93]. Although a near complete cessation of cerebral blood has been demonstrated in both models, their extensive use has been limited. The same may be said of other global-ischemia producing strategies which have included decapitation, the use of a neck tourniquet, elevating the cerebrospinal fluid pressure and cardiac arrest by the pharmcological induction of asphyxiation [23,94]. However, the limitation of such models by high mortality rates, complexity of technique, and their lack of conduciveness to long

term recovery and selective neuronal vulnerability, hinders their application to murine global cerebral ischemia.

Then, what alternative strategies may be employed to reproducibly yield delayed neuronal death in the CA1 region of the mouse hippocampus? In rat and gerbil models of global ischemia, blood flow changes during reperfusion are characterized by a sequence of initial hyperemia followed by a period of delayed and prolonged hypoperfusion[86,152]. Studies have shown that a series of nonlethal cerebral ischemic insults repeated at one hour intervals, produces extensive neuronal damage, possibly by increasing ischemic severity by cumulative degrees of hypoperfusion[153]. Thus, a similar approach may be applied to our murine four-vessel model of global cerebral ischemia.

As previously mentioned, neuronal viability and function is dependent upon the sensitive balance between the circulatory supply of nutrients and the metabolic demands of the cerebral tissue. It is possible that a model may be derived from the perturbation of those factors that dictate cerebral blood flow: intracranial pressure, cerebral perfusion pressure, blood viscosity, arterial blood gases, and the diameter and distribution of collateral channels[14]. Additional strategies have included compromising the oxygen carrying capacity of hemoglobin by exposing mice to carbon monoxide, hypobaric or normobaric hypoxia and injections of KCN[92,154,155]. Moreover, conditions that perturb the delicate energy balance of cerebral tissue, such as hyperglycemia and the elevation of the cerebral metabolic rate of oxygen consumption ($CMRO_2$) during times of arterial

occlusion, remain potential strategies for inducing hippocampal damage in murine models of global ischemia.

However, by further modifying the ischemia in order to establish a murine model, its relevance to stroke lessens as does the clinical application of successful neuroprotective strategies derived therein.

Scenario 2: Cerebral Blood Flow Below Ischemia Threshold

In the event that the reduction of blood flow during the four-vessel occlusion is as severe as per the rat, the lack of delayed CA1 neuronal death in the mouse hippocampus may most effectively be explained by the neuroprotective effects of hypothermia. Although the rectal temperature of all mice was monitored and maintained at normothermic ranges of 37.5 +/- 0.5 °C throughout all surgical procedures, intracranial temperature was never measured. Studies have clearly demonstrated that during ischemia of 5 to 20 minutes of duration, brain temperature, if not controlled, may fall 2 to 4 °C[29,156]. This reduction in temperature has been shown to completely prevent the neuronal death in selectively vulnerable regions of both the rat and gerbil hippocampus [92,93]. In fact, hippocampal neuronal death was not observed in any mice subjected to temperatures of 31 to 33 °C during 20 min of bilateral carotid artery occlusion[157]. Prolonged hypothermia initiated 1 to 2 hours post-ischemia was effective in reducing CA1 loss in both gerbils and rats[14,158,159]. Therefore, the continuous monitoring of intra- and post-ischemic brain temperature will be required to determine whether mice

subjected to the four-vessel occlusion benefited from hypothermia. Thus, implantation of brain temperature probes would facilitate data collection during both the occlusion and the critical phase of early reperfusion when the animals are awake and freely-moving.

It is worth repeating that although regions of selective vulnerability succumb to delayed neuronal death following global cerebral ischemia, the precise mechanism by which this occurs remains unknown. However, the pathogenesis of ischemia is known to evolve more rapidly with increasing degrees of the ischemic insult, described as the "maturation phenomenon" [73-76]. Studies in the rat four-vessel model have yielded >90% CA1 neuronal loss 7 days after ischemia [95]. The duration of post-ischemia reperfusion time required for the initiation of delayed neuronal death has yet to be fully established in the mouse. For this reason, we assessed CA1 hippocampal damage at 7 and 14 days following the four-vessel occlusion. Our study found that C57Bl/6 mice, considered the most susceptible to ischemic injury,[96,157] failed to produce significant neuronal loss in the CA1 region of the hippocampus either 7 or 14 days following 20 min of four-vessel occlusion. Thus, in light of the "maturation phenomenon", even though highly unlikely, studies with reperfusion times in excess of 14 days may be required to yield the hypothesized ischemic outcome in the mouse hippocampus.

In addition, a less likely yet possible, explanation for this study's findings may be attributed to the induction of ischemic tolerance following the initial vertebral artery occlusion. A 2 min sublethal ischemic insult followed by 1 to 7 days of reperfusion has been shown to protect vulnerable neurons to subsequent periods of ischemia[160,161].

Whether a period of "ischemia" necessary for tolerance induction was initiated following the occlusion of the vertebral arteries has yet to be determined.

Another possibility is the induction of heat shock protein 70 (HSP70) expression following the first stage of the surgical preparation of the mouse four-vessel occlusion model. In general, heat shock proteins are responsible for maintaining the tertiary structure of normal or partially denatured proteins. There is evidence to suggest that HSP70 is selectively induced in hippocampal neurons made tolerant to ischemia by an initial exposure to hyperthermia[162]. It is possible that elevated brain temperatures resulting from the electrocauterization of the vertebral arteries may have increased levels of HSP70, and thereby inducing ischemic tolerance. This hypothesis may be tested by probing the hippocampus of mice subjected to electrocautery of the vertebral arteries with an antibody specific for HSP70.

Contextual Significance

Previous studies attempting to develop mouse versions of either the four-vessel occlusion or two-vessel occlusion in combination with controlled systemic hypotension were hindered by excessive animal mortality[24,96,140]. Accordingly, current strategies to produce mouse global ischemia exploit potential strain-related susceptibilities to ischemia, owing to differences in the completeness of their Circle of Willis, in models of bilateral carotid artery occlusion[96,140,157]. Interestingly, by successfully occluding both vertebral and carotid arteries in the mouse, our study is the first to explore the ischemic

response of mouse hippocampal neurons, independent of the degree of anastamoses between the anterior and posterior circulation of the forebrain.

Nevertheless, how do we reconcile the apparent discrepancy between the results of this investigation and those in which mouse ischemia produced by the occlusion of only the carotid arteries yields CA1 hippocampal damage? To address this issue, one must realize that the reliability of any model is dependent on the statistical validity of its quantitative data. The significant increases in the loss of CA1 pyramidal neurons following bilateral carotid occlusion that have been published have only been detected by qualitative assessments of mouse hippocampal damage[96,141,163,164]. The use of scores, defined by ranges of cell death, to qualitatively evaluate hippocampal damage eliminates the variability that would normally preclude statistical significance if the number of ischemic CA1 neurons were actually counted.

In this study, a significant loss of CA1 hippocampal neurons was not observed in CD1 mice following 20-min of ischemia. In stark contrast, Murakami *et al.* reported that 3-min of bilateral carotid artery occlusion under controlled ventilation was sufficient to produce hippocampal damage in the same strain of mouse[141].

The success of the rat version of the four-vessel occlusion model of global ischemia lies in its reproducibility and consistency in yielding > 90% CA1 hippocampal neuronal death following seven days of reperfusion. The near complete loss of this region of the hippocampus provides a stable baseline upon which neuroprotective

strategies may be compared. Therefore, in developing a model of global ischemia in the mouse, both the statistical significance and measure of delayed CA1 hippocampal neuronal death must be taken into account. The present murine four-vessel occlusion model fails to meet both of these criteria.

It has been published that the mortality rate of the four-vessel occlusion is at least 50% in rats, even when performed by the most experienced investigators. A similarly high rate was observed in testing the mouse four-vessel occlusion model owing to the tortuosity of the surgical procedures and the severity of the ischemia[23]. To accommodate for this mortality, a larger number of mice must be challenged in order to obtain statistically significant sample sizes. This presents a dilemna, as mutant mice, for which the model is intended, are generally very expensive to construct and breed. In fairness, the majority of the mortalities were recorded during the first stage of the model during which the vertebral arteries are occluded by electrocautery. Therefore, had the hypothesized ischemic outcome been observed, i.e. >90% CA1 hippocampal neuronal death, the proposal of alternative strategies to permanently occlude the vertebral arteries would have been warranted.

The results of the present investigation failed to demonstrate a strain-dependent susceptibility to ischemia in the four-vessel model. It has been postulated that the reduced patency of the posterior communicating artery is responsible for the increased susceptibility of C57Bl/6 and BALB/c mice to ischemia in models of bilateral carotid artery occlusion[96,140,157]. The occlusion of the vertebral arteries in the four-vessel model,

however, should have effectively eliminated any significant contribution of the posterior circulation to cerebral blood flow. Paradoxically, in contrast to the results of studies of only the two-vessel occlusion, the four-vessel model did not yield significant hippocampal death after 15- and 20-min of ischemia in either CD1 or C57Bl/6 mice.

The maintained spontaneous electrical activity recorded by the EEG in 7 of 10 SV-129J mice during the four-vessel occlusion may be attributed to this strain's enhanced ischemic resistance demonstrated in both models of focal and transient forebrain ischemia[53,96]. The death of SV-129J mice (n=3) registering flat EEG records may likely be attributed to a fatal restriction of blood flow to the respiratory centres in the midbrain.

Even though hippocampal damage has been produced by two-vessel models of mouse ischemia, such studies neglect to report either the selectivity of CA1 death or its temporal profile. The results of such studies may possibly be attributed to widespread necrosis induced by the severity of prolonged durations of bilateral carotid artery occlusion. In fact, Murakami *et al.* reported that hippocampal injury was more delayed following 3-min of bilateral carotid artery occlusion, than when compared to that observed after 10-min[141]. Moreover, the absence of significant hippocampal death in C57Bl/6 mice subjected to 20 min of four-vessel occlusion, and the 100% animal mortality following an additional 5 min insult suggests that a heterogeneous response of murine brain tissue to global ischemia may not exist. It may be possible that the hippocampal physiology of mice may be intrinsically distinct from that of other rodents.

In this study, hippocampal damage was reported as a percentage of dead pyramidal neurons compared to the total number of neurons in the CA1 subfield. Alternative methods to quantify hippocampal neuronal death include ranked scores and measures of neuronal density. In particular, neuronal death using the latter method is expressed as the number of neurons per unit length, e.g. 1 mm, and facilitates the detection of changes in total cell counts resulting from the clearance of dead neurons by scavengers. However, the lack of significant differences in the percentage of hippocampal neuronal death and in the total cell counts (Appendix D) at each of the septotemporal levels (Bregma coordinates: -1.70, -2.06, -2.70, -3.16) suggest that such additional measures to control for counting variability may not be warranted.

Dead pyramidal neurons were identified by light microscopy using cresyl violet staining according to the appearance of darkly staining neurons with pyknotic nuclei. It is widely believed that delayed hippocampal neuronal death produced by global cerebral ischemia is mediated by apoptosis[142]. Although the morphological features of nuclear and cytoplasmic shrinking, chromatin condensation and plasma membrane blebbing typical of apoptosis sharply contrasts the cell swelling, karyorrhexis and cytoplasmic hypereosinophilia of necrosis[29], the histological analysis employed in this study cannot reliably distinguish between them. Moreover, it is also difficult to determine whether pyknotic nuclei, as presented by cresyl violet staining, truly reflect dead neurons, or rather, viable non-neuronal cells. For instance, microglia are known to invade the CA1 pyramidal layer following an ischemic insult[142]. Consequently, their mis-identification as

dead neurons would result in an overestimation of neuronal cell death. Thus, the use of cell-type specific markers, e.g. NeuN for neurons and GFAP for astroglia, in combination with TUNEL staining would detect nuclear changes, such as DNA fragmentation, in CA1 pyramidal neurons undergoing programmed cell death.

Therefore, is a murine model of global cerebral ischemia possible? The answer is a resounding - maybe. Again, the regulation of brain temperature and the measurement of blood flow changes during the four-vessel occlusion are of critical importance to this issue.

Historically, the development and validation of standard models of cerebral ischemia were tested in a variety of animal species and strains. It was apparent that the animals were chosen to fit the model. Ironically, with the introduction of genetically engineered mice, the situation has been reversed. Now investigators have the daunting task of developing models that are amenable to the mouse. Success has been achieved in establishing reproducible murine models of focal cerebral ischemia. Unfortunately, the results of this investigation may now be added to a list of failed studies attempting to produce a reliable model of mouse global cerebral ischemia.

However, there is room for optimism. A recent study of global ischemia published in the Journal of Neuroscience investigated the effects of the overexpression of a superoxide dismutase in a transgenic "rat" using Pulsinelli's four-vessel occlusion

model[165]. Thus, if geneticists lean towards mutant rats, the roles of specific genes in stroke pathophysiology may be further elucidated in already established models of global cerebral ischemia.

VII.ii. A New Direction

It should be noted that such efforts were invested in the development of this model for the purpose of studying the response of the GluR2 null mutant mouse to global cerebral ischemia. Without a reproducible model of delayed neuronal death, however, it is not possible to test the GluR2 Hypothesis using this mutant mouse, or any other. Rather than improving upon the methodological aspects of this model, as described in the Discussions, or exploring a potential species-dependent resistance to global ischemia, i.e. rat vs. mouse, it was decided that it was necessary to take advantage of the availability of the GluR2 null mutant mouse. For this reason, the GluR2 knockout mouse was tested in a model of permanent focal cerebral ischemia. In contrast to murine global ischemia, this model has been well-described and established in the literature.

VII.iii. Response of GluR2 Knockout Mice in a Model of Permanent Focal Cerebral Ischemia

Description & Validity of the Model

Prior to testing valuable mutant mice to a middle cerebral artery occlusion, it was necessary to reproduce and validate an established model of permanent focal cerebral ischemia. In so doing, the intraluminal occlusion model of focal ischemia was chosen on account of its minimal invasiveness, and its preservation of intracranial pressure, blood brain barrier permeability and intracerebral temperature. In addition, the absence of the mechanical and thermal trauma associated with the more well-established rat models of focal ischemia is a great advantage to the intraluminal model.

The success of this model lies in the careful preparation and selection of the occluding filament[47,139]. The suture must fit the lumen of the carotid arteries, be pliable to facilitate its advancement through the vasculature, and thin enough to traverse through the carotid foramen at the base of the skull. However, this filament must also possess the thickness to completely occlude the origin of the middle cerebral artery, yet be flexible enough to prevent the accidental perforation of its sheathing artery. To this end, a number of methodology papers have been published emphasizing the appropriate matching of the filament calibre to the body weight of the murine subject[47,48,50,139]. We tested the occlusion success of different suture types and sizes and found that for mice weighing 25-40g (CD1 strain; n=17), a 6-0 monofilament suture, though inadequate in yielding infarctions, did not perforate the middle cerebral artery as did those sutures of greater thickness. By convention, the filament is modified at its tip with a coating of

biocompatible dental silicone which provides the necessary augmentation to the filament calibre without comprising its flexibility.

Although the use of an intraluminal filament presents the opportunity to study reperfusion injury by the reversibility of the occlusion, we decided to establish a model of permanent focal cerebral ischemia. In this model, the mouse would be sacrificed 24 hours following the filamentous occlusion of its middle cerebral artery as a means of controlling the size and distribution of the ischemic lesion. Thus, by reducing infarct variability, a stable baseline may be created against which the changes in infarction volume ascribed to potential therapeutic strategies may be measured and compared. Studies have demonstrated that this model yields near maximally evolved infarctions, with the least variability, 24 hours following the onset of ischemia[28,65].

Therefore, a pilot study was conducted to establish a model of permanent focal ischemia by the intraluminal occlusion of the middle cerebral artery. To validate the model, male CD1 mice were subjected to similar experimental conditions and protocols as described in the Methods and Materials section (VI.iv.). This particular strain of mouse was tested since the GluR2 null mutants were generated on a CD1 background[131].

Cerebral infarction, as detected by 2% TTC staining, was produced in 16 of 21 (76.2%) male CD1 mice, 24 hours following the permanent filamentous occlusion of the middle cerebral artery, (Figure 9a). Ischemic damage, although distributed throughout the ischemic hemisphere, was most severe in the antero-temporal region of the brain, and

reproducibly encompassed both cortical and striatal tissue. Intuitively, the distribution of tissue injury reflected the described vascular territory of the middle cerebral artery. Edematous swelling of cerebral tissue was apparent in each of the ischemic hemispheres. However, it should be noted that the described method of infarct volume quantification does not include a correction for edema.

Of the total 25 mice tested in the model, 4 did not survive the 24 hour ischemic time period (16% mortality rate.) The mean infarction volume and standard deviation in those mice that survived was 69.33 +/- 14.36 mm^3.

Variability in the infarction volume following the middle cerebral artery occlusion is typical in models of focal ischemia. However, the limits of this statistical variation is dependent upon the measure of control over those experimental parameters known to influence the lesion size. In this pilot study, core rectal temperature was controlled between 37 +/- 0.5°C during all operative procedures. The variability may also be attributed to differences in animal physiology as described by arterial blood gases, pH and arterial blood pressure. Due to technical limitations, i.e. lack of appropriate physiological monitoring devices, such parameters could not be measured. Nevertheless, a 20.7% (14.36 / 69.33) variability in the infarction volumes may be considered scientifically acceptable since it lies within the statistical range published in studies in which ischemically-challenged mice were monitored for the said parameters[48,53,171,172].

An additional source of variability lies with the efficacy of the MCA occlusion. Despite the advancement of the filament over a length of 10+/- 0.5mm, the surgeon is blind to the actual occlusion of the middle cerebral artery. Therefore, a suture that is too thin may not reduce cerebral blood flow to ischemic levels. In other instances, the suture may be repositioned within the artery by vasospasm and / or retrograde perfusion through the Circle of Willis. In fact, the absence of infarction in 5 of the 21 (23.8%) mice tested may be attributed to any of these reasons. As a solution, the use of laser Doppler flowmetry allows for the monitoring of cerebral blood flow changes following the insertion of the occluding filament. With this technique, criteria may be established such that the occlusion is deemed successful only if the measure of flow post-MCAO is equal to or less than 20% of the baseline, as measured prior to the insertion of the filament. It was decided at the conclusion of the pilot study to monitor regional cerebral blood flow in the GluR2 project with a laser Doppler device to improve the success of the model.

GluR2 Knockout Mice are Not More Susceptible to Permanent Focal Ischemia

This study reveals that the infarction volumes and neurobehavioural deficits sustained 24 hours following the permanent intraluminal occlusion of the middle cerebral artery did not differ between wild-type mice and those with a mutated GluR2 gene. These results were not attributed to differences in cerebral blood flow measured both pre- and 15-min post-MCA occlusion by laser Doppler flowmetry.

This is the first study to test the GluR2 null mutant mice in an in vivo model of cerebral ischemia. It is also the first study to explore the potential role of the GluR2 subunit in the pathophysiology of focal cerebral ischemia. As the results infer, the mutation of the GluR2 gene does not render mutant mice more susceptible to ischemic injury in a permanent model of focal ischemia.

This finding supports the null hypothesis of the study, since it was believed that the knockouts would have larger infarction volumes than their wild-type controls. The lack of a statistical difference between these two experimental groups may not be attributed to infarct variability resulting from inadequate physiological monitoring. The variability in the wild-type and knockout lesions were 28.2% and 22.6%, respectively, both of which are within the statistical range of papers published with controls for arterial blood pressure and gases[48,53,171,172]. In addition, each animal that recorded an acceptable reduction in cerebral blood flow (<20% residual rCBF) following the filament insertion proceeded to infarction.

A caveat of all studies employing *in vivo* genetic manipulation is the veritable possibility that the response of the mutant mice to the ischemia may be adulterated by developmental compensation. In addition, it may be surmised that all GluR2-dependent interactions have been eliminated in the knockout mice, and the resulting functional perturbations not fully known. However, neuronal excitability and cellularity are relatively normal in the GluR2 null mutant mice[131]. And more importantly, the expression of calcium binding proteins including calbindin, parvalbumin, calmodulin and

calretinin, which were hypothesized to be upregulated as a means of buffering enhanced Ca^{2+} permeability in the knockouts, were shown to not differ from wild-type littermates[173].

Genetically engineered mice are tools used to better appreciate the contextual significance of specific genes and their proteins in the mechanisms underlying ischemic cell death. Although they may be the star attraction of a given study, they are not the show. Their importance lies in how their role influences the scientific story. For instance, a major drawback to the scientific merit of the present study is the inappropriateness of the model used to test the knockout. It was originally hypothesized that the GluR2 mutant mice would have larger infarction volumes as compared to wild-type controls in this model of permanent focal ischemia. However, this model is ischemically very severe, such that the available margin of lesion growth to be limited to only about 10% of that present at 24 hours post-MCAO[28,48,65]. Therefore, it is possible that the lack of a difference between the knockouts and the controls may be due to a ceiling effect ascribed to the model.

Contextual Significance

The quinoxalinedione class of AMPA receptor antagonists, including NBQX, YM872 and YM890, have conferred neuroprotection in models of both temporary and permanent focal ischemia in rats and cats[101,120-125]. However, the exact mechanisms by which they do so are not completely understood. It may be surmised that the blockade of AMPA receptor physiology during ischemia may deny NMDA and voltage gated Ca^{2+}

channels the necessary membrane depolarization required for their activation. And although the indirect inactivation of calcium conductances through these channels has been proposed to explain the efficacy of these drugs[34,125], evidence to support an AMPA receptor GluR2-dependent mechanism in models of focal ischemia has yet to be reported.

The results of this study argue against the importance of the GluR2 subunit in mediating tissue damage in a severe model of focal ischemia. However, it should be noted that the most compelling evidence to support a role for AMPA receptors, and more specifically the GluR2 subunit, in cerebral ischemia has been derived from models of delayed neuronal death[135-137]. In fact, the GluR2 Hypothesis is established upon observations made from studies of transient forebrain ischemia and status epilepticus. Hence, one would ideally test the GluR2 knockout mice in a murine model of global cerebral ischemia. Although some have been reported[24,96,140,141], a reproducible model of transient forebrain ischemia requiring minimal technical expertise has yet to be published.

For this reason, the GluR2 mutant mice were tested in a model of permanent focal ischemia. However, mild models of focal ischemia have been recently described in the rat and mouse[174,175]. Thus, it is possible that in a model of mild focal ischemic severity, GluR2 mRNA may be selectively downregulated, and the consequent formation of Ca^{2+}-permeable AMPA receptors may contribute to the final infarct volume. To this end, penumbral changes in glutamate receptor mRNA expression may be detected by standard methods of immunohistochemistry. Moreover, the functional significance of potential

GluR2 expression changes after mild focal cerebral ischemia may be further explored by the ability of 1-naphthylacetyl spermine (1-NA-Spm) to reduce infarction volumes. An analogue of spider joro toxin, this antagonist to calcium permeable AMPA receptors, was recently shown to be a potent anticonvulsant when administered intracerebroventricularly in a rat seizure model of amygdala-kindling[176-179].

Validity of the GluR2 Hypothesis

The GluR2 Hypothesis states that the mRNA of the GluR2 subunit is downregulated in vulnerable neurons destined to die by global ischemia. This will then lead to the formation of Ca^{2+}-permeable AMPA receptors lacking the GluR2 subunit. Consequently, in the presence of endogenous glutamate, Ca^{2+} influx through these GluR2-less receptors contributes to or causes ischemic cell death[136,137]. Interestingly, the data supporting the GluR2 Hypothesis has not been fully embraced nor reproduced. Specifically, the causal relationship between the selective downregulation of the GluR2 subunit, and its functional consequences leading to neuronal degeneration has been questioned[180]. In fact, studies have shown that GluR2 mRNA is not selectively downregulated following global ischemia, including one such paper published by Pelligrini-Giampietro; coauthor of the hypothesis itself[133]. Regardless, this downregulation in the GluR2 mRNA reportedly occurs 48 to 72 hours post-ischemia in the CA1 hippocampus[132]. In consideration of the time course of ischemia-induced delayed neuronal, however, the likelihood of new Ca^{2+}-permeable AMPA channel formation occurring within this time frame must be questioned. In fact, direct evidence

of newly formed AMPA channels subsequent to the selective downregulation of GluR2 mRNA has yet to be reported. More recently, studies have shown that AMPA receptor-mediated excitoxicity in cultured cortical neurons derived from the GluR2 mutant mice to be mediated not by Ca^{2+} permeability, but rather, Na^{+} influx [173].

The findings of the present investigation indicate that the absence of the GluR2 subunit, rendering AMPA channels Ca^{2+}-permeable, does not worsen the ischemic outcome following permanent focal ischemia. However, the severity of the ischemia attributed to the model used in this study may mask the potential importance of the GluR2 subunit in more delayed forms of neuronal death. Further evaluation of this role will necessitate the testing of the GluR2 mutant mice in a reproducible murine model of global cerebral ischemia.

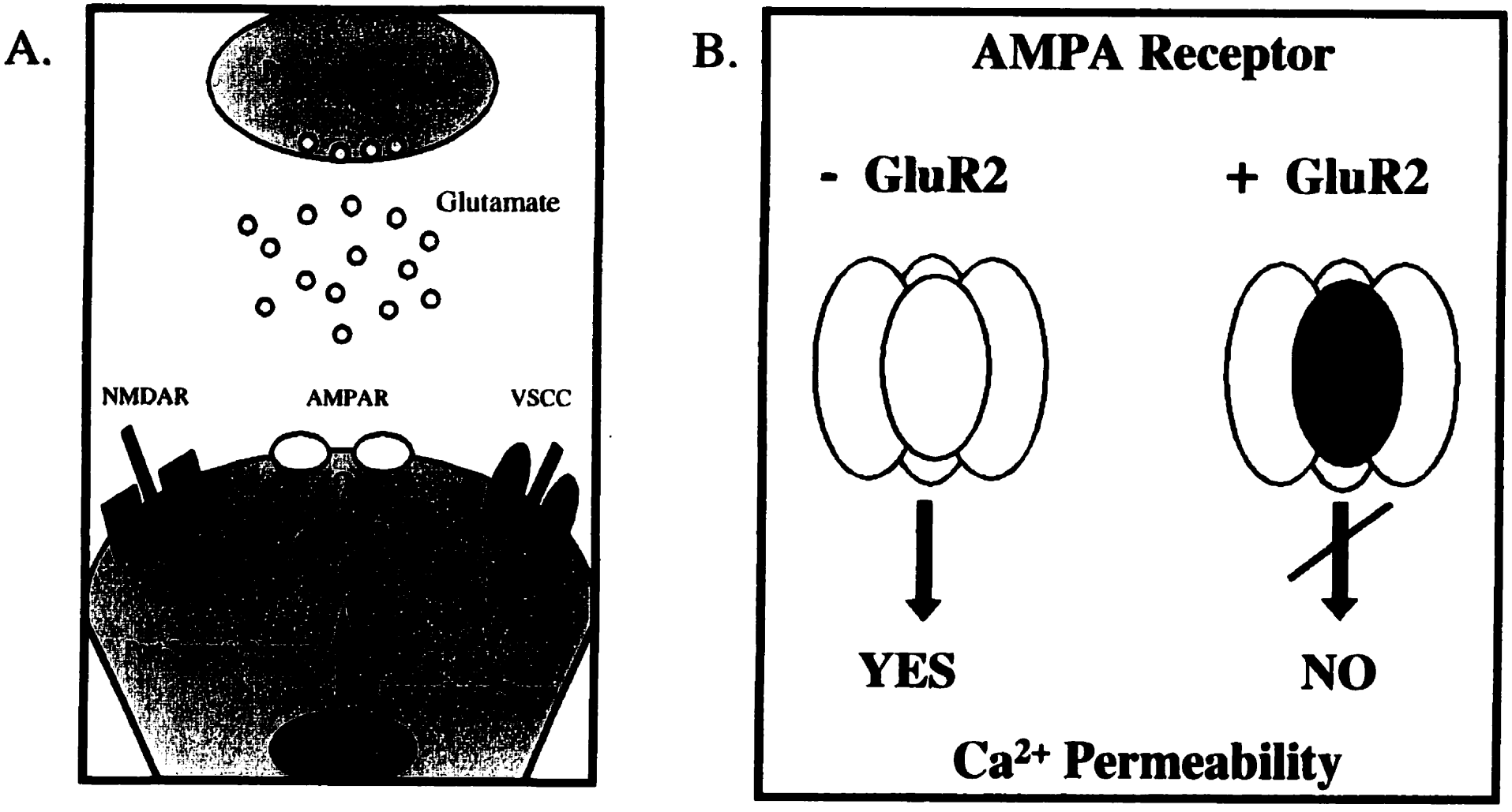

Figure 1. A. Routes of Ca^{2+} Influx through Voltage Sensitive Calcium Channels (VSCC), and NMDA and AMPA receptor linked ion channels following glutamate activation. B. Ca^{2+} permeability through AMPA receptors is dependent upon the inclusion of the GluR2 subunit in its ion channel composition.

Four-Vessel Occlusion Does Not Produce Significant CA1 Hippocampal Damage Following 5-, 10- & 15 min of Global Ischemia in CD1 Mice

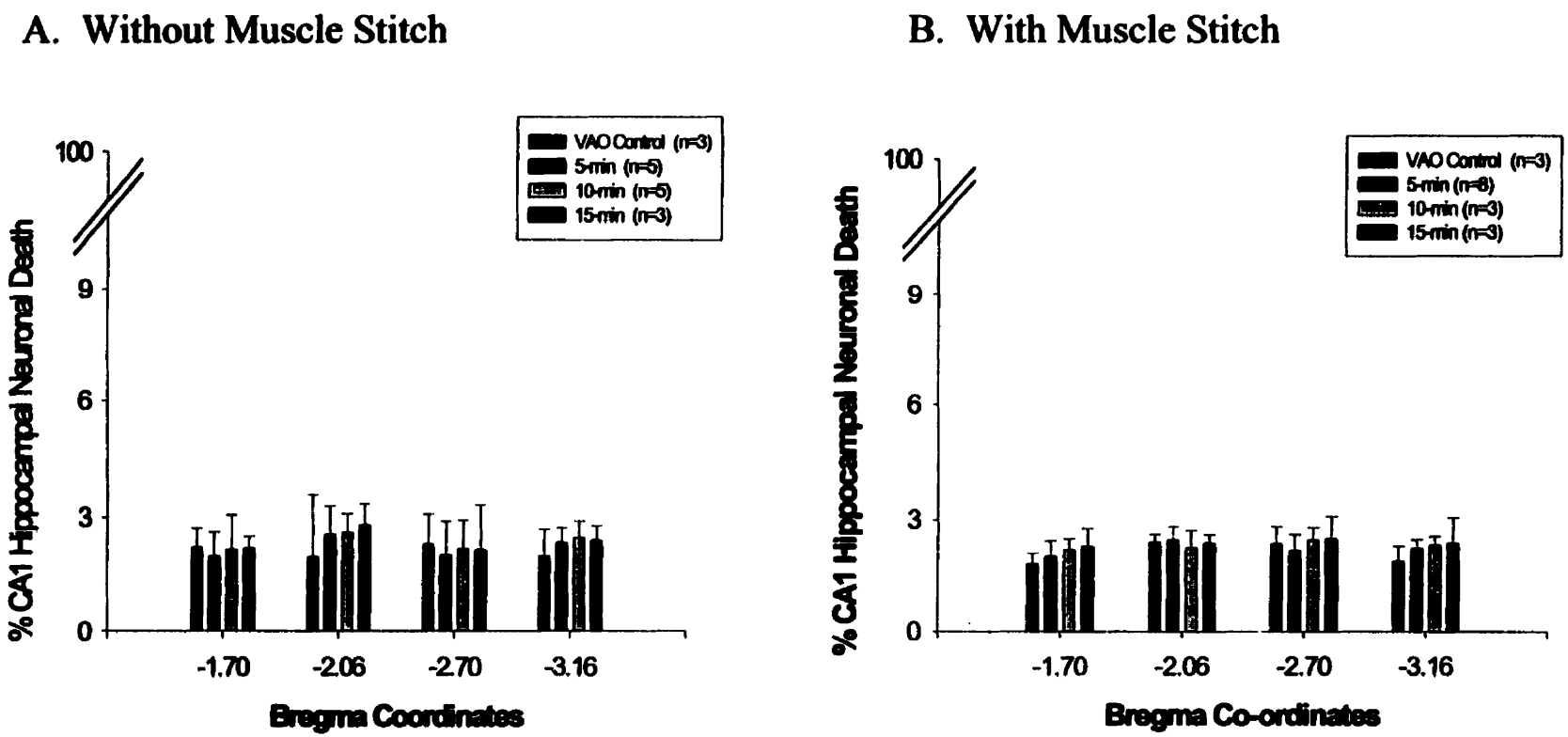

Figure 2. Bar graphs show lack of statistically significant differences between the percentage of CA1 neuronal death at dorsal (Bregma -1.70 & -2.06) and ventral (Bregma -2.70 & -3.16) levels of the hippocampus in mice subjected to the four-vessel occlusion model with (B) and without (A) a paravertebral muscle stitch. Neuronal death (~3%) was assessed on the appearance of pyknotic nuclei in the CA1 subfield of the CD1 mouse hippocampus.

No Difference in CA1 Hippocampal Damage Between CD1 & C57Bl/6 Mouse Strains Following 15- and 20-min Four-Vessel Occlusion

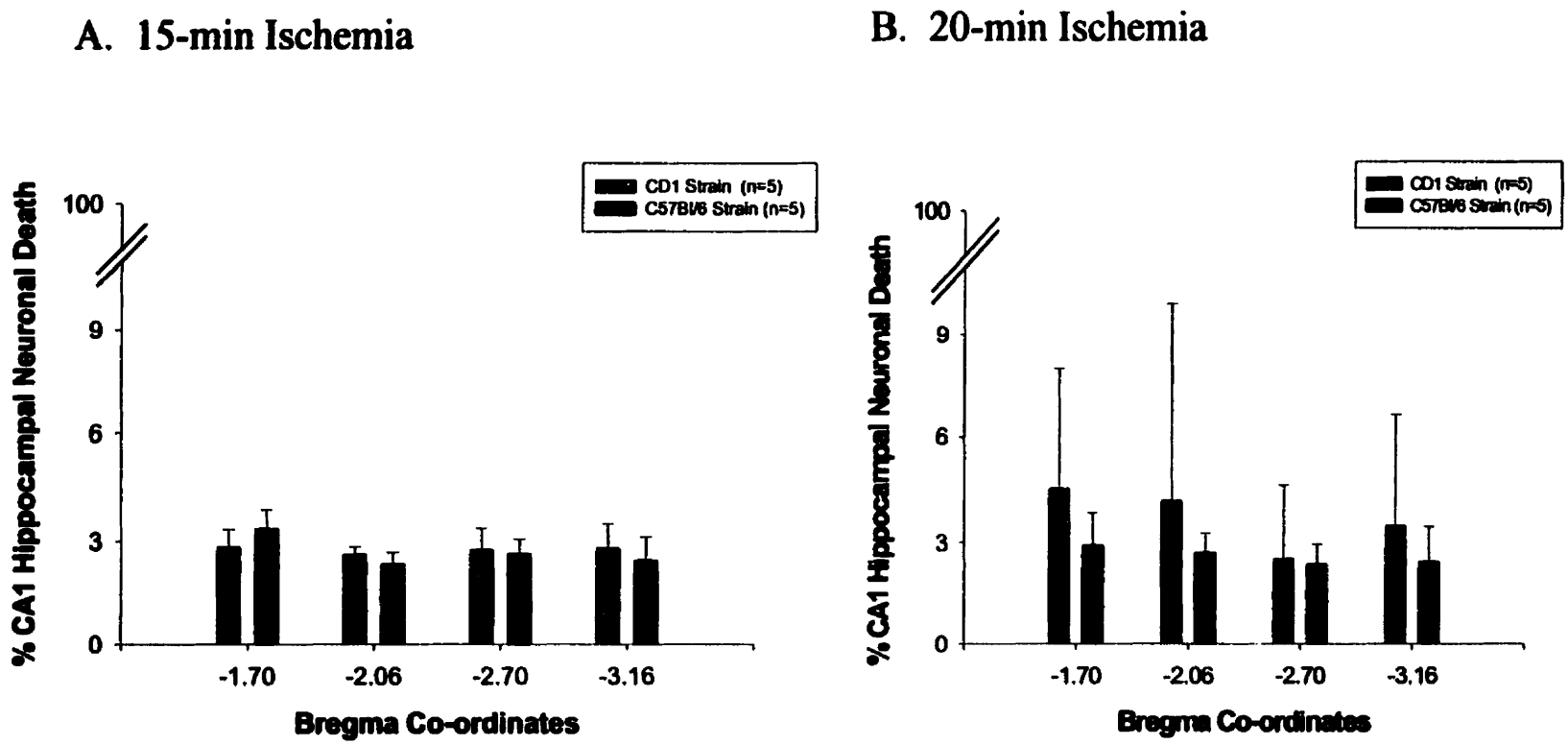

Figure 3. Bar graphs show lack of statistically significant differences in the percentage of CA1 neuronal death at dorsal (Bregma -1.70 & -2.06) and ventral (Bregma -2.70 & -3.16) levels of the hippocampus in CD1 and C57Bl/6 mice subjected to (A) 15 min and (B) 20 min of four-vessel occlusion. Neuronal death (~3%) was assessed on the appearance of pyknotic nuclei in the CA1 subfield of the mouse hippocampus.

No Difference in CA1 Hippocampal Damage in C57Bl/6 Mice 7 or 14 Days Following 20-min Four-Vessel Occlusion

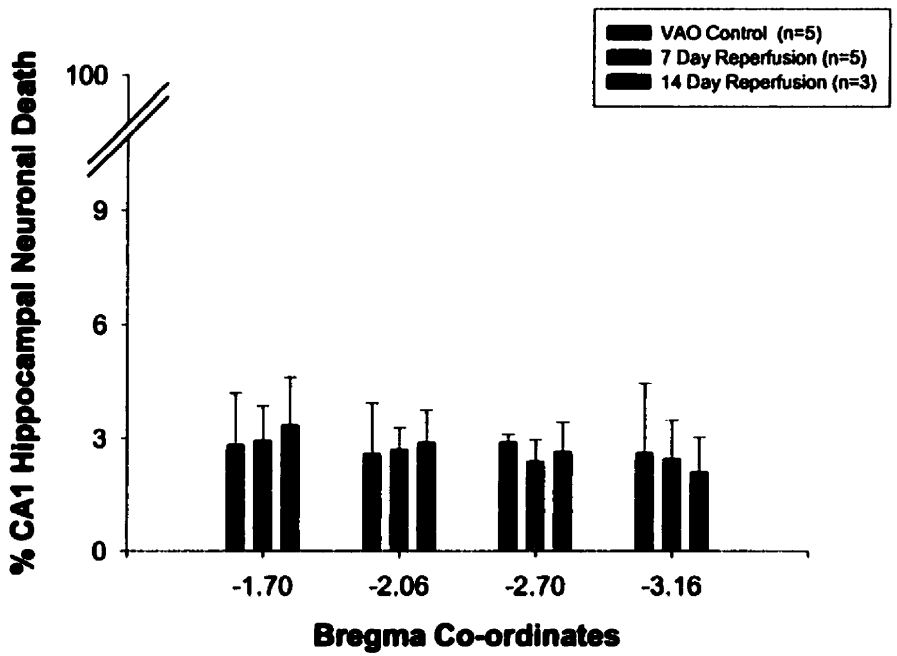

Figure 4. Bar graph shows lack of statistically significant differences in the percentage of CA1 neuronal death at dorsal (Bregma -1.70 & -2.06) and ventral (Bregma -2.70 & -3.16) levels of the hippocampus in C57Bl/6 mice 7 and 14 days following 20 min of four-vessel occlusion. Neuronal death (~3%) was assessed on the appearance of pyknotic nuclei in the CA1 subfield of the mouse hippocampus.

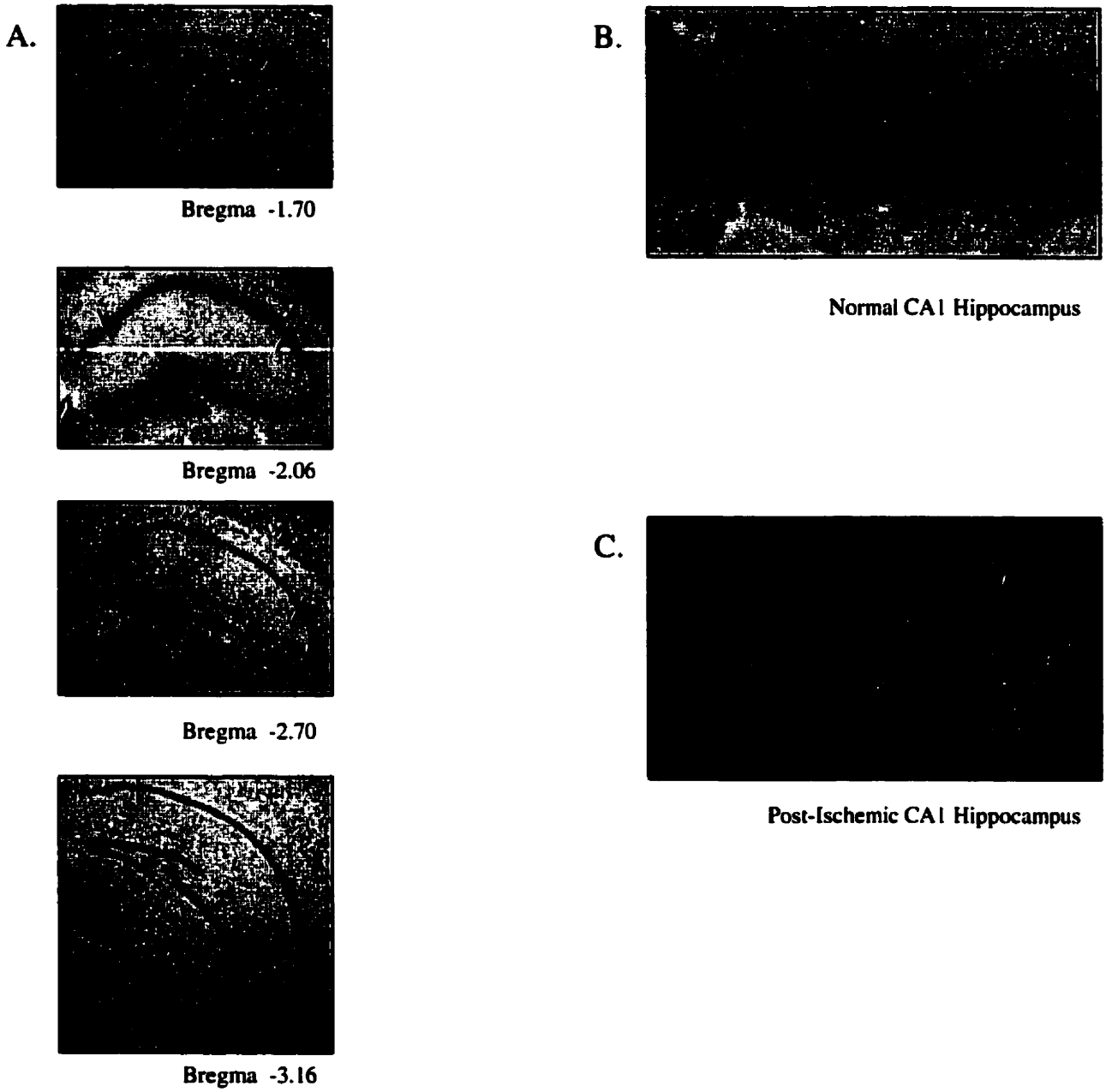

Figure 5. A. Septotemporal levels of mouse hippocampus used to quantify CA1 neuronal death. CA1 pyramidal layer lies within the bounded region of each represented level of the hippocampus. Hippocampal damage was evaluated at four levels to establish a potential dorsal (Bregma coordinates: -1.70, -2.06) to ventral (Bregma coordinates: -2.70, -3.16) gradient of delayed neuronal death. High magnification (X 500) of CA1 subfield depicting normal, viable neurons (B) and highly eosinophilic, pyknotic neurons from a post-ischemic mouse hippocampus (arrowheads, C). Cresyl violet staining was used for Panels A and B; Panel C was stained by hematoxylin & eosin (H&E).

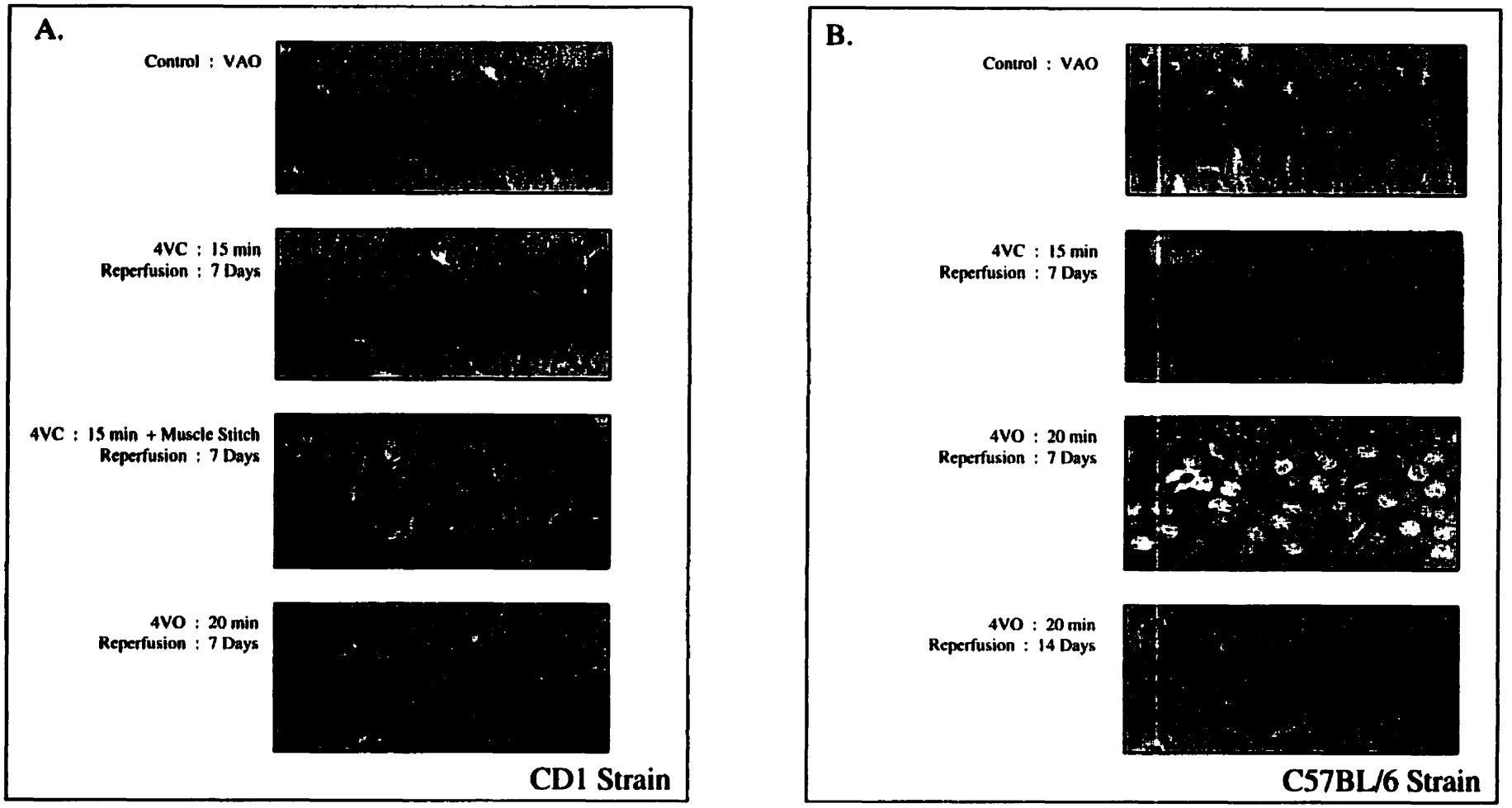

Figure 6. Photographs of cresyl violet stained CA1 pyramidal neurons taken at high magnification (X 500) in mice subjected to the labeled durations of ischemia (vertebral artery occlusion (VAO)-control, 5-, 10-, 15- & 20-min of four vessel occlusion) and reperfusion periods (7 & 14 days). Note that the CA1 hippocampal neurons appear normal in both CD1 (A) and C57Bl/6 (B) mice regardless of the ischemic challenge, as compared to controls.

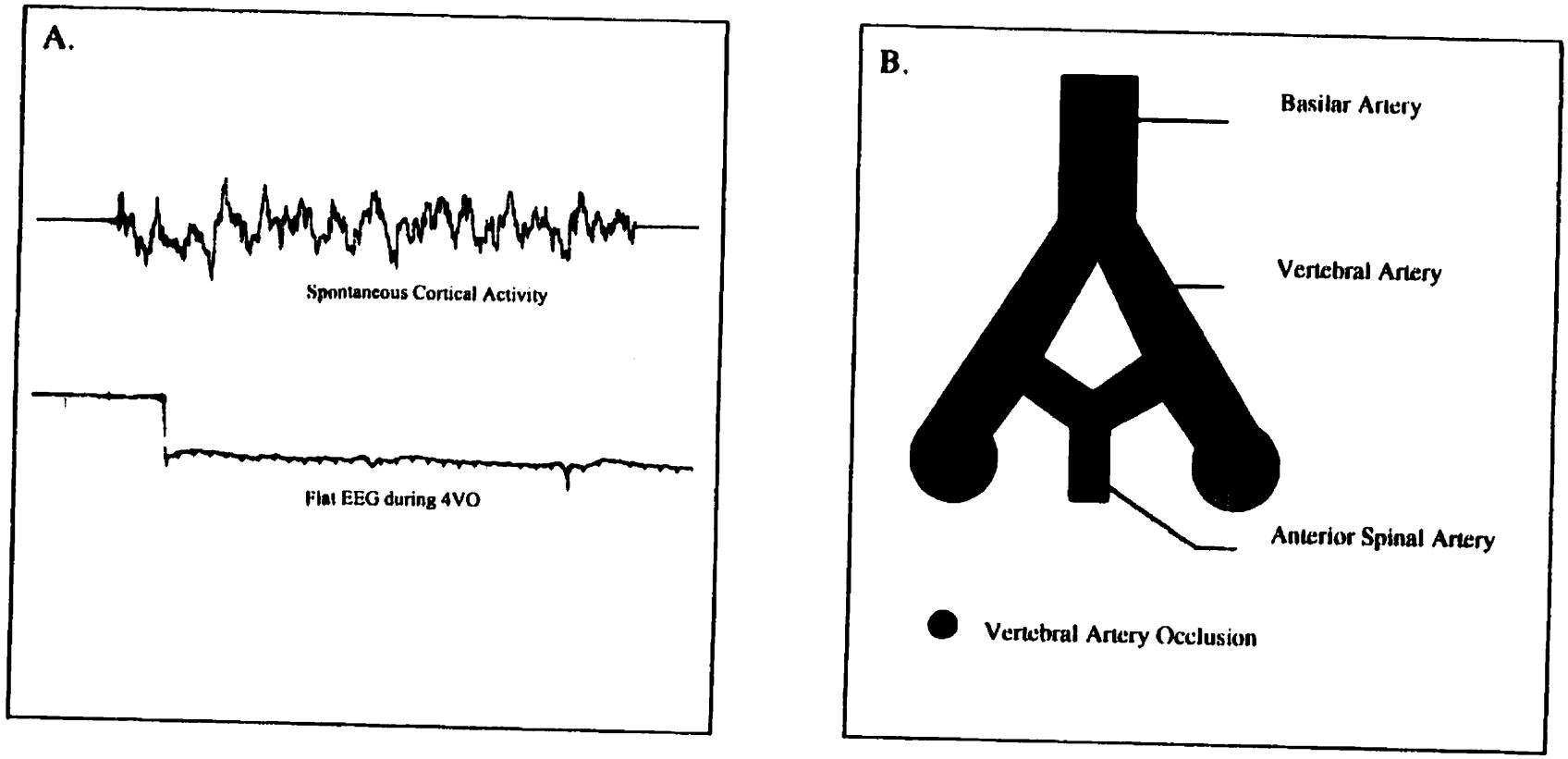

Figure 7. A. Recording of cortical electrical activity by the electroencephalogram (EEG). Pre-Ischemia recording of spontaneous cortical activity (upper trace) followed by isoelectric quiescence during four-vessel occlusion. B. Collateral circulation originating from the anterior spinal artery bypasses both vertebral artery occlusions.

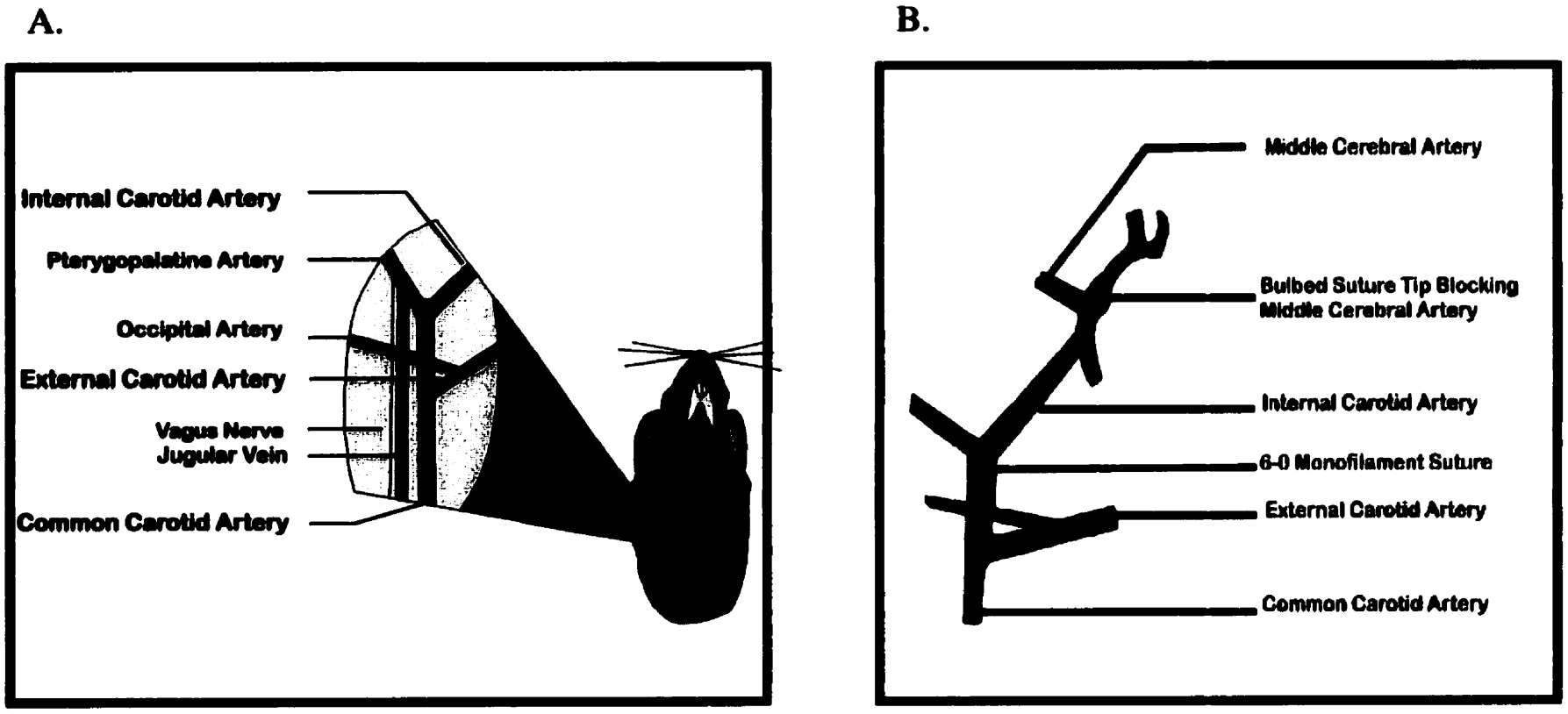

Figure 8. A. Surgical window created in the mouse following a ventral midline neck incision. B. Intraluminal occlusion of the middle cerebral artery by a silicone-coated 6-0 monofilament suture.

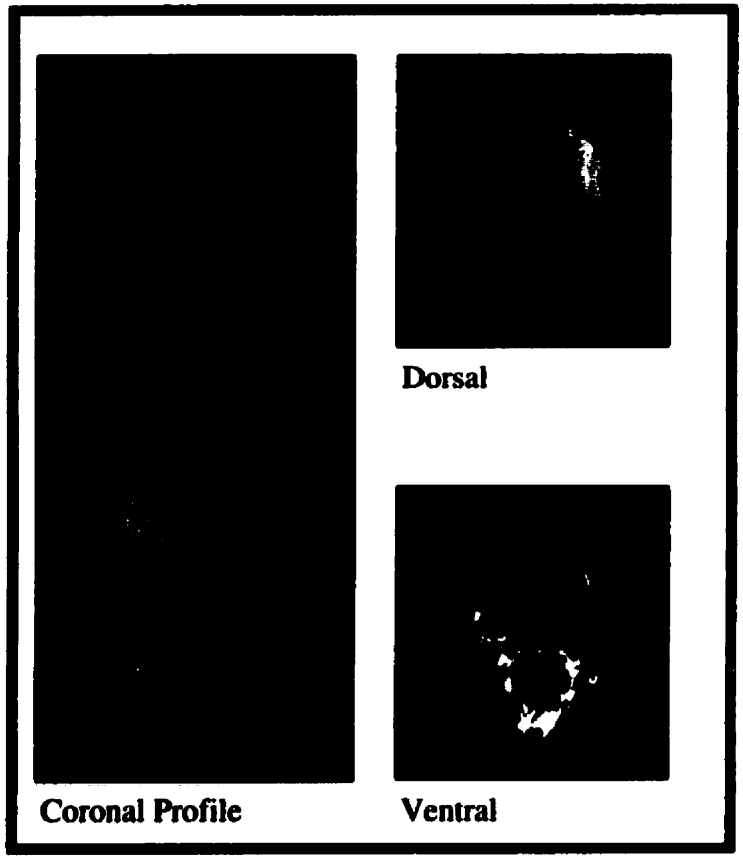

A.

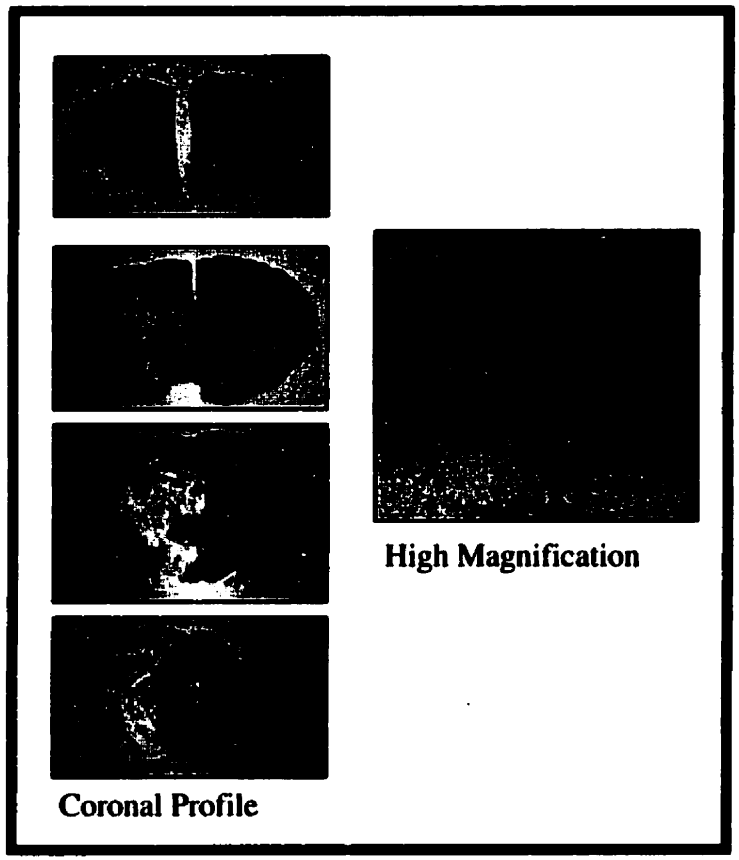

B.

Figure 9. A. Photograph of brain tissue stained with 2% 2,3,5-triphenyltetrazolium chloride solution (TTC). Infarcted tissue in the right hemisphere remains unstained; viable tissue is stained brick red. Dorsal / ventral profiles, and coronal slices (2 mm thick) of the ischemic brain are presented. B. Histological representation of the ischemic brain. Lesion is characterized by regions of pallor, tissue swelling and pyknotic nuclei. Border of the ischemic lesion is readily apparent in the high magnification (X 400) photograph where the infarct lies to the left of viable tissue.

Response of GluR2 Knockout Mice to Permanent Focal Cerebral Ischemia

A. rCBF

B. Neurological Scores

C. Infarction Volume

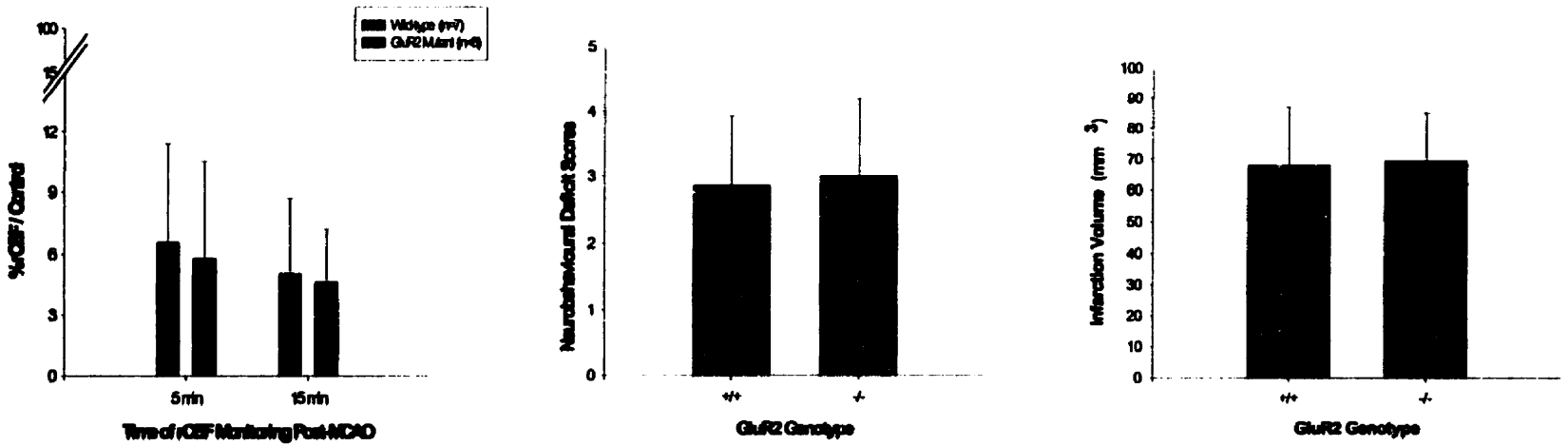

Figure 10. Wild-type (n=7) and GluR2 null mutant mice (n=8) did not differ in their susceptibility to permanent focal cerebral ischemia. Infarction volumes (C) and neurobehavioural deficits (B) sustained 24 hours following the intraluminal occlusion of the middle cerebral artery did not differ between wild-type and knockout mice. (A) Residual cerebral blood flow measured 5- & 15- min after MCAO was less than 20% of thepre-MCAO baseline, without a statistical difference in the relative reduction between mutant and wild-type mice.

Validation of the Frustrum Summation Method for Infarction Quantification

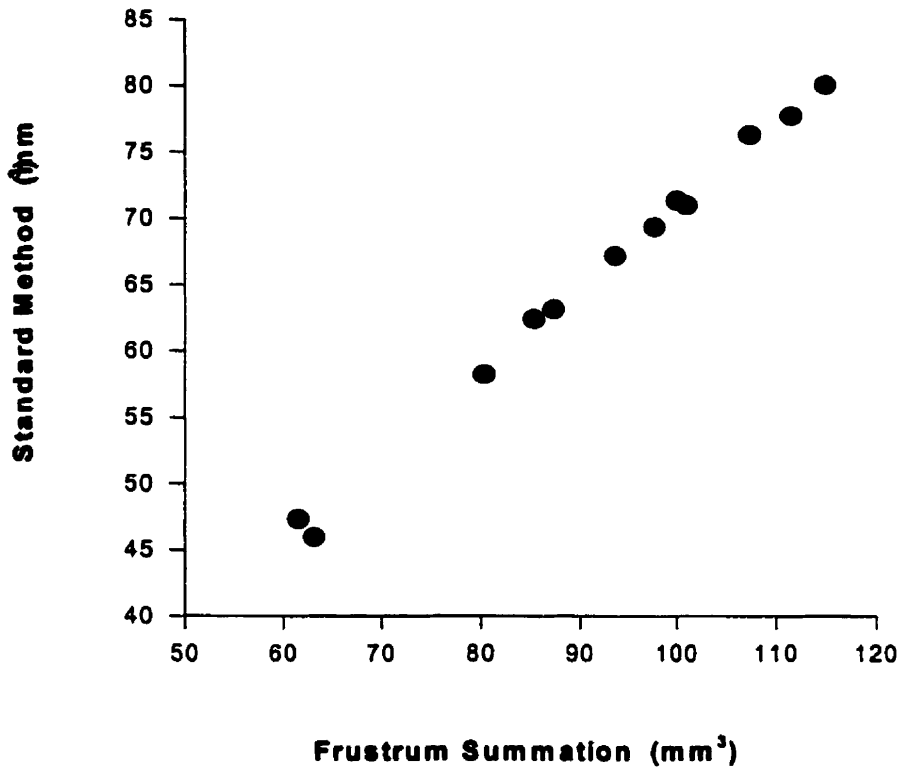

Figure 11. Correlation analysis comparing a standard method to calculate rat infarction volumes & the frustrum summation method of murine lesion quantification. A pearson correlation coefficient of 0.998 was generated statistically to validate the methodology.

IX. References

1. Thompson DW, Furlan AJ: Clinical epidemiology of stroke. *Neurosurg Clin N Am* 1997;8:265-269

2. Sacco RL: Current epidemiology of stroke, in Fisher M, Bogousslavsky J (eds): *Current review of cerebrovascular disease*. 1993,

3. Camarata PJ, Heros RC, Latchaw RE: "Brain attack": the rationale for treating stroke as a medical emergency. *Neurosurgery* 1994;34:144-57; discussion 157-8

4. Heros RC, Camarata PJ, Latchaw RE: Brain attack. Introduction. *Neurosurg Clin N Am* 1997;8:135-144

5. Dobkin B: The economic impact of stroke. *Neurology* 1995;45:S6-9

6. Sacco RL: Risk factors, outcomes, and stroke subtypes for ischemic stroke. *Neurology* 1997;49:S39-44

7. Wang YF, Tsirka SE, Strickland S, Stieg PE, Soriano SG, Lipton SA: Tissue plasminogen activator (tPA) increases neuronal damage after focal cerebral ischemia in wild-type and tPA-deficient mice [see comments]. *Nat Med* 1998;4:228-231

8. Hacke W, Hennerici M, Gelmers HJ, Kramer G: Pathophysiology of cerebral ischemia, in Hacke W (ed): *Cerebral ischemia*. 1991,

9. Chillon JM, Baumbach GL: Autoregulation of cerebral blood flow, in Welch KMA, Weir B, Caplan LR, Reis DJ, Siesjo BK (eds): *Primer on cerebrovascular diseases*. 1996,

10. Day A: Arterial distributions and variants, in wood j (ed): *Cerebral blood flow: physiologic and clinical aspects*. 1987, pp 19-36

11. Sokoloff L: Anatomy of cerebral circulation, in Welch KMA, Caplan LR, Reis DJ, Siesjo BK, Weir B (eds): *Primer on cerebrovascular diseases*. 1997,

12. Ratcheson RA, kiefer s, Selman WR: Pathophysiology and clinical evaluation of ischemic cerebrovascular disease, in Anonymous*Youman's neurological surgery*. 1996,

13. Traystman RJ: Regulation of cerebral blood flow by carbon dioxide, in caplan l, reis d, siesjo b, weir b, welch k (eds): *Primer on cerebrovascular diseases*. 1997,

14. Daffertshofer M, Hennerici M: Cerebrovascular regulation and vasoneuronal coupling. *J Clin Ultrasound* 1995;23:125-138

15. Goadsby PJ, Edvinsson L: Extrinsic Innervation: Transmitters, Receptors, and Functions - The Sympathetic Nervous System, in Welch KMA, Caplan LR, Reis DJ, Siesjo BK, Weir B (eds): *Primer on Cerebrovascular Diseases*. Toronto, Academic Press, 1997,

16. Goadsby PJ, Edvinsson L: Extrinsic Innervation: Transmitters, Receptors, and Functions - The Parasympathetic Nervous System, in Welch KMA, Caplan LR, Reis DJ, Siesjo BK, Weir B (eds): *Primer on Cerebrovascular Diseases*. Toronto, Academic Press, 1997, pp 63-67

17. Lassen NA, Astrup J: Ischemic penumbra, in wood j (ed): *Cerebral blood flow*. 1987, pp 458-466

18. Symon L: Pathological regulation in cerebral ischemia, in Wood JH (ed): *Cerebral blood flow: physiologic and clinical aspects*. 1987, pp 413-424

19. Astrup J, Siesjo BK, Symon L: Thresholds in cerebral ischemia - the ischemic penumbra. *Stroke* 1981;12:723-725

20. Jafar JJ, Crowell RM: Focal ischemic thresholds, in Wood JH (ed): *Cerebral blood flow: physiologic and clinical aspects*. Academic press, 1987, pp 449-457

21. Brust JCM: Cerebral circulation: Stroke, in Kandel ER, Schwartz JH, Jessel TM (eds): *Principles of neural science*. 1991,

22. Gamache FW: Comparison of global and focal cerebral ischemia, in Wood JH (ed): *Cerebral blood flow: physiologic and clinical aspects*. 1991, pp 518-530

23. Ginsberg MD, Busto R: Rodent models of cerebral ischemia. *Stroke* 1989;20:1627-1642

24. Panahian N, Yoshida T, Huang PL, Hedley-Whyte ET, Dalkara T, Fishman MC, Moskowitz MA: Attenuated hippocampal damage after global cerebral ischemia in mice mutant in neuronal nitric oxide synthase. *Neuroscience* 1996;72:343-354

25. Duverger D, MacKenzie ET: The quantification of cerebral infarction following focal ischemia in the rat: influence of strain, arterial pressure, blood glucose concentration, and age. *J Cereb Blood Flow Metab* 1988;8:449-461

26. Brint S, Jacewicz M, Kiessling M, Tanabe J, Pulsinelli W: Focal brain ischemia in the rat: methods for reproducible neocortical infarction using tandem occlusion of the distal middle cerebral and ipsilateral common carotid arteries. *J Cereb Blood Flow Metab* 1988;8:474-485

27. Tamura A, Graham DI, McCulloch J, Teasdale GM: Focal cerebral ischaemia in the rat: 1. Description of technique and early neuropathological consequences following middle cerebral artery occlusion. *J Cereb Blood Flow Metab* 1981;1:53-60

28. Buchan AM, Xue D, Slivka A: A new model of temporary focal neocortical ischemia in the rat. *Stroke* 1992;23:273-279

29. Buja LM, Eigenbrodt ML, Eigenbrodt EH: Apoptosis and necrosis. Basic types and mechanisms of cell death. *Arch Pathol Lab Med* 1993;117:1208-1214

30. Busto R, Dietrich WD, Globus MY, Valdes I, Scheinberg P, Ginsberg MD: Small differences in intraischemic brain temperature critically determine the extent of ischemic neuronal injury. *J Cereb Blood Flow Metab* 1987;7:729-738

31. Green EJ, Dietrich WD, van Dijk F, Busto R, Markgraf CG, McCabe PM, Ginsberg MD, Schneiderman N: Protective effects of brain hypothermia on behavior and histopathology following global cerebral ischemia in rats. *Brain Res* 1992;580:197-204

32. Colbourne F, Corbett D: Delayed and prolonged post-ischemic hypothermia is neuroprotective in the gerbil. *Brain Res* 1994;654:265-272

33. Smith ML, Bendek G, Dahlgren N, Rosen I, Wieloch T, Siesjo BK: Models for studying long-term recovery following forebrain ischemia in the rat. 2. A 2-vessel occlusion model. *Acta Neurol Scand* 1984;69:385-401

34. Siesjo BK, Bengtsson F: Calcium fluxes, calcium antagonists, and calcium-related pathology in brain ischemia, hypoglycemia, and spreading depression: a unifying hypothesis. *J Cereb Blood Flow Metab* 1989;9:127-140

35. Wagner KR, Kleinholz M, de Courten-Myers GM, Myers RE: Hyperglycemic versus normoglycemic stroke: topography of brain metabolites, intracellular pH, and infarct size. *J Cereb Blood Flow Metab* 1992;12:213-222

36. Garcia JH: The evolution of brain infarcts. A review. *J Neuropathol Exp Neurol* 1992;51:387-393

37. Slivka A, Murphy E, Horrocks L: Cerebral edema after temporary and permanent middle cerebral artery occlusion in the rat. *Stroke* 1995;26:1061-5; discussion 1065-6

38. Fox G, Gallacher D, Shevde S, Loftus J, Swayne G: Anatomic variation of the middle cerebral artery in the Sprague-Dawley rat. *Stroke* 1993;24:2087-92; discussion 2092-

39. Bederson JB, Pitts LH, Tsuji M, Nishimura MC, Davis RL, Bartkowski H: Rat middle cerebral artery occlusion: evaluation of the model and development of a neurologic examination. *Stroke* 1986;17:472-476

40. Osborne KA, Shigeno T, Balarsky AM, Ford I, McCulloch J, Teasdale GM, Graham DI: Quantitative assessment of early brain damage in a rat model of focal cerebral ischaemia. *J Neurol Neurosurg Psychiatry* 1987;50:402-410

41. Burda J, Marsala M, Radonak J, Marsala J: Graded postischemic reoxygenation ameliorates inhibition of cerebral cortical protein synthesis in dogs. *J Cereb Blood Flow Metab* 1991;11:1001-1005

42. Selman WR, VanDerVeer C, Whittingham TS, LaManna JC, Lust WD, Ratcheson RA: Visually defined zones of focal ischemia in the rat brain. *Neurosurgery* 1987;21:825-830

43. Tamura A, Graham DI, McCulloch J, Teasdale GM: Focal cerebral ischaemia in the rat: 2. Regional cerebral blood flow determined by [14C]iodoantipyrine autoradiography following middle cerebral artery occlusion. *J Cereb Blood Flow Metab* 1981;1:61-69

44. Chan PH: Oxygen radicals in focal cerebral ischemia. *Brain Pathol* 1994;4:59-65

45. Markgraf CG, Kraydieh S, Prado R, Watson BD, Dietrich WD, Ginsberg MD: Comparative histopathologic consequences of photothrombotic occlusion of the distal middle cerebral artery in Sprague-Dawley and Wistar rats. *Stroke* 1993;24:286-92; discussion 292-3

46. Robinson MJ, Macrae IM, Todd M, Reid JL, McCulloch J: Reduction in local cerebral blood flow induced by endothelin-1 applied topically to the middle cerebral artery in the rat. *J Cardiovasc Pharmacol* 1991;17 Suppl 7:S354-7:S354-7

47. Clark WM, Lessov NS, Dixon MP, Eckenstein F: Monofilament intraluminal middle cerebral artery occlusion in the mouse. *Neurol Res* 1997;19:641-648

48. Connolly ES, Jr., Winfree CJ, Stern DM, Solomon RA, Pinsky DJ: Procedural and strain-related variables significantly affect outcome in a murine model of focal cerebral ischemia. *Neurosurgery* 1996;38:523-31; discussion 532

49. Kamii H, Kinouchi H, Sharp FR, Koistinaho J, Epstein CJ, Chan PH: Prolonged expression of hsp70 mRNA following transient focal cerebral ischemia in transgenic mice overexpressing CuZn-superoxide dismutase. *J Cereb Blood Flow Metab* 1994;14:478-486

50. Hata R, Mies G, Wiessner C, Fritze K, Hesselbarth D, Brinker G, Hossmann KA: A reproducible model of middle cerebral artery occlusion in mice: hemodynamic, biochemical, and magnetic resonance imaging. *J Cereb Blood Flow Metab* 1998;18:367-375

51. Kogure K, Kato H: Altered gene expression in cerebral ischemia. *Stroke* 1993;24:2121-2127

52. Dirnagl U, Kaplan B, Jacewicz M, Pulsinelli W: Continuous measurement of cerebral cortical blood flow by laser-Doppler flowmetry in a rat stroke model. *J Cereb Blood Flow Metab* 1989;9:589-596

53. Huang Z, Huang PL, Panahian N, Dalkara T, Fishman MC, Moskowitz MA: Effects of cerebral ischemia in mice deficient in neuronal nitric oxide synthase. *Science* 1994;265:1883-1885

54. Laing RJ, Jakubowski J, Laing RW: Middle cerebral artery occlusion without craniectomy in rats. Which method works best? [see comments]. *Stroke* 1993;24:294-7; discussion 297-8

55. Bederson JB, Pitts LH, Germano SM, Nishimura MC, Davis RL, Bartkowski HM: Evaluation of 2,3,5-triphenyltetrazolium chloride as a stain for detection and quantification of experimental cerebral infarction in rats. *Stroke* 1986;17:1304-1308

56. Isayama K, Pitts LH, Nishimura MC: Evaluation of 2,3,5-triphenyltetrazolium chloride staining to delineate rat brain infarcts. *Stroke* 1991;22:1394-1398

57. Uno M, Matsumoto K, Wallace MC: Neutral red staining for the assessment of acute outcome in rat focal cerebral ischemia models. *Neurol Med Chir (Tokyo)* 1995;35:561-566

58. Rosenblum WI: Histopathologic clues to the pathways of neuronal death following ischemia/hypoxia. *J Neurotrauma* 1997;14:313-326

59. Swanson RA, Morton MT, Tsao-Wu G, Savalos RA, Davidson C, Sharp FR: A semiautomated method for measuring brain infarct volume [see comments]. *J Cereb Blood Flow Metab* 1990;10:290-293

60. Persson L, Hardemark HG, Bolander HG, Hillered L, Olsson Y: Neurologic and neuropathologic outcome after middle cerebral artery occlusion in rats. *Stroke* 1989;20:641-645

61. Iadecola C: Principles and methods for measurement of cbf: experimental methods, in welch k, kaplan l, reis d, siesjo b, weir b (eds): *Primer on cerebrovascular disease.* academic press, 1997,

62. Todd NV, Picozzi P, Crockard HA, Russell RR: Reperfusion after cerebral ischemia: influence of duration of ischemia. *Stroke* 1986;17:460-466

63. Siesjo BK: Pathophysiology and treatment of focal cerebral ischemia. Part II: Mechanisms of damage and treatment. *J Neurosurg* 1992;77:337-354

64. Siesjo BK: Pathophysiology and treatment of focal cerebral ischemia. Part I: Pathophysiology. *J Neurosurg* 1992;77:169-184

65. Chiamulera C, Terron A, Reggiani A, Cristofori P: Qualitative and quantitative analysis of the progressive cerebral damage after middle cerebral artery occlusion in mice. *Brain Res* 1993;606:251-258

66. Wang LC, Futrell N, Wang DZ, Chen FJ, Zhai QH, Schultz LR: A reproducible model of middle cerebral infarcts, compatible with long- term survival, in aged rats. *Stroke* 1995;26:2087-2090

67. Lo EH, Rogowska J, Bogorodzki P, Trocha M, Matsumoto K, Saffran B, Wolf GL: Temporal correlation analysis of penumbral dynamics in focal cerebral ischemia. *J Cereb Blood Flow Metab* 1996;16:60-68

68. Hakim AM: Ischemic penumbra: the therapeutic window. *Neurology* 1998;51:S44-6

69. Hakim AM: The cerebral ischemic penumbra. *Can J Neurol Sci* 1987;14:557-559

70. Garcia JH: Morphology of global cerebral ischemia. *Crit Care Med* 1988;16:979-987

71. White BC, Grossman LI, Krause GS: Brain injury by global ischemia and reperfusion: a theoretical perspective on membrane damage and repair [see comments]. *Neurology* 1993;43:1656-1665

72. Brierley JB, Graham DI: Hypoxia and vascular disorders of the central nervous system, in Adams JH, Corsellis JAN, Duchen LW (eds): *Greenfield's neuropathology*. New York, John Wiley & Sons, 1984, pp 125-207

73. Ito U, Spatz M, Walker JT, Jr., Klatzo I: Experimental cerebral ischemia in mongolian gerbils. I. Light microscopic observations. *Acta Neuropathol (Berl)* 1975;32:209-223

74. Kirino T, Sano K: Fine structural nature of delayed neuronal death following ischemia in the gerbil hippocampus. *Acta Neuropathol (Berl)* 1984;62:209-218

75. Kirino T, Sano K: Selective vulnerability in the gerbil hippocampus following transient ischemia. *Acta Neuropathol (Berl)* 1984;62:201-208

76. Kirino T, Tamura A, Sano K: Delayed neuronal death in the rat hippocampus following transient forebrain ischemia. *Acta Neuropathol (Berl)* 1984;64:139-147

77. Kirino T: Delayed neuronal death in the gerbil hippocampus following ischemia. *Brain Res* 1982;239:57-69

78. Pulsinelli WA, Brierley JB, Plum F: Temporal profile of neuronal damage in a model of transient forebrain ischemia. *Ann Neurol* 1982;11:491-498

79. Suzuki R, Yamaguchi T, Kirino T, Orzi F, Klatzo I: The effects of 5-minute ischemia in Mongolian gerbils: I. Blood-brain barrier, cerebral blood flow, and local cerebral glucose utilization changes. *Acta Neuropathol (Berl)* 1983;60:207-216

80. Petito CK, Feldmann E, Pulsinelli WA, Plum F: Delayed hippocampal damage in humans following cardiorespiratory arrest. *Neurology* 1987;37:1281-1286

81. Cummings JL, Tomiyasu U, Read S, Benson DF: Amnesia with hippocampal lesions after cardiopulmonary arrest. *Neurology* 1984;34:679-681

82. Bachevalier J, Meunier M: Cerebral ischemia: are the memory deficits associated with hippocampal cell loss? *Hippocampus* 1996;6:553-560

83. Blomqvist P, Mabe H, Ingvar M, Siesjo BK: Models for studying long-term recovery following forebrain ischemia in the rat. 1. Circulatory and functional effects of 4-vessel occlusion. *Acta Neurol Scand* 1984;69:376-384

84. Pulsinelli WA, Brierley JB: A new model of bilateral hemispheric ischemia in the unanesthetized rat. *Stroke* 1979;10:267-272

85. Clifton GL, Taft WC, Blair RE, Choi SC, DeLorenzo RJ: Conditions for pharmacologic evaluation in the gerbil model of forebrain ischemia. *Stroke* 1989;20:1545-1552

86. Kato H, Araki T, Kogure K, Murakami M, Uemura K: Sequential cerebral blood flow changes in short-term cerebral ischemia in gerbils. *Stroke* 1990;21:1346-1349

87. Furlow TW, Jr. Cerebral ischemia produced by four-vessel occlusion in the rat: a quantitative evaluation of cerebral blood flow. *Stroke* 1982;13:852-855

88. Ashton D, Van Reempts J, Haseldonckx M, Willems R: Dorsal-ventral gradient in vulnerability of CA1 hippocampus to ischemia: a combined histological and electrophysiological study. *Brain Res* 1989;487:368-372

89. McGrail KM: Intraoperative use of electroencephalography as an assessment of cerebral blood flow. *Neurosurg Clin N Am* 1996;7:685-692

90. Sugio K, Horigome N, Sakaguchi T, Goto M: A model of bilateral hemispheric ischemia--modified four-vessel occlusion in rats [letter]. *Stroke* 1988;19:922

91. Pulsinelli WA, Buchan AM: The four-vessel occlusion rat model: method for complete occlusion of vertebral arteries and control of collateral circulation. *Stroke* 1988;19:913-914

92. Pulsinelli WA, Levy DE, Duffy TE: Cerebral blood flow in the four-vessel occlusion rat model [letter]. *Stroke* 1983;14:832-834

93. Shirane R, Shimizu H, Kameyama M, Weinstein PR: A new method for producing temporary complete cerebral ischemia in rats. *J Cereb Blood Flow Metab* 1991;11:949-956

94. Katz L, Ebmeyer U, Safar P, Radovsky A, Neumar R: Outcome model of asphyxial cardiac arrest in rats. *J Cereb Blood Flow Metab* 1995;15:1032-1039

95. Rod MR, Auer RN: Combination therapy with nimodipine and dizocilpine in a rat model of transient forebrain ischemia. *Stroke* 1992;23:725-732

96. Fujii M, Hara H, Meng W, Vonsattel JP, Huang Z, Moskowitz MA: Strain-related differences in susceptibility to transient forebrain ischemia in SV-129 and C57black/6 mice. *Stroke* 1997;28:1805-10; discussion 1811

97. Landis DM: The early reactions of non-neuronal cells to brain injury. *Annu Rev Neurosci* 1994;17:133-51:133-151

98. Choi DW: Cerebral hypoxia: some new approaches and unanswered questions. *J Neurosci* 1990;10:2493-2501

99. Choi DW: Calcium: still center-stage in hypoxic-ischemic neuronal death. *Trends Neurosci* 1995;18:58-60

100. Tymianski M: Cytosolic calcium concentrations and cell death in vitro. *Adv Neurol* 1996;71:85-105:85-105

101. Kawasaki-Yatsugi S, Yatsugi S, Takahashi M, Toya T, Ichiki C, Shimizu-Sasamata M, Yamaguchi T, Minematsu K: A novel AMPA receptor antagonist, YM872, reduces infarct size after middle cerebral artery occlusion in rats [In Process Citation]. *Brain Res* 1998;793:39-46

102. Choi DW: Calcium-mediated neurotoxicity: relationship to specific channel types and role in ischemic damage. *Trends Neurosci* 1988;11:465-469

103. Choi DW: Glutamate neurotoxicity and diseases of the nervous system. *Neuron* 1988;1:623-634

104. Osuga H, Hakim AM: Relationship between extracellular glutamate concentration and voltage- sensitive calcium channel function in focal cerebral ischemia in the rat. *J Cereb Blood Flow Metab* 1996;16:629-636

105. Lipton SA, Rosenberg PA: Excitatory amino acids as a final common pathway for neurologic disorders [see comments]. *N Engl J Med* 1994;330:613-622

106. Hollmann M, Heinemann S: Cloned glutamate receptors. *Annu Rev Neurosci* 1994;17:31-108:31-108

107. Rothman SM, Olney JW: Glutamate and the pathophysiology of hypoxic--ischemic brain damage. *Ann Neurol* 1986;19:105-111

108. Dugan LL, Choi DW: Excitotoxicity, free radicals, and cell membrane changes. *Ann Neurol* 1994;35 Suppl:S17-21:S17-21

109. MacDermott AB, Mayer ML, Westbrook GL, Smith SJ, Barker JL: NMDA-receptor activation increases cytoplasmic calcium concentration in cultured spinal cord neurones [published erratum appears in Nature 1986 Jun 26-Jul 2;321(6073):888]. *Nature* 1986;321:519-522

110. Albers GW, Goldberg MP, Choi DW: Do NMDA antagonists prevent neuronal injury? Yes. *Arch Neurol* 1992;49:418-420

111. Buchan AM: Do NMDA antagonists protect against cerebral ischemia: are clinical trials warranted? *Cerebrovasc Brain Metab Rev* 1990;2:1-26

112. Buchan AM, Li H, Cho S, Pulsinelli WA: Blockade of the AMPA receptor prevents CA1 hippocampal injury following severe but transient forebrain ischemia in adult rats. *Neurosci Lett* 1991;132:255-258

113. Park CK, Nehls DG, Graham DI, Teasdale GM, McCulloch J: The glutamate antagonist MK-801 reduces focal ischemic brain damage in the rat. *Ann Neurol* 1988;24:543-551

114. McCulloch J, Ozyurt E, Park CK, Nehls DG, Teasdale GM, Graham DI: Glutamate receptor antagonists in experimental focal cerebral ischaemia. *Acta Neurochir Suppl (Wien)* 1993;57:73-9:73-79

115. Lanier WL, Perkins WJ, Karlsson BR, Milde JH, Scheithauer BW, Shearman GT, Michenfelder JD: The effects of dizocilpine maleate (MK-801), an antagonist of the N-methyl-D-aspartate receptor, on neurologic recovery and histopathology following complete cerebral ischemia in primates. *J Cereb Blood Flow Metab* 1990;10:252-261

116. Buchan A, Li H, Pulsinelli WA: The N-methyl-D-aspartate antagonist, MK-801, fails to protect against neuronal damage caused by transient, severe forebrain ischemia in adult rats. *J Neurosci* 1991;11:1049-1056

117. Buchan A, Pulsinelli WA: Hypothermia but not the N-methyl-D-aspartate antagonist, MK-801, attenuates neuronal damage in gerbils subjected to transient global ischemia. *J Neurosci* 1990;10:311-316

118. Li H, Buchan AM: Treatment with an AMPA antagonist 12 hours following severe normothermic forebrain ischemia prevents CA1 neuronal injury. *J Cereb Blood Flow Metab* 1993;13:933-939

119. Sheardown MJ, Nielsen EO, Hansen AJ, Jacobsen P, Honore T: 2,3-Dihydroxy-6-nitro-7-sulfamoyl-benzo(F)quinoxaline: a neuroprotectant for cerebral ischemia. *Science* 1990;247:571-574

120. Shimizu-Sasamata M, Kano T, Rogowska J, Wolf GL, Moskowitz MA, Lo EH, Iadecola C: YM872, a highly water-soluble AMPA receptor antagonist, preserves the hemodynamic penumbra and reduces brain injury after permanent focal ischemia in rats [In Process Citation]. *Stroke* 1998;29:2141-2148

121. Kawasaki-Yatsugi S, Shimizu-Sasamata M, Yatsugi S, Yamaguchi T: Delayed treatment with YM90K, an AMPA receptor antagonist, protects against ischaemic damage after middle cerebral artery occlusion in rats [In Process Citation]. *J Pharm Pharmacol* 1998;50:891-898

122. Shimizu-Sasamata M, Kawasaki-Yatsugi S, Okada M, Sakamoto S, Yatsugi S, Togami J, Hatanaka K, Ohmori J, Koshiya K, Usuda S, Murase K: YM90K: pharmacological characterization as a selective and potent alpha- amino-3-hydroxy-5-methylisoxazole-4-propionate/kainate receptor antagonist. *J Pharmacol Exp Ther* 1996;276:84-92

123. Xue D, Huang ZG, Barnes K, Lesiuk HJ, Smith KE, Buchan AM: Delayed treatment with AMPA, but not NMDA, antagonists reduces neocortical infarction. *J Cereb Blood Flow Metab* 1994;14:251-261

124. Gill R, Nordholm L, Lodge D: The neuroprotective actions of 2,3-dihydroxy-6-nitro-7-sulfamoyl-benzo(F)quinoxaline (NBQX) in a rat focal ischaemia model. *Brain Res* 1992;580:35-43

125. Gill R: The pharmacology of alpha-amino-3-hydroxy-5-methyl-4-isoxazole propionate (AMPA)/kainate antagonists and their role in cerebral ischaemia. *Cerebrovasc Brain Metab Rev* 1994;6:225-256

127. Hollmann M, Hartley M, Heinemann S: Ca2+ permeability of KA-AMPA--gated glutamate receptor channels depends on subunit composition. *Science* 1991;252:851-853

128. Hume RI, Dingledine R, Heinemann SF: Identification of a site in glutamate receptor subunits that controls calcium permeability. *Science* 1991;253:1028-1031

129. Burnashev N: Calcium permeability of glutamate-gated channels in the central nervous system. *Curr Opin Neurobiol* 1996;6:311-317

130. Geiger JR, Melcher T, Koh DS, Sakmann B, Seeburg PH, Jonas P, Monyer H: Relative abundance of subunit mRNAs determines gating and Ca2+ permeability of AMPA receptors in principal neurons and interneurons in rat CNS. *Neuron* 1995;15:193-204

131. Jia Z, Agopyan N, Miu P, Xiong Z, Henderson J, Gerlai R, Taverna FA, Velumian A, MacDonald J, Carlen P, Abramow-Newerly W, Roder J: Enhanced LTP in mice deficient in the AMPA receptor GluR2. *Neuron* 1996;17:945-956

132. Gorter JA, Petrozzino JJ, Aronica EM, Rosenbaum DM, Opitz T, Bennett MV, Connor JA, Zukin RS: Global ischemia induces downregulation of Glur2 mRNA and increases AMPA receptor-mediated Ca2+ influx in hippocampal CA1 neurons of gerbil. *J Neurosci* 1997;17:6179-6188

133. Pellegrini-Giampietro DE, Pulsinelli WA, Zukin RS: NMDA and non-NMDA receptor gene expression following global brain ischemia in rats: effect of NMDA and non-NMDA receptor antagonists. *J Neurochem* 1994;62:1067-1073

134. Pellegrini-Giampietro DE, Zukin RS, Bennett MV, Cho S, Pulsinelli WA: Switch in glutamate receptor subunit gene expression in CA1 subfield of hippocampus following global ischemia in rats [published erratum appears in Proc Natl Acad Sci U S A 1993 Jan 15;90(2):780]. *Proc Natl Acad Sci U S A* 1992;89:10499-10503

135. Pollard H, Heron A, Moreau J, Ben-Ari Y, Khrestchatisky M: Alterations of the GluR-B AMPA receptor subunit flip/flop expression in kainate-induced epilepsy and ischemia. *Neuroscience* 1993;57:545-554

136. Pellegrini-Giampietro DE, Gorter JA, Bennett MV, Zukin RS: The GluR2 (GluR-B) hypothesis: Ca(2+)-permeable AMPA receptors in neurological disorders [see comments]. *Trends Neurosci* 1997;20:464-470

137. Bennett MV, Pellegrini-Giampietro DE, Gorter JA, Aronica E, Connor JA, Zukin RS: The GluR2 hypothesis: Ca(++)-permeable AMPA receptors in delayed neurodegeneration. *Cold Spring Harb Symp Quant Biol* 1996;61:373-84:373-384

138. Kinouchi H, Epstein CJ, Mizui T, Carlson E, Chen SF, Chan PH: Attenuation of focal cerebral ischemic injury in transgenic mice overexpressing CuZn superoxide dismutase. *Proc Natl Acad Sci U S A* 1991;88:11158-11162

139. Schmid-Elsaesser R, Zausinger S, Hungerhuber E, Baethmann A, Reulen HJ, Garcia JH: A critical reevaluation of the intraluminal thread model of focal cerebral ischemia : evidence of inadvertent premature reperfusion and subarachnoid hemorrhage in rats by laser-doppler flowmetry [In Process Citation]. *Stroke* 1998;29:2162-2170
140. Barone FC, Knudsen DJ, Nelson AH, Feuerstein GZ, Willette RN: Mouse strain differences in susceptibility to cerebral ischemia are related to cerebral vascular anatomy. *J Cereb Blood Flow Metab* 1993;13:683-692

141. Murakami K, Kondo T, Kawase M, Chan PH: The development of a new mouse model of global ischemia: focus on the relationships between ischemia duration, anesthesia, cerebral vasculature, and neuronal injury following global ischemia in mice. *Brain Res* 1998;780:304-310

142. Nitatori T, Sato N, Waguri S, Karasawa Y, Araki H, Shibanai K, Kominami E, Uchiyama Y: Delayed neuronal death in the CA1 pyramidal cell layer of the gerbil hippocampus following transient ischemia is apoptosis. *J Neurosci* 1995;15:1001-1011

143. Shigeno T, Yamasaki Y, Kato G, Kusaka K, Mima T, Takakura K, Graham DI, Furukawa S: Reduction of delayed neuronal death by inhibition of protein synthesis. *Neurosci Lett* 1990;120:117-119

144. Xu DG, Crocker SJ, Doucet JP, St-Jean M, Tamai K, Hakim AM, Ikeda JE, Liston P, Thompson CS, Korneluk RG, MacKenzie A, Robertson GS: Elevation of neuronal expression of NAIP reduces ischemic damage in the rat hippocampus. *Nat Med* 1997;3:997-1004

145. MacManus JP, Buchan AM, Hill IE, Rasquinha I, Preston E: Global ischemia can cause DNA fragmentation indicative of apoptosis in rat brain. *Neurosci Lett* 1993;164:89-92

146. Goto K, Ishige A, Sekiguchi K, Iizuka S, Sugimoto A, Yuzurihara M, Aburada M, Hosoya E, Kogure K: Effects of cycloheximide on delayed neuronal death in rat hippocampus. *Brain Res* 1990;534:299-302

147. Todd NV, Picozzi P, Crockard A, Russell RW: Duration of ischemia influences the development and resolution of ischemic brain edema. *Stroke* 1986;17:466-471

148. Nedergaard M, Jakobsen J, Diemer NH: Autoradiographic determination of cerebral glucose content, blood flow, and glucose utilization in focal ischemia of the rat brain: influence of the plasma glucose concentration. *J Cereb Blood Flow Metab* 1988;8:100-108

149. Pulsinelli WA, Levy DE, Duffy TE: Regional cerebral blood flow and glucose metabolism following transient forebrain ischemia. *Ann Neurol* 1982;11:499-502

150. Kuroiwa T, Bonnekoh P, Hossmann KA: Laser doppler flowmetry in CA1 sector of hippocampus and cortex after transient forebrain ischemia in gerbils. *Stroke* 1992;23:1349-1354

151. Miller CL, Lampard DG, Alexander K, Brown WA: Local cerebral blood flow following transient cerebral ischemia. I. Onset of impaired reperfusion within the first hour following global ischemia. *Stroke* 1980;11:534-541

152. Kadotani H, Namura S, Katsuura G, Terashima T, Kikuchi H: Attenuation of focal cerebral infarct in mice lacking NMDA receptor subunit NR2C. *Neuroreport* 1998;9:471-475

153. Inoue T, Kato H, Araki T, Kogure K: Emphasized selective vulnerability after repeated nonlethal cerebral ischemic insults in rats. *Stroke* 1992;23:739-745

154. Koida M, Nakamuta H, Yasuda K, Muguruma K, Hiramatsu Y, Ogawa Y, Kato Y: Carbon monoxide (CO)-induced hypoxia in mice: evaluation as an experimental model of cerebral ischemia for drug screening. *Jpn J Pharmacol* 1989;51:273-278

155. Ishimaru H, Katoh A, Suzuki H, Fukuta T, Kameyama T, Nabeshima T: Effects of N-methyl-D-aspartate receptor antagonists on carbon monoxide- induced brain damage in mice. *J Pharmacol Exp Ther* 1992;261:349-352

156. Andou Y, Mitani A, Masuda S, Arai T, Kataoka K: Re-evaluation of ischemia-induced neuronal damage in hippocampal regions in the normothermic gerbil. *Acta Neuropathol (Berl)* 1992;85:10-14

157. Yang G, Kitagawa K, Matsushita K, Mabuchi T, Yagita Y, Yanagihara T, Matsumoto M: C57BL/6 strain is most susceptible to cerebral ischemia following bilateral common carotid occlusion among seven mouse strains: selective neuronal death in the murine transient forebrain ischemia. *Brain Res* 1997;752:209-218

158. Coimbra C, Wieloch T: Hypothermia ameliorates neuronal survival when induced 2 hours after ischaemia in the rat. *Acta Physiol Scand* 1992;146:543-544

159. Colbourne F, Nurse SM, Corbett D: Temperature changes associated with forebrain ischemia in the gerbil. *Brain Res* 1993;602:264-267

160. Kato H, Kogure K, Araki T, Liu XH, Kato K, Itoyama Y: Immunohistochemical localization of superoxide dismutase in the hippocampus following ischemia in a gerbil model of ischemic tolerance. *J Cereb Blood Flow Metab* 1995;15:60-70

161. Kitagawa K, Matsumoto M, Tagaya M, Hata R, Ueda H, Niinobe M, Handa N, Fukunaga R, Kimura K, Mikoshiba K: 'Ischemic tolerance' phenomenon found in the brain. *Brain Res* 1990;528:21-24

162. Liu Y, Kato H, Nakata N, Kogure K: Temporal profile of heat shock protein 70 synthesis in ischemic tolerance induced by preconditioning ischemia in rat hippocampus. *Neuroscience* 1993;56:921-927

163. Murakami K, Kondo T, Epstein CJ, Chan PH: Overexpression of CuZn-superoxide dismutase reduces hippocampal injury after global ischemia in transgenic mice [published erratum appears in Stroke 1997 Dec;28(12):2573]. *Stroke* 1997;28:1797-1804

164. Terashima T, Namura S, Hoshimaru M, Uemura Y, Kikuchi H, Hashimoto N: Consistent injury in the striatum of C57BL/6 mice after transient bilateral common carotid artery occlusion [In Process Citation]. *Neurosurgery* 1998;43:900-7; discussion 907-8

165. Chan PH, Kawase M, Murakami K, Chen SF, Li Y, Calagui B, Reola L, Carlson E, Epstein CJ: Overexpression of SOD1 in transgenic rats protects vulnerable neurons against ischemic damage after global cerebral ischemia and reperfusion [In Process Citation]. *J Neurosci* 1998;18:8292-8299

166. Wityk RJ, Stern BJ: Ischemic stroke: today and tomorrow [see comments]. *Crit Care Med* 1994;22:1278-1293

167. Obrenovitch TP, Urenjak J: Is high extracellular glutamate the key to excitotoxicity in traumatic brain injury? *J Neurotrauma* 1997;14:677-698

168. Burnashev N, Khodorova A, Jonas P, Helm PJ, Wisden W, Monyer H, Seeburg PH, Sakmann B: Calcium-permeable AMPA-kainate receptors in fusiform cerebellar glial cells. *Science* 1992;256:1566-1570

169. Petralia RS, Wang YX, Mayat E, Wenthold RJ: Glutamate receptor subunit 2-selective antibody shows a differential distribution of calcium-impermeable AMPA receptors among populations of neurons. *J Comp Neurol* 1997;385:456-476

170. Longa EZ, Weinstein PR, Carlson S, Cummins R: Reversible middle cerebral artery occlusion without craniectomy in rats. *Stroke* 1989;20:84-91

171. Yang G, Chan PH, Chen J, Carlson E, Chen SF, Weinstein P, Epstein CJ, Kamii H: Human copper-zinc superoxide dismutase transgenic mice are highly resistant to reperfusion injury after focal cerebral ischemia. *Stroke* 1994;25:165-170

172. Huang Z, Huang PL, Ma J, Meng W, Ayata C, Fishman MC, Moskowitz MA: Enlarged infarcts in endothelial nitric oxide synthase knockout mice are attenuated by nitro-L-arginine. *J Cereb Blood Flow Metab* 1996;16:981-987

173. Roder JC: Normal expression of intracellular calcium ion binding proteins in GluR2 mutant mice. 1999;(Abstract)

174. Du C, Hu R, Csernansky CA, Hsu CY, Choi DW: Very delayed infarction after mild focal cerebral ischemia: a role for apoptosis? *J Cereb Blood Flow Metab* 1996;16:195-201

175. Endres M, Namura S, Shimizu-Sasamata M, Waeber C, Zhang L, Gomez-Isla T, Hyman BT, Moskowitz MA: Attenuation of delayed neuronal death after mild focal ischemia in mice by inhibition of the caspase family. *J Cereb Blood Flow Metab* 1998;18:238-247

176. Tsubokawa H, Oguro K, Masuzawa T, Nakaima T, Kawai N: Effects of a spider toxin and its analogue on glutamate-activated currents in the hippocampal CA1 neuron after ischemia. *J Neurophysiol* 1995;74:218-225

177. Blaschke M, Keller BU, Rivosecchi R, Hollmann M, Heinemann S, Konnerth A: A single amino acid determines the subunit-specific spider toxin block of alpha-amino-3-hydroxy-5-methylisoxazole-4-propionate/kainate receptor channels. *Proc Natl Acad Sci U S A* 1993;90:6528-6532

178. Takazawa A, Yamazaki O, Kanai H, Ishida N, Kato N, Yamauchi T: Potent and long-lasting anticonvulsant effects of 1-naphthylacetyl spermine, an analogue of Joro spider toxin, against amygdaloid kindled seizures in rats. *Brain Res* 1996;706:173-176

179. Koike M, Iino M, Ozawa S: Blocking effect of 1-naphthyl acetyl spermine on Ca(2+)-permeable AMPA receptors in cultured rat hippocampal neurons. *Neurosci Res* 1997;29:27-36

180. Ben-Ari Y, Khrestchatisky M: The GluR2 (GluRB) hypothesis in ischemia: missing links [letter; comment]. *Trends Neurosci* 1998;21:241-242

181. Sokal RR, Rohlf FJ: Assumptions of Analysis of Variance: the arcsine transformation, in Emerson R, Kennedy D, Park RB (eds): *Biometry: principles and practice of statistics in biological research.* San Francisco, W.H. Freeman & Co, 1969, pp 386-387

X. Appendix A: Literature Summary Tables

X.i. Table 1: Mutant Mice Tested in Models of Focal Cerebral Ischemia

Gene	Protein	Mutating Strategy	Model of Ischemia	Change in Infarction Volume	Reference
NNOS	Neuronal nitric oxide synthase	Knockout	Permanent	Reduction	[63]
NNOS	Neuronal nitric oxide synthase	Knockout	Temporary	Reduction	[106]
ENOS	Endothelial nitric oxide synthase	Knockout	Temprorary	Exacerbation	[108]
INOS	Inducible nitric oxide synthase	Knockout	Permanent	Reduction	[297]
PARP	poly(ADP-ribose) polymerase	Knockout	Temporary	Reduction	[296]
CPLA2	Cytosolic phospholipase A_2	Knockout	Transient	Reduction	[298]
p53	p53	Knockout	Permanent	Reduction	[99]
p55	p55 Receptor of Tumor Necrosis Factor-alpha	Knockout	Temporary	Reduction	[288]

Table 1 Continued:

Gene	Protein	Mutating Strategy	Model of Ischemia	Change in Infarction Volume	Reference
BCL-2	Human Bcl2 protein	Transgenic	Permanent	Reduction	[303]
ICAM-1	Intercellular adhesion molecule-1	Knockout	Transient	Reduction	[291,302]
CREB	cAMP-responsive element-binding protein	Knockout	Permanent	No Change	[290]
ICE	IL-1 beta converting enzyme	Transgenic	Transient	Reduction	[301]
ApoE	Apolipoprotein-E	Transgenic	Transient	Reduction	[293]
ApoE	Apolipoprotein-E	Knockout	Transient	Exacerbation	[300]
NGF	Nerve growth factor	Transgenic	Permanent	Reduction	[289]
TPA	tissue plasminogen activator (tPA)	Knockout	Transient	Reduction	[295]
PS	P-Selectin	Knockout	Transient	Reduction	[299]
CuZn-SOD-1	CuZn-superoxide dismutase	Transgenic	Transient	Reduction	[66]

Table 1 Continued:

Gene	Protein	Mutating Strategy	Model of Ischemia	Change in Infarction Volume	Reference
CuZn-SOD-1	CuZn-superoxide dismutase	Transgenic	Permanent	No Difference	[73]
CuZn-SOD-1	CuZn-superoxide dismutase	Transgenic	Permanent	Reduction	[72]
CuZn-SOD-1	CuZn-superoxide dismutase	Knockout	Transient	Reduction	[74]
Mn-SOD-2	Mitochondrial manganese superoxide dismutase	Knockout	Permanent	Exacerbation	[76]
GP1	glutathione peroxidase	Transgenic	Transient	Reduction	[292]
NR2A	epsilon subunit of NMDAR	Knockout	Transient	Reduction	[287]
NR2C	NR2C subunit of NMDAR	Knockout	Permanent	Reduction	[77]
GluR2 flip	Flip-variant of GluR2 subunit of AMPAR	Transgenic	Permanent	Exacerbation	[31]
GluR2	GluR2 subunit of AMPAR	Knockout	Permanent	No Difference	

X.ii. Table 2: Mutant Mice Tested in Models of Global Cerebral Ischemia

Gene	Protein	Mutating Strategy	Model Type	Effect on CA1 Death	Reference
BCL-2	Human BCL-2 protein	Transgenic	BCCAO	Reduction	[304]
CuZn-SOD-1	CuZn-superoxide dismutase	Transgenic	BCCAO	Reduction	[75]
NNOS	Neuronal nitric oxide synthase	Knockout	Three-Vessel Occlusion	Reduction	[2]

XI. Appendix B: Data Summary Tables

XI.i. Data Table I: Percent CA1 Hippocampal Damage Sustained in a Four-Vessel Occlusion Model of Murine Global Cerebral Ischemia

XI.i.a. Data Table Ii: % CA1 Hippocampal Damage 7 Days Following 5-, 10- & 15-min of Four-Vessel Occlusion in CD1 Mice

Hippocampal	Dorsal 1		Dorsal 2		Ventral 1		Ventral 2	
Coordinates	Bregma -1.70		Bregma -2.06		Bregma -2.70		Bregma -3.16	
Ischemia	Mean	SD	Mean	SD	Mean	SD	Mean	SD
Without Muscle Stitch								
VAO-Control	2.23	0.49	1.98	1.59	2.32	0.77	2.00	0.70
5 min	1.99	0.63	2.56	0.72	2.02	0.89	2.36	0.37
10 min	2.18	0.89	2.61	0.49	2.19	0.75	2.47	0.44
15 min	2.20	0.30	2.81	0.54	2.15	1.16	2.41	0.37
With Muscle Stitch								
VAO-Control	1.82	0.28	2.42	0.19	2.37	0.44	1.89	0.40
5 min	2.02	0.42	2.47	0.34	2.17	0.43	2.23	0.25
10 min	2.20	0.29	2.25	0.45	2.47	0.31	2.33	0.22
15 min	2.29	0.47	2.38	0.21	2.50	0.59	2.38	0.68

Statistics	Two-Way ANOVA		
Without Muscle Stitch		With Muscle Stitch	
Ischemia Duration	$p = 0.8848$	Ischemia Duration	$p = 0.2380$
Septotemporal Level	$p = 0.6925$	Septotemporal Level	$p = 0.2615$
Interaction	$p = 0.9551$	Interaction	$p = 0.8155$

XI.i.b. Data Table Iii: % CA1 Hippocampal Damage 7 Days Following 15- & 20-min of Four-Vessel Occlusion in C57Bl/6 and CD1 Mice

Hippocampal Coordinates	Dorsal 1 Bregma -1.70		Dorsal 2 Bregma -2.06		Ventral 1 Bregma -2.70		Ventral 2 Bregma -3.16	
Mouse Group	Mean	SD	Mean	SD	Mean	SD	Mean	SD
CD1 - 15 min	2.86	1.05	2.65	0.47	2.78	1.32	2.81	1.52
CD1 - 20 min	4.55	3.44	4.21	5.71	2.55	2.08	3.50	3.13
C57Bl/6 - 15 min	3.35	1.18	2.35	0.73	2.65	0.91	2.47	1.45
C57Bl/6 - 20 min	2.94	0.92	2.72	0.57	2.40	0.56	2.47	1.01

Statistics	Two-Way ANOVA		
15 min Ischemia		20 min Ischemia	
Strain (CD1 vs C57Bl/6)	p = 0.8972	Strain (CD1 vs C57Bl/6)	p = 0.4588
Septotemporal Level	p = 0.6552	Septotemporal Level	p = 0.6199
Interaction	p = 0.8656	Interaction	p = 0.9405

XI.i.c. Data Table Iiii: % CA1 Hippocampal Damage 7 & 14 Days Following 20-min of Four-Vessel Occlusion in C57Bl/6 Mice

Hippocampal Coordinates	Dorsal 1 Bregma -1.70		Dorsal 2 Bregma -2.06		Ventral 1 Bregma -2.70		Ventral 2 Bregma -3.16	
Mouse Group	Mean	SD	Mean	SD	Mean	SD	Mean	SD
VAO-Control	2.83	1.38	2.61	1.33	2.90	0.20	2.63	1.84
7 Day	2.94	0.92	2.72	0.57	2.40	0.56	2.47	1.01
14 Day	3.36	1.27	2.89	0.87	2.66	0.81	2.13	0.89

Statistics	Two-Way ANOVA
Reperfusion	$p = 0.9785$
Septotemporal Level	$p = 0.4120$
Interaction	$p = 0.9628$

XI.ii. Data Table II: Response of GluR2 Knockout Mice to 24 Hours of Permanent Focal Cerebral Ischemia

XI.ii.a. Data Table IIi: % Residual Cerebral Blood Flow 5- & 15-min Post-Middle Cerebral Artery Occlusion in Wild-type and GluR2 Knockout Mice

Wild-type	GluR2 (+/+)		Knockout	GluR2 (-/-)	
Mouse #	% Residual Blood Flow		Mouse #	% Residual Blood Flow	
	5-min Post MCAO	15-min Post MCAO		5-min Post MCAO	15-min Post MCAO
2	2.65	2.51	5	13.59	10.43
14	4.54	2.30	6	2.23	2.72
19	3.24	3.13	11	5.04	4.95
20	4.93	3.62	17	2.49	3.30
23	13.88	13.50	24	3.59	3.74
28	13.16	11.66	31	5.11	3.48
33	3.74	3.88	35	3.14	2.73
			36	5.12	5.74
Mean +/- SD	6.59 +/- 4.80	5.80 +/- 4.70	Mean +/- SD	5.04 +/- 3.65	4.64 +/- 2.57

XI.ii.b. Data Table IIii: **Infarction Volumes Sustained in Wild-type and GluR2 Knockout Mice 24 Hours Following Permanent Focal Cerebral Ischemia**

Wild-type	GluR2 (+/+)		Knockout	GluR2 (-/-)
Mouse #	Infarct Volume (mm^3)		Mouse #	Infarct Volume (mm^3)
2	88.84		5	63.92
14	65.28		6	79.16
19	49.81		11	82.63
20	48.37		17	87.44
23	82.02		24	43.98
28	49.89		31	49.63
33	90.53		35	71.83
			36	75.93
Mean +/- SD	67.82 +/- 19.10		Mean +/- SD	69.32 +/- 15.64

XI.ii.c. Data Table IIiii: Neurobehavioural Deficit Scores Assessed in Wild-type and GluR2 Knockout Mice 24 Hours Following Permanent Focal Cerebral Ischemia

Wild-type	GluR2 (+/+)		Knockout	GluR2 (-/-)
Mouse #	Neurobehavioural Deficit Score		Mouse #	Neurobehavioural Deficit Score
2	4		5	4
14	2		6	4
19	4		11	4
20	2		17	2
23	2		24	4
28	2		31	1
33	4		35	3
			36	2
Mean +/- SD	2.86 +/- 1.07		Mean +/- SD	3.00 +/- 1.20

Note: Neurobehavioural Deficit Score System

0 - absence of apparent neurobehavioural deficit
1 - inability to extend right forepaw
2 - circling behaviour
3 - tendency to fall to its side
4 - no spontaneous movement

XII. Appendix C: Statistical Analysis Tables

Statistical Table XIIi: Septotemporal Level Comparisons of the Number of Dead Neurons and Total Number of CA1 Hippocampal Neurons following 5-, 10- & 15-min of Four-Vessel Occlusion With and Without a Paravertebral Muscle Stitch (One Way ANOVA)

Statistical Method:		One-Way ANOVA	Statistical Method:		One-Way ANOVA
Without Muscle Stitch			With Muscle Stitch		
Bregma Coordinate			Bregma Coordinate		
-1.70			-1.70		
	Dead CA1 Neurons	p=0.8797		Dead CA1 Neurons	p=0.9299
	Total CA1 Neurons	p=0.5107		Total CA1 Neurons	p=0.9346
-2.06			-2.06		
	Dead CA1 Neurons	p=0.1920		Dead CA1 Neurons	p=0.8656
	Total CA1 Neurons	p=0.4397		Total CA1 Neurons	p=0.6880
-2.70			-2.70		
	Dead CA1 Neurons	p=0.9549		Dead CA1 Neurons	p=0.3084
	Total CA1 Neurons	p=0.8634		Total CA1 Neurons	p=0.5558
-3.16			-3.16		
	Dead CA1 Neurons	p=0.3513		Dead CA1 Neurons	p=0.4789
	Total CA1 Neurons	p=0.7321		Total CA1 Neurons	p=0.9322

Statistical Table XIIii: Septotemporal Level Comparisons of the Number of Dead Neurons and Total Number of CA1 Hippocampal Neurons following 15- & 20-min of Four-Vessel Occlusion in CD1 and C57Bl/6 Mouse Strains (t-test)

Statistical Method:		t-test	Statistical Method:		t-test
CD1 vs C57Bl/6 Strains	15 min Ischemia		CD1 vs C57Bl/6 Strains	20 min Ischemia	
Bregma Coordinate			Bregma Coordinate		
-1.70			-1.70		
	Dead CA1 Neurons	p=0.2995		Dead CA1 Neurons	p=0.4333
	Total CA1 Neurons	p=0.0949		Total CA1 Neurons	p=0.8317
-2.06			-2.06		
	Dead CA1 Neurons	p=0.2336		Dead CA1 Neurons	p=0.4296
	Total CA1 Neurons	p=0.1141		Total CA1 Neurons	p=0.4508
-2.70			-2.70		
	Dead CA1 Neurons	p=0.8845		Dead CA1 Neurons	p=0.9091
	Total CA1 Neurons	p=0.5567		Total CA1 Neurons	p=0.5697
-3.16			-3.16		
	Dead CA1 Neurons	p=0.8092		Dead CA1 Neurons	p=0.7128
	Total CA1 Neurons	p=0.3216		Total CA1 Neurons	p=0.9806

Statistical Table XIIiii:Septotemporal Level Comparisons of the Number of Dead Neurons and Total Number of CA1 Hippocampal Neurons following 7 & 14 Days of Reperfusion in C57Bl/6 Mice (One-Way ANOVA)

Statistical Method:		One-Way ANOVA
Reperfusion Period		
Bregma Coordinate		
-1.70		
	Dead CA1 Neurons	p=0.8101
	Total CA1 Neurons	p=0.9207
-2.06		
	Dead CA1 Neurons	p=0.9719
	Total CA1 Neurons	p=0.8333
-2.70		
	Dead CA1 Neurons	p=0.9743
	Total CA1 Neurons	p=0.4889
-3.16		
	Dead CA1 Neurons	p=0.7529
	Total CA1 Neurons	p=0.7293

Statistical Analysis

Study 1: CD1 Mice - 5, 10, 15 min Ischemia

Without a Paravertebral Muscle Stitch

Individual Animal Percentages

Total Neuronal Counts

Statistical Analysis

Study 1: CD1 Mice - 5, 10, 15 min ischemia

With a Paravertebral Muscle Stitch

Individual Animal Percentages / Total Neuronal Counts

Group: [illegible]

Animal #		% CA1 Neuronal Death -1.70	[illegible]	-2.70	-3.16
1		2.00	[illegible]	[illegible]	1.84
2		[illegible]	[illegible]	[illegible]	2.31
3		1.94	2.37	[illegible]	[illegible]
	Mean	[illegible]	[illegible]	[illegible]	[illegible]
	SD	[illegible]	[illegible]	[illegible]	[illegible]

	-1.70 Dead	Alive	Total	% Dead	[illegible] Dead	Alive	Total	% Dead	-2.70 Dead	Alive	Total	% Dead	-3.16 Dead	Alive	Total	% Dead
1	[illegible]	434	[illegible]	[illegible]	17	[illegible]	[illegible]	[illegible]	24	618	642	[illegible]	18	[illegible]	[illegible]	1.84
2	[illegible]	[illegible]	[illegible]	[illegible]	11	478	[illegible]	[illegible]	16	[illegible]	[illegible]	[illegible]	[illegible]	1067	[illegible]	2.31
3	[illegible]	[illegible]	[illegible]	[illegible]	8	330	[illegible]	[illegible]	11	647	[illegible]	[illegible]	17	1108	1128	[illegible]
Mean	7	[illegible]	[illegible]	[illegible]	12	470	481	[illegible]	17	[illegible]	[illegible]	[illegible]	[illegible]	1042	[illegible]	[illegible]
SD	[illegible]	70	71	[illegible]	[illegible]	[illegible]	[illegible]	[illegible]	7	[illegible]	[illegible]	[illegible]	4	70	70	[illegible]

Group: 5 min

Animal #		% CA1 Neuronal Death -1.70	[illegible]	-2.70	-3.16
1		[illegible]	[illegible]	[illegible]	2.76
2		[illegible]	3.14	[illegible]	[illegible]
3		1.76	[illegible]	[illegible]	[illegible]
4		[illegible]	[illegible]	[illegible]	2.18
5		[illegible]	[illegible]	1.72	2.12
6		2.10	2.31	[illegible]	[illegible]
7		[illegible]	[illegible]	2.10	[illegible]
8		2.21	[illegible]	[illegible]	[illegible]
	Mean	[illegible]	[illegible]	2.17	[illegible]
	SD	[illegible]	[illegible]	[illegible]	[illegible]

	-1.70 Dead	Alive	Total	% Dead	[illegible] Dead	Alive	Total	% Dead	-2.70 Dead	Alive	Total	% Dead	-3.16 Dead	Alive	Total	% Dead
1	6	[illegible]	[illegible]	[illegible]	17	[illegible]	714	[illegible]	14	[illegible]	[illegible]	[illegible]	[illegible]	919	[illegible]	[illegible]
2	5	[illegible]	370	[illegible]	21	[illegible]	[illegible]	3.14	16	[illegible]	777	[illegible]	37	1277	[illegible]	[illegible]
3	6	[illegible]	[illegible]	[illegible]	8	402	410	[illegible]	13	613	[illegible]	[illegible]	[illegible]	[illegible]	[illegible]	[illegible]
4	17	[illegible]	[illegible]	[illegible]	12	614	[illegible]	[illegible]	16	[illegible]	721	[illegible]	31	[illegible]	[illegible]	2.18
5	9	[illegible]	319	[illegible]	10	[illegible]	[illegible]	[illegible]	10	671	[illegible]	[illegible]	31	[illegible]	[illegible]	2.12
6	[illegible]	[illegible]	[illegible]	2.10	14	[illegible]	[illegible]	2.31	22	[illegible]	717	[illegible]	[illegible]	1119	[illegible]	[illegible]
7	[illegible]	[illegible]	[illegible]	[illegible]	16	673	[illegible]	[illegible]	13	[illegible]	619	2.10	17	[illegible]	[illegible]	[illegible]
8	7	[illegible]	317	[illegible]	18	[illegible]	[illegible]	[illegible]	13	[illegible]	674	[illegible]	[illegible]	[illegible]	[illegible]	[illegible]
Mean	[illegible]	[illegible]	[illegible]	[illegible]	14	[illegible]	[illegible]	[illegible]	16	[illegible]	[illegible]	2.17	[illegible]	[illegible]	[illegible]	[illegible]
SD	4	[illegible]	[illegible]	[illegible]	4	[illegible]	113	[illegible]	4	[illegible]	[illegible]	[illegible]	4	[illegible]	[illegible]	[illegible]

Group: 10 min

Animal #		% CA1 Neuronal Death -1.70	[illegible]	-2.70	-3.16
1		2.21	1.73	[illegible]	[illegible]
2		[illegible]	[illegible]	[illegible]	2.11
3		[illegible]	[illegible]	[illegible]	[illegible]
	Mean	[illegible]	[illegible]	[illegible]	[illegible]
	SD	[illegible]	[illegible]	0.21	[illegible]

	-1.70 Dead	Alive	Total	% Dead	[illegible] Dead	Alive	Total	% Dead	-2.70 Dead	Alive	Total	% Dead	-3.16 Dead	Alive	Total	% Dead
1	[illegible]	[illegible]	[illegible]	2.21	12	[illegible]	[illegible]	1.73	18	[illegible]	[illegible]	[illegible]	[illegible]	917	941	[illegible]
2	[illegible]	[illegible]	[illegible]	[illegible]	16	614	[illegible]	[illegible]	21	[illegible]	[illegible]	[illegible]	18	[illegible]	[illegible]	2.11
3	11	[illegible]	444	[illegible]	13	611	[illegible]	[illegible]	16	[illegible]	[illegible]	[illegible]	30	1315	1344	[illegible]
Mean	[illegible]	[illegible]	[illegible]	[illegible]	14	[illegible]	916	[illegible]	[illegible]	728	[illegible]	[illegible]	[illegible]	[illegible]	[illegible]	[illegible]
SD	3	[illegible]	[illegible]	[illegible]	2	[illegible]	[illegible]	[illegible]	3	[illegible]	110	[illegible]	[illegible]	[illegible]	[illegible]	[illegible]

Group: 15 min

Animal #		% CA1 Neuronal Death -1.70	[illegible]	-2.70	-3.16
1		2.70	[illegible]	3.14	3.16
2		[illegible]	[illegible]	2.37	1.87
3		[illegible]	2.2	[illegible]	2.12
	Mean	[illegible]	[illegible]	[illegible]	[illegible]
	SD	0.47	0.21	[illegible]	[illegible]

	-1.70 Dead	Alive	Total	% Dead	[illegible] Dead	Alive	Total	% Dead	-2.70 Dead	Alive	Total	% Dead	-3.16 Dead	Alive	Total	% Dead
1	7	[illegible]	[illegible]	2.70	18	[illegible]	773	[illegible]	19	[illegible]	[illegible]	3.14	[illegible]	[illegible]	1013	3.16
2	[illegible]	[illegible]	[illegible]	[illegible]	7	[illegible]	[illegible]	[illegible]	[illegible]	[illegible]	[illegible]	2.37	[illegible]	[illegible]	[illegible]	1.87
3	11	410	[illegible]	[illegible]	[illegible]	[illegible]	[illegible]	2.2	18	[illegible]	[illegible]	[illegible]	[illegible]	[illegible]	[illegible]	2.12
Mean	[illegible]	[illegible]	[illegible]	[illegible]	16	[illegible]	[illegible]	[illegible]	19	767	[illegible]	[illegible]	[illegible]	1077	[illegible]	[illegible]
SD	3	116	[illegible]	0.47	7	[illegible]	[illegible]	[illegible]	1	[illegible]	[illegible]	[illegible]	[illegible]	[illegible]	111	[illegible]

Statistical Analysis

Study 2: **CD1 & C57Bl/6 Mice - Comparison Between 15 & 20 min Ischemia**

CD1 Mice

Individual Animal Percentages

Ischemia: 15 min

Animal #		% CA1 Neuronal Death -1.7	-2.06	-2.7	-3.16
1		3.91	3.05	3.66	3.65
2		3.13	2.66	1.55	4.62
3		3.32	2.68	4.50	3.27
4		1.12	2.96	2.70	1.63
5		2.83	1.86	1.48	0.89
	Mean	2.86	2.66	2.70	2.61
	SD	1.05	0.47	1.31	1.52

Total Neuronal Counts

	-1.70 Dead	Alive	Total	% Dead	-2.06 Dead	Alive	Total	% Dead	-2.70 Dead	Alive	Total	% Dead	-3.16 Dead	Alive	Total	% Dead
	14	344	358	3.91	18	572	590	3.05	26	684	710	3.66	38	1003	1041	3.65
	16	496	512	3.13	19	690	709	2.66	10	634	644	1.55	65	1343	1408	4.62
	15	437	452	3.32	18	653	671	2.68	30	701	734	4.50	50	1481	1531	3.27
	6	530	536	1.12	21	680	700	2.96	20	720	740	2.70	12	723	735	1.63
	17	584	601	2.83	10	530	540	1.86	10	664	674	1.48	6	666	672	0.89
Mean	14	478	492	2.86	17	628	644	2.66	20	681	700	2.70	34	1043	1077	2.61
SD	4	88	92	1.05	4	72	76	0.47	10	39	41	1.31	25	369	397	1.52

Ischemia: 20 min

Animal #		% CA1 Neuronal Death -1.7	-2.06	-2.7	-3.16
1		4.23	2.33	0.89	5.06
2		4.41	1.96	2.02	1.79
3		10.31	14.39	5.94	8.26
4		2.10	1.56	2.95	1.85
5		1.70	0.83	0.95	0.73
	Mean	4.55	4.21	2.55	3.50
	SD	3.44	5.71	2.00	3.13

	-1.70 Dead	Alive	Total	% Dead	-2.06 Dead	Alive	Total	% Dead	-2.70 Dead	Alive	Total	% Dead	-3.16 Dead	Alive	Total	% Dead
	15	340	355	4.23	13	544	557	2.33	6	666	674	0.89	16	300	316	5.06
	16	347	363	4.41	8	400	408	1.96	16	776	792	2.02	23	1265	1288	1.79
	63	549	611	10.31	143	861	994	14.39	42	665	707	5.94	100	1110	1210	8.26
	9	420	429	2.10	10	632	642	1.56	15	494	509	2.95	19	1072	1091	1.85
	7	404	411	1.70	5	600	605	0.83	6	631	636	0.95	9	1220	1229	0.73
Mean	22	412	434	4.55	36	605	641	4.21	18	720	740	2.55	33	993	1026	3.50
SD	23	84	106	3.44	60	166	216	5.71	14	106	109	2.00	39	397	465	3.13

Statistical Analysis

Study 2: CD1 & C57Bl/6 Mice - Comparison Between 15 & 20 min Ischemia

C57Bl/6 Mice

Individual Animal Percentages / Total Neuronal Counts

Ischemia: 15 min

Animal #		% CA1 Neuronal Death -1.7	-3.06	-2.7	-3.16
1		1.61	2.72	2.81	2.77
2		4.60	1.52	3.43	1.42
3		3.34	3.21	2.44	4.83
4		4.27	2.62	3.38	1.27
5		2.95	1.67	1.20	2.07
	Mean	3.36	2.35	2.65	2.47
	SD	1.18	0.73	0.81	1.45

	-1.70 Dead	Alive	Total	% Dead	-3.06 Dead	Alive	Total	% Dead	-2.70 Dead	Alive	Total	% Dead	-3.16 Dead	Alive	Total	% Dead
	6	367	373	1.61	14	500	514	2.72	19	656	675	2.81	32	1123	1155	2.77
	12	249	261	4.60	7	455	462	1.52	20	563	583	3.43	20	1391	1411	1.42
	13	376	389	3.34	20	603	623	3.21	18	720	738	2.44	60	1181	1241	4.83
	5	112	117	4.27	16	594	610	2.62	28	801	829	3.38	16	1245	1261	1.27
	16	527	543	2.95	10	590	600	1.67	10	823	833	1.20	26	1232	1258	2.07
Mean	10	326	337	3.36	13	548	562	2.35	19	713	732	2.65	31	1234	1265	2.47
SD	5	155	160	1.18	5	67	70	0.73	6	107	106	0.81	17	100	82	1.45

Ischemia: 20 min

Animal #		% CA1 Neuronal Death -1.7	-3.06	-2.7	-3.16
1		2.44	3.48	2.95	2.88
2		2.43	2.70	2.96	2.30
3		2.43	1.94	1.64	2.88
4		2.85	2.51	2.16	0.79
5		4.56	2.99	2.26	3.40
	Mean	2.94	2.73	2.40	2.47
	SD	0.92	0.67	0.58	1.01

	-1.70 Dead	Alive	Total	% Dead	-3.06 Dead	Alive	Total	% Dead	-2.70 Dead	Alive	Total	% Dead	-3.16 Dead	Alive	Total	% Dead
	8	320	328	2.44	14	526	540	2.59	19	626	645	2.95	32	1077	1109	2.89
	9	361	370	2.43	7	419	426	1.64	26	620	646	2.96	22	922	944	2.33
	10	402	412	2.43	20	455	475	4.29	10	600	610	1.64	29	962	991	2.93
	12	409	421	2.85	16	700	716	2.23	13	590	603	2.16	7	882	889	0.79
	26	544	570	4.56	10	604	614	1.63	18	777	795	2.26	42	1192	1234	3.40
Mean	13	407	420	3	13	541	554	3	17	661	668	3	26	1027	1053	2
SD	7	84	92	1	5	114	116	1	6	100	114	1	13	130	135	1

Statistical Analysis

Study 3: C57Bl/6 Mice - Comparison Between 7 & 14 Day Reperfusion Periods

C57Bl/6 Strain

Individual Percentages / Total Neuronal Counts

Control: VAC

Animal #		% CA1 Neuronal Death -1.70	-2.06	-2.70	-3.16
1		1.82	3.34	2.95	4.43
2		4.41	1.07	3.07	0.79
3		2.27	3.41	2.89	2.69
	Mean	2.83	2.61	2.90	2.63
	SD	1.30	1.30	0.30	1.94

	-1.70 Dead	Alive	Total	% Dead	-2.06 Dead	Alive	Total	% Dead	-2.70 Dead	Alive	Total	% Dead	-3.16 Dead	Alive	Total	% Dead
	7	378	385	1.82	12	347	359	3.34	17	559	576	2.95	33	712	745	4.43
	13	282	295	4.41	8	740	748	1.07	18	568	586	3.07	9	1175	1184	0.76
	11	473	484	2.27	24	680	704	3.41	18	657	669	2.69	31	1121	1152	2.69
Mean	10	378	388	2.83	15	589	604	2.61	18	595	610	2.90	24	1003	1027	2.63
SD	3	96	95	1.30	8	211	210	1.30	1	61	61	0.20	13	253	245	1.84

Reperfusion: 7 Days

Animal #		% CA1 Neuronal Death -1.70	-2.06	-2.70	-3.16
1		2.44	3.49	2.95	2.89
2		2.43	2.70	2.88	2.33
3		2.43	1.94	1.64	2.93
4		2.85	2.51	2.19	0.79
5		4.55	2.89	2.36	3.40
	Mean	2.94	2.72	2.40	2.47
	SD	0.93	0.57	0.55	1.01

	-1.70 Dead	Alive	Total	% Dead	-2.06 Dead	Alive	Total	% Dead	-2.70 Dead	Alive	Total	% Dead	-3.16 Dead	Alive	Total	% Dead
	8	320	328	2.44	19	530	549	3.49	19	626	645	2.95	32	1077	1109	2.89
	9	361	370	2.43	12	419	431	2.70	25	860	845	2.88	22	922	944	2.33
	10	402	412	2.43	9	460	469	1.94	10	600	610	1.64	27	892	921	2.93
	12	409	421	2.85	18	700	718	2.51	13	585	598	2.19	7	882	889	0.79
	26	544	570	4.55	18	604	622	2.89	18	777	795	2.26	42	1192	1234	3.40
Mean	13	407	420	2.94	15	541	556	2.72	17	681	698	2.40	26	1037	1063	2.47
SD	7	84	92	0.93	4	114	117	0.57	6	109	114	0.55	13	125	130	1.01

Reperfusion: 14 Days

Animal #		% CA1 Neuronal Death -1.70	-2.06	-2.70	-3.16
1		2.37	2.07	2.72	2.83
2		2.92	3.80	3.40	2.66
3		4.76	2.80	1.87	1.10
	Mean	3.35	2.89	2.66	2.13
	SD	1.25	0.87	0.77	0.90

	-1.70 Dead	Alive	Total	% Dead	-2.06 Dead	Alive	Total	% Dead	-2.70 Dead	Alive	Total	% Dead	-3.16 Dead	Alive	Total	% Dead
	14	576	590	2.37	11	520	531	2.07	23	625	648	3.40	21	779	790	2.83
	12	399	411	2.92	21	532	553	3.80	15	656	671	2.24	27	987	1014	2.66
	10	190	200	4.76	15	520	535	2.80	16	727	743	2.15	11	993	1004	1.10
Mean	12	391	400	3.35	16	524	540	2.89	17	669	687	2.66	20	919	939	2.13
SD	2	190	191	1.25	5	7	12	0.87	3	57	59	0.81	8	125	121	0.90

Statistical Analysis

Note: Analysis of Variance of Percentage CA1 Neuronal Death Requires an Arcsine Transformation

Transformation: Angle = Arcsine (Square Root (Percentage / 100))

Study 1 CD1 Mice - 4VO: 5, 10, 15 min Ischemia

Without Paravertebral Muscle Stitch

Ischemia:	VAO					Ischemia:	5 min					Ischemia:	10 min					Ischemia:	15 min				
		% CA1 Neuronal Death					% CA1 Neuronal Death						% CA1 Neuronal Death						% CA1 Neuronal Death			
Animal #		-1.70	-0.69	-0.70	-0.10	Animal #	-1.70	-0.69	-0.70	-0.10		Animal #	-1.70	-0.69	-0.7	-0.10		Animal #	-1.70	-0.69	-0.70	-0.10
1		3.70	3.91	3.14	1.35	1	2.34	2.34	3.65	2.71		1	1.74	2.69	2.67	2.68		1	2.61	2.35	2.45	2.67
2		2.39	0.95	2.19	2.73	2	2.65	1.95	1.84	2.10		2	2.69	2.85	3.21	2.76		2	2.10	2.74	1.23	2.61
3		1.73	1.14	1.62	1.35	3	1.73	1.69	1.35	1.65		3	2.49	2.64	1.65	2.73		3	1.62	2.51	1.77	2.35
						4	1.62	2.64	2.76	2.65		4	0.95	2.65	2.65	2.65						
						5	1.19	2.61	1.64	2.64		5	2.16	2.65	1.44	1.65						

Arcsine Transformation

Animal #		-1.70	-0.69	-0.70	-0.10	Animal #	-1.70	-0.69	-0.70	-0.10	Animal #	-1.70	-0.69	-0.7	-0.10	Animal #	-1.70	-0.69	-0.70	-0.10
1		0.17	0.20	0.16	0.12	1	0.16	0.16	0.16	0.17	1	0.13	0.16	0.16	0.14	1	0.16	0.16	0.16	0.14
2		0.16	0.10	0.15	0.17	2	0.17	0.14	0.14	0.16	2	0.16	0.16	0.16	0.17	2	0.16	0.17	0.11	0.17
3		0.13	0.11	0.13	0.14	3	0.13	0.13	0.12	0.14	3	0.16	0.14	0.12	0.17	3	0.14	0.16	0.15	0.16
						4	0.14	0.17	0.17	0.16	4	0.00	0.17	0.16	0.17					
						5	0.11	0.17	0.16	0.16	5	0.16	0.16	0.12	0.14					

With Paravertebral Muscle Stitch

Ischemia:	VAO					Ischemia:	5 min					Ischemia:	10 min					Ischemia:	15 min				
		% CA1 Neuronal Death					% CA1 Neuronal Death						% CA1 Neuronal Death						% CA1 Neuronal Death			
Animal #		-1.70	-0.69	-0.70	-0.10	Animal #	-1.70	-0.69	-0.70	-0.10		Animal #	-1.70	-0.69	-0.70	-0.10		Animal #	-1.70	-0.69	-0.70	-0.10
1		2.65	2.65	2.65	1.94	1	2.69	2.39	1.82	2.70		1	2.21	1.73	2.84	2.65		1	2.70	2.39	2.14	2.16
2		1.69	2.26	2.39	2.31	2	1.35	2.14	2.65	2.67		2	1.69	2.84	2.35	2.11		2	1.84	2.61	2.27	1.97
3		1.84	2.27	1.97	1.81	3	1.75	1.65	2.47	2.39		3	2.49	2.49	2.69	2.39		3	2.39	2.2	1.69	2.16
						4	2.65	2.39	2.69	2.16												
						5	2.65	2.49	1.72	2.12												
						6	2.16	2.31	2.67	2.39												
						7	1.97	2.65	2.16	1.69												
						8	2.31	2.64	1.69	2.69												

Arcsine Transformation

Animal #		-1.70	-0.69	-0.70	-0.10	Animal #	-1.70	-0.69	-0.70	-0.10	Animal #	-1.70	-0.69	-0.70	-0.10	Animal #	-1.70	-0.69	-0.70	-0.10
1		0.14	0.16	0.17	0.14	1	0.14	0.16	0.14	0.17	1	0.16	0.13	0.16	0.16	1	0.17	0.16	0.16	0.16
2		0.12	0.16	0.16	0.16	2	0.12	0.16	0.14	0.14	2	0.14	0.16	0.16	0.16	2	0.14	0.16	0.16	0.14
3		0.14	0.16	0.14	0.12	3	0.13	0.14	0.16	0.16	3	0.16	0.16	0.17	0.16	3	0.16	0.16	0.14	0.16
						4	0.14	0.16	0.16	0.16										
						5	0.17	0.16	0.13	0.16										
						6	0.16	0.16	0.16	0.16										
						7	0.14	0.16	0.16	0.14										
						8	0.16	0.16	0.14	0.16										

Statistical Analysis

Note: Analysis of Variance of Percentage CA1 Neuronal Death Requires an Arcsine Transformation

Transformation: Angle = Arcsine (Square Root (Percentage / 100))

Study 2: CD1 & C57Bl/6 Mice - Comparison Between 15 & 20 min Ischemia

CD1 Mice

Ischemia: 15 min

Animal #	% CA1 Neuronal Death			
	-1.70	-0.60	-0.70	-0.10
1	3.04	3.05	3.05	3.05
2	2.13	2.05	1.05	4.05
3	3.30	2.05	4.05	3.07
4	1.13	2.05	2.70	1.03
5	2.05	1.05	1.45	0.05

Arcsine Transformation

Animal #	-1.70	-0.60	-0.70	-0.10
1	0.20	0.15	0.15	0.15
2	0.15	0.15	0.12	0.20
3	0.15	0.15	0.21	0.15
4	0.11	0.17	0.17	0.13
5	0.17	0.14	0.12	0.05

C57Bl/6 Mice

Ischemia: 15 min

Animal #	% CA1 Neuronal Death			
	-1.70	-0.60	-0.70	-0.10
1	1.01	2.73	2.01	2.77
2	4.05	1.05	3.45	1.45
3	3.34	3.21	2.04	4.05
4	4.07	2.05	3.20	1.27
5	2.05	1.07	1.20	2.07

Arcsine Transformation

Animal #	-1.70	-0.60	-0.70	-0.10
1	0.13	0.17	0.17	0.17
2	0.20	0.15	0.15	0.12
3	0.15	0.15	0.15	0.20
4	0.01	0.15	0.15	0.11
5	0.17	0.13	0.11	0.14

CD1 Mice

Ischemia: 20 min

Animal #	% CA1 Neuronal Death			
	-1.70	-0.60	-0.70	-0.10
1	4.20	2.30	0.60	0.60
2	4.41	1.05	2.05	1.70
3	10.51	14.35	0.04	0.35
4	2.15	1.05	2.05	1.05
5	1.70	0.53	0.55	0.73

Arcsine Transformation

Animal #	-1.70	-0.60	-0.70	-0.10
1	0.21	0.15	0.09	0.23
2	0.21	0.14	0.14	0.13
3	0.30	0.30	0.25	0.20
4	0.15	0.13	0.17	0.13
5	0.13	0.09	0.15	0.09

C57Bl/6 Mice

Ischemia: 20 min

Animal #	% CA1 Neuronal Death			
	-1.70	-0.60	-0.70	-0.10
1	2.44	3.45	2.05	2.05
2	2.45	2.70	2.05	2.30
3	2.45	1.04	1.04	2.05
4	2.05	2.51	2.15	0.70
5	4.05	2.05	2.20	3.45

Arcsine Transformation

Animal #	-1.70	-0.60	-0.70	-0.10
1	0.15	0.15	0.17	0.17
2	0.15	0.17	0.17	0.15
3	0.15	0.14	0.13	0.17
4	0.17	0.15	0.15	0.09
5	0.09	0.17	0.15	0.15

Statistical Analysis

Note: Analysis of Variance of Percentage CA1 Neuronal Death Requires an Arcsine Transformation

Transformation: Angle = Arcsine (Square Root (Percentage / 100))

Study 3: C57BV6 Mice - Comparison Between 7 & 14 Day Reperfusion Periods Following 30 min Ischemia

Control	VAO	Reperfusion: 7 Days								Reperfusion: 14 Days					
		% CA1 Neuronal Death					% CA1 Neuronal Death					% CA1 Neuronal Death			
Animal #		-1.70	-0.69	-0.70	-0.10	Animal #	-1.70	-0.69	-0.70	-0.10	Animal #	-1.70	-0.69	-0.70	-0.10
1		1.88	3.34	2.95	4.43	1	2.44	3.48	2.95	2.89	1	2.37	2.97	3.70	3.89
2		4.41	1.87	3.07	0.70	2	2.48	2.70	2.68	2.20	2	2.82	2.89	2.48	2.68
3		2.37	3.41	2.89	2.89	3	2.48	1.84	1.84	2.95	3	4.70	2.89	1.87	1.10
						4	2.89	2.01	2.10	0.70					
						5	4.89	2.89	2.28	2.48					
Arcsine Transformation															
Animal #		-1.70	-0.69	-0.70	-0.10	Animal #	-1.70	-0.69	-0.70	-0.10	Animal #	-1.70	-0.69	-0.70	-0.10
1		0.14	0.18	0.17	0.21	1	0.16	0.18	0.17	0.17	1	0.16	0.14	0.17	0.18
2		0.21	0.18	0.16	0.08	2	0.16	0.17	0.17	0.16	2	0.17	0.20	0.19	0.16
3		0.18	0.19	0.16	0.16	3	0.16	0.14	0.13	0.17	3	0.20	0.17	0.14	0.16
						4	0.17	0.16	0.16	0.08					
						5	0.20	0.17	0.16	0.16					

XIII. Appendix D: Infarct Volume Quantification

XIII.i. Lesion Quantification Following Permanent Focal Cerebral Ischemia

A novel method of infarct volume calculation was used to quantitate the cerebral damage sustained from the permanent occlusion of the mouse middle cerebral artery. Although this approach shares in the use of an image analysis system to quantify lesion areas per slice of brain tissue, it differs from other methods in terms of its integration of those areas into a final infarct volume.

Investigators have typically calculated the overall lesion size by summing the infarct volumes per slice of brain tissue; the latter of which is calculated from the product of the infarct area per slice and the slice thickness. By convention, the infarct area from the caudal face of each tissue section is used for this calculation. Thus, for an ischemic brain cut into four coronal slices of 2 mm thickness, the infarct volume would be calculated as follows:

$$\text{Slice Infarct Volume } (mm^3) = \text{Infarct Area } (mm^2) \bullet \text{Tissue Thickness}$$

$$\text{Overall Lesion Volume } (mm^3) = \text{Sum of Infarct Volumes } (mm^3) \text{ Per Four Brain Slices}$$

The general criticism of this method of calculation lies in its conceptualization of the infarct volume within a given slice to be cylindrical. Therefore, this approach assumes that the infarct areas on either side of a coronal brain slice to be equal. However, this is not true. For two consecutive ischemic brain slices, the caudal face of

the first is representative of the rostral face of the second. With the spatial evolution of the lesion within the ischemic hemisphere, rarely are the caudal and rostral infarct areas of a given slice equal, and likewise, the caudal infarct areas from two adjacent sections of 2 mm thickness.

To better represent the evolution of the infarct within a tissue slice, I have conceptualized the lesion as a frustrum. This is a conical section with two circular sides with differing radii. This approach more adequately represents the disparate infarct areas quantified from both the rostral and caudal faces of a given brain slice. Therefore, for an ischemic brain cut into four coronal slices of 2 mm thickness, the infarct volume would be calculated as follows:

Slice Infarct Volume (mm^3) = 1/3 • Pi • Tissue Thickness * (R1*R1 + R1 * R2 + R2 * R 2)

where R1 = Radius of the Rostral Face of the Slice

R2 = Radius of the Caudal Face of the Slice

R1 & R2 are calculated from the infarct areas of a slice, therefore:

e.g. R1 = Square Root (Infarct Area / Pi)

Remember: Area of Circle = Pi • Radius • Radius

To calculate the Infarct Area of Slice 1:

R1 is derived from the caudal face of Slice 1

R2 is derived from the rostral face of Slice 2

Therefore,

Overall Lesion Volume (mm^3) = Sum of Infarct Volumes (mm^3) Per Four Brain Slices

To validate this method of infarct volume calculation, data from a rat focal ischemia study unrelated to the current work was inputted into the "Frustrum" formula. The results were then correlated to that calculated by an already established method of lesion quantification. A Pearson correlation coefficient of 0.998014 was calculated by statistical software, (Figure 11).

XIII.ii.a. Data Table IIIi: Correlation Analysis & Infarction Volume Data Derived from Both the Frustrum Summation and an Established Method of Lesion Quantification

Rat #	Established Method Infarct Volume (mm^3)	Frustrum Quantification Infarct Volume (mm^3)	Pearson Correlation Coefficient
1	87.3	63.14	**0.998041**
2	101.0	71.02	
3	97.7	69.34	
4	100.0	71.35	
5	63.1	45.97	
6	107.4	76.30	
7	80.3	58.23	
8	61.5	47.34	
9	93.6	67.19	
10	85.3	62.41	
11	114.9	80.06	
12	111.5	77.74	

Note: Differences in the absolute value of infarction volumes derived from each method is attributed to differences in a magnification factor used to their respective quantification formulae. This factor is used to correct the infarct area measured by the image analysis system from a histological slide preparation of the ischemic tissue, so that it is more representative of the area of damage in an unprocessed brain slice.

XIII.iii. Infarction Volume Program Source Code

```
const Pi:= 3.1459
var Area_1, Area_2, Area_3, Area_4 : real
var t : real
loop
        var reply : string
        put skip, "Please enter the thickness of each slice of tissue (mm):  ".."
        get t
        put skip, "Please enter the value of Area_1:  ".."
        get Area_1
        put "Please enter the value of Area_2:  ".."
        get Area_2
        put "Please enter the value of Area_3:  ".."
        get Area_3
        put "Please enter the value of Area_4:  ".."
        get Area_4
        put skip, "Slice    Raw Infarct Area (sq. mm)"
        for Row : 1..1
                put "  ", "1", "          ",
                        Area_1
                put "  ", "2", "          ",
                        Area_2
                put "  ", "3", "          ",
                        Area_3
                put "  ", "4", "          ",
                        Area_4
        end for
        put skip, "Are the data correct (y/n)?  ".."
        get reply
        exit when reply = "y"
end loop
var ca_1,ca_2, ca_3, ca_4 : real
var mag : real
put skip, "Please enter the magnification factor, e.g. mouse = 6:  ".."
get mag
ca_1:= Area_1/mag**2
ca_2:= Area_2/mag**2
ca_3:= Area_3/mag**2
ca_4:= Area_4/mag**2
put skip, "Slice    Raw Infarct Area (sq. mm)    Corrected Infarct Area (sq. mm)"
for Row : 1..1
        put "  ", "1", "          ",
                Area_1, "                    ",
                ca_1
```

```
        put "  ", "2", "          ",
                Area_2, "                    ",
                ca_2
        put "  ", "3", "          ",
                Area_3, "                    ",
                ca_3
        put "  ", "4", "          ",
        Area_4, "                    ",
        ca_4
end for
var Volume_1, Volume_2, Volume_3, Volume_4 : real
var TotVol : real
var R_1, R_2, R_3, R_4 : real
var CV_1, CV_2, CV_3, CV_4 : real
var CR_1, CR_2, CR_3, CR_4 : real
var CVTot : real
R_1:= sqrt(Area_1/Pi)
R_2:= sqrt(Area_2/Pi)
R_3:= sqrt(Area_3/Pi)
R_4:= sqrt(Area_4/Pi)
CR_1:= sqrt(ca_1/Pi)
CR_2:= sqrt(ca_2/Pi)
CR_3:= sqrt(ca_3/Pi)
CR_4:= sqrt(ca_4/Pi)
const R_5 := 0
const Area_5 := 0
const CR_5 := 0
const ca_5 := 0
Volume_1:= 1/3*Pi*t*(R_1**2 + R_1 * R_2 + R_2**2)
Volume_2:= 1/3*Pi*t*(R_2**2 + R_2 * R_3 + R_3**2)
Volume_3:= 1/3*Pi*t*(R_3**2 + R_3 * R_4 + R_4**2)
Volume_4:= 1/3*Pi*t*(R_4**2 + R_4 * R_5 + R_5**2)
TotVol:= Volume_1 + Volume_2 + Volume_3 + Volume_4
put skip, "The total volume of infarction is ", TotVol, " cu. mm."
CV_1:= 1/3*Pi*t*(CR_1**2 + CR_1 * CR_2 + CR_2**2)
CV_2:= 1/3*Pi*t*(CR_2**2 + CR_2 * CR_3 + CR_3**2)
CV_3:= 1/3*Pi*t*(CR_3**2 + CR_3 * CR_4 + CR_4**2)
CV_4:= 1/3*Pi*t*(CR_4**2 + CR_4 * CR_5 + CR_5**2)
CVTot:= CV_1 + CV_2 + CV_3 + CV_4
put skip, "The total corrected volume of infarction is ", CVTot, " cu. mm."
```

XIII.iv. Infarction Volume Program Monitor Output:

Display of Program Prompts

Please enter the thickness of each slice of tissue (mm) : _____

Please enter the value of Area_1: _____

Please enter the value of Area_2: _____

Please enter the value of Area_3: _____

Please enter the value of Area_4: _____

Slice	Raw Infarct Area (mm2)
1	_____
2	_____
3	_____
4	_____

Are the data correct (y / n)? _____

Please enter the magnification factor, e.g. mouse = 6 : _____

Slice	Raw Infarct Area (mm2)	Corrected Infarct Area (mm2)
1	_____	_____
2	_____	_____
3	_____	_____
4	_____	_____

The total corrected volume of infarction is _____ mm^3.